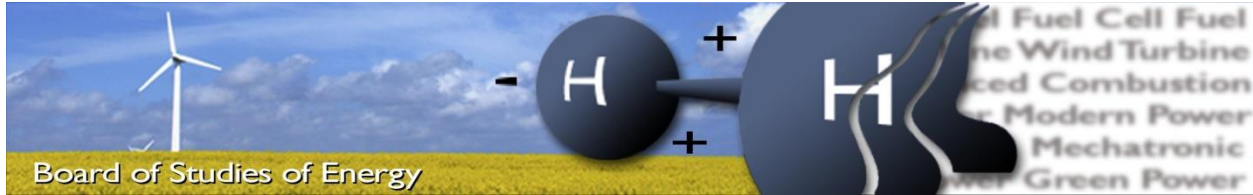




Coordination of Battery Energy Storage and Power-to-Gas in Distribution Systems

Master Thesis

Teodor Ognyanov Trifonov



Title : **Coordination of Battery Energy Storage and Power-to-Gas in Distribution Systems**

Project type : **Master Thesis**

Project period : **01.02.2016 – 10.01.2017**

Student : **Teodor Ognyanov Trifonov**

Student № : **20147778**

Supervisor : **Jiakun Fang**

Abstract:

Concerning the rapid development and deployment of Renewable Energy Systems and the need to store that energy, the target of this thesis is to coordinate between an Energy Storage System and a Power-to-Gas system in a manner that fully utilizes their complementary advantages. Different technologies concerning the Energy Storage System and Power-to-Gas systems are investigated, as well as suitable roles for the Energy Storage System in the electrical grid. Steady-state models are created of Renewable Energy Systems and of a Power-to-Gas system as well as the respected grids. Charging strategies are created for the Energy Storage System and production strategies for the Power-to-Gas system. The size of the Energy Storage System is then observed with regards to the Renewable Energy Systems and in coordination with the Power-to-Gas system. As a result it is found that it is possible to store surplus energy from Renewable Energy Systems and it can further on be stored in the form of methane and that with a proper charging strategy the capacity of the Energy Storage System can be lowered.

Teodor Trifonov

Copies : 3

Pages, total : 77

Appendix : 17

Supplements : 3 CDs

Table of Contents

NOMENCLATURE	V
CHAPTER 1 – INTRODUCTION	1
1.1 Background and motivation	1
1.2 Background and motivation	1
1.2 Problem Formulation	3
1.3 Project Limitations	3
1.4 Methodology	4
1.5 The organization of the thesis	4
CHAPTER 2 OVERVIEW OF ENERGY STORAGE SYSTEMS	5
2.1 Role of the energy storage system in the grid	5
2.1.1 Bulk Energy Services (BES)	6
2.1.2 Ancillary Services	6
2.1.3 Transmission Infrastructure Services	7
2.1.4 Distribution Infrastructure Services	7
2.1.5 Customer Energy Management Services	7
2.2 Electrochemical Energy Storage	9
2.2.1 Lead-Acid Batteries (LA)	9
2.2.2 Lithium – Ion	11
2.2.3 Vanadium Redox	12
2.2.4 Compressed Air Energy Storage (CAES)	14
2.3 Heat storage	15
2.3.1 Aquifer Thermal Energy Storage (ATES)	16
2.3.2 Pit Thermal Energy Storage (PTES)	16
2.4 Power-to-Gas (PtG)	17
2.4.1 Alkaline Electrolysis (AE)	18
2.4.2 Proton Exchange Membrane (PEM)	19
2.4.3 Chemical Methanation	20
2.5 Technology Comparison	20
2.6 Conclusions	22
CHAPTER 3 POWER SYSTEM WITH RENEWABLES	24

3.1 Grid Layout	24
3.2 Electrical Demand	24
3.3 Wind Turbine Modelling	25
3.4 Modelling of Photovoltaic Modules	26
3.5 Renewable Power Generation	28
3.5.1 Wind Power	28
3.5.2 PV power generation	32
3.6 Conclusion	34
CHAPTER 4 NATURAL GAS SYSTEM SIMULATION	35
4.1 Supporting Gas Grid	35
4.1.1 Natural Gas Grid Parameters	35
4.1.2 Newton-Raphson method	36
4.2 Power-to-Gas Simulation	38
4.3 Gas Powered Generator Regulation	39
4.3.1 Kalman Filter	40
4.3.2 Least Error Squares (LES)	42
4.4 Gas Grid Simulation and Demand	42
4.4.1 Least Error Squares	42
4.4.2 Kalman Filter	43
4.4.3 Power-to-Gas Gas Demand	45
4.5 Conclusions	45
CHAPTER 5 ENERGY STORAGE AND ITS OPTIMAL SIZING	46
5.1. Obtaining the Storage System Size	46
5.1.1 Flowchart for obtaining Storage System Capacity	46
5.1.2 Sizing Storage System with regards to the import/export	46
5.1.3 Sizing Storage System with regards to the price of electrical power	47
5.2 Sizing of the ESS	49
5.3.1 Sizing Storage System Capacity with Surplus Power Method	49
5.3.2 Sizing Storage System Capacity with Surplus Power and Price Method	51
5.4 Sizing ESS with PtG via Surplus Power and Price Method	53
5.5 Sizing of ESS with Electrochemical Characteristics	54
5.6 Conclusions	56

CHAPTER 6 CONCLUSION AND FUTURE WORK	57
6.1 Conclusions	57
6.2 Future work	57
BIBLIOGRAPHY	58
APPENDIX A	61
APPENDIX B	70
Appendix B.1 Wind Turbines	70
Appendix B.2 Solar Panels	75

Nomenclature

Symbol	Description	Unit
Indices		
m	Indices of numerical procedure (iteration step)	
Input Parameters – Grid		
R_{per}	Residual percentage	%
Input Parameters – Photovoltaic		
G	Solar irradiance	W/m^2
T	Ambient temperature	$^{\circ}C$
Input Parameters – Wind Turbine		
V	Velocity of the wind	m/s
ρ	Air Density	kg/m^3
Datasheet Parameters – Photovoltaic		
G_s	Reference solar irradiance	W/m^2
I_{mpps}, I_{scs}	Maximum power point and Short circuit current at STC	A
NOCT	Nominal Operation Cell Temperature	$^{\circ}C$
$NOCT_s$	Ambient Nominal Operation Cell Temperature	$^{\circ}C$
T_s	Reference ambient temperature	$^{\circ}C$
V_{mpps}, V_{ocs}	Maximum power point and Short circuit voltage at STC	V
α, β, γ	Current, Voltage and Power temperature coefficients	$\%/^{\circ}C$
Datasheet Parameters – Wind Turbine		
A	Swept Area of Blades	m^2
$C_{p,wt}$	Efficiency coefficient of the wind turbine	
Variables – Grid		
$P_{c,g}, P_{g,g}$	Power consumption and generation in the grid	MW
$P_{pr,g}, P_{prl,g}$	Price and price limit of electrical power in the grid	Currency/MWh
$P_{r,g}$	Residual power in the grid	MW
Variables – Energy Storage System		
$E_{cap,ss}$	Energy capacity of the ESS	MWh
$P_{i/o,ess}$	Input/output power at the ESS	MW
$P_{c,ess}, P_{g,ess}$	Power consumed and generated by ESS	MW
η_{ESS}	Efficiency of the ESS	%
Variables – Photovoltaic		
C_1, C_2	Coefficient	
I_p	Output current	A
I_{mpp}, I_{sc}	Maximum power point and Short circuit current	A
I_{scg}	Short-circuit current at G	A
$P_{g,pv}$	Power generation photo voltaic	MW
$P_{gn,pv}$	Power generation photovoltaic type “n”	MW
V_{oc}, V_{ocg}	Open circuit voltage and open circuit voltage at G	V
V_p	Output voltage [V]	V
$V_{min,pv}, V_{max,pv}$	Maximum and Minimum voltage [V]	V
$V_{mpp,pv}$	Maximum power point voltage [V]	V
y_p	Number of Photovoltaics from type “p”	
ΔT	Temperature variation	

ΔV	Voltage variation	
M_s	Modules connected in series	
M_p	Modules connected in parallel	
Variables – Wind Turbine		
$P_{g,wt}$	Power generation wind turbine	MW
$P_{gn,wt}$	Power generation Wind turbine type “n”	MW
X_n	Number of WTs from type “n”	
Variables – Power-to-Gas		
C_{PtG}	PtG constant	
$E_{d,PtG}$	Energy demand	MWh
$E_{d,\Delta H}$	Energy demand for creating 1 mol of CH ₄	MWh
$G_{d,PtG}$	Gas demand from the PtG system	mol
$G_{p,PtG}$	Gas production PtG	m^3/h
LHV	Lower Heating Value	
η_{PtG}	Efficiency of the PtG	%
ΔH	Energy demand for creating 1 mol of CH ₄	kJ
Variables & Parameters – Gas Grid		
D_{k-l}	Diameter of pipe between nodes k and l	mm
$G_{d,GPGv}$	Gas demand from the GPG at city ‘v’	m^3
L_{k-l}	Diameter of pipe between nodes k and l	km
p_k, p_l	Nodal Gas pressure at both ends of the pipeline	kPa
$P_{d,GPGv}$	Power demand from the GPG at city ‘v’	MW
$P_{c,cityv}^m$	Power consumption at city ‘v’ at moment ‘m’	MW
$Q_{gas,k-l}$	Gas flow rate measured in section k-l	m^3/h
$Q_{s\ gas,k}, Q_{d\ gas,k}$	Gas supply and demand at node k	m^3/h
Z_{k-l}	Resistance coefficient of the pipeline	
Π_k, Π_l	$\Pi_k = p_k^2, \Pi_l = p_l^2$	
η_{GPGv}	Efficiency of GPG at city ‘v’	%
Variables & Parameters – Load Prediction		
K^m	Kalman gain for moment m	
p_{error}^m	Prediction error for moment m	
p_{error}^{m-1}	Prediction error for moment $m-1$	
p_{error}^{m-}	Prediction error estimation based on a previous estimate	
R	Noise of the environment	
s^m	Past data	
u^m	Contro signal	
w^{m-1}	Process noise	
\hat{X}^m	Estimated load at moment m .	
\hat{X}^{m-1}	Estimation for moment $m-1$	
\hat{x}^{m-}	Estimation based on a previous estimate	
Z^m	Past observed data at moment m	
$a_0, a_1 \dots$	Regression coefficients	
y_1, y_2, y_3	Factors affecting the load	
Y	Factor matrix	
\hat{X}	Estimated load	
θ	Regression coefficient matrix	

Chapter 1 – Introduction

With the increasing development and deployment of renewables, energy system integration draws broad interest as a way to make energy systems work more efficiently. The purpose of this master thesis is to propose the concepts and methodology to coordinate the Electrical Energy Storage System (ESS) and the Power-to-Gas (PtG) system. This chapter contains basic concepts that are needed to understand why coordination is necessary between an ESS and a PtG.

1.1 Background and motivation

1.2 Background and motivation

In the future of energy supply, Renewable Energy Sources (RES) will have more and more impact on the power grid. In the past, humanity has mainly depended on fossil-fuel technologies to satisfy its energy

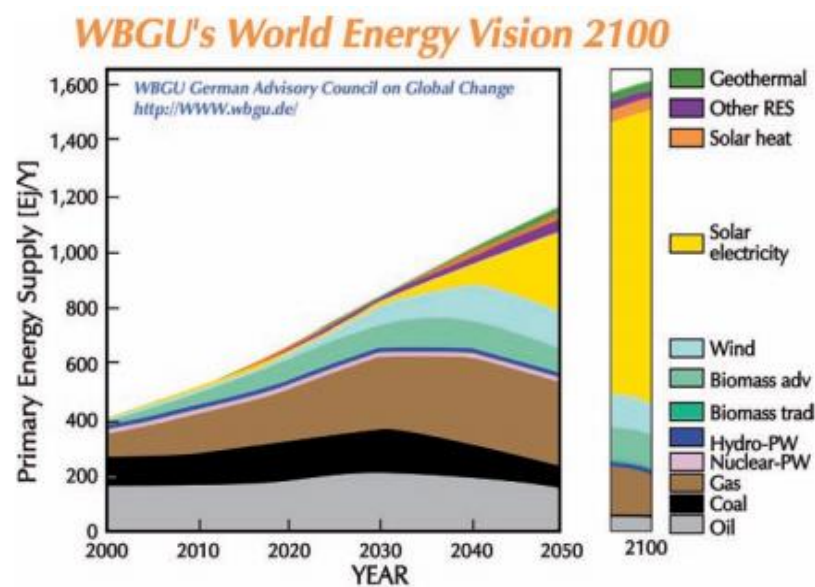


Figure 1 The World Energy Vision 2100 [2]

needs [1]. Figure 1 presents the vision of where the worlds energy should come from in the year 2100 according to the German Advisory Council on Global Change .It can be seen that the time to phase out the fossil-fuel based energy is closer than ever. With years passing, humanity will increase its energy demand and fossil fuels alone will not be able to meet that demand. When that time comes, researchers and engineers working on different RES projects will have to make sure that this demand can be

satisfied only with the use of green technologies. According to Figure 1, this turning point will occur around the year 2030 and by then a lot of work needs to be done as to how different RES can be more efficient. This can happen through new technologies ., finding specific optimal geographical locations for placing RES, or even creating new RES [2].

Denmark has set an ambitious goal where 100% of the energy supply must come from Renewable Energy Systems (RES). Due to this in the next years, it is expected that more and more of the energy supply needs of the country will be covered by RES. In the future, most of the energy supply needs will be covered by wind power parks, both onshore and offshore.

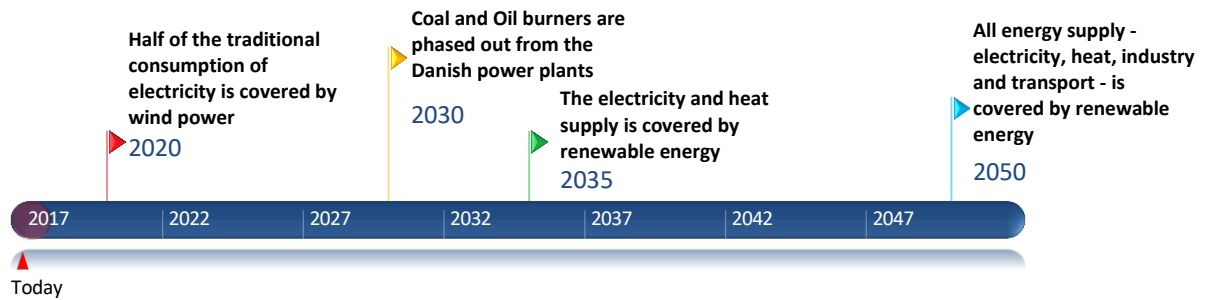


Table 1 Energy policy for Denmark until 2050 [3]

Table 1 presents the Danish government's energy policy milestones until 2050. Until the year 2020 half of the electrical supply must be covered by wind power, Recent studies reveal that as of January 2015 total wind power penetration in Denmark has reached 39% [4].

By the year 2030, according to Table 1, coal and oil burners must be phased out from the electrical system. Coal and oil burners are fundamental to the power system of any country due to their high power output and mature technology. Due to this most coal and oil burner power plants are used for covering the bulk of the electrical needs of citizens. One way of dealing with this issue is through an increase in the offshore wind power parks [5]. In recent years, wind energy has been dramatically increased.

By the year 2035, both electrical and heat supply must be covered by RES. At the moment heating for homes comes from cogeneration, also called Combined Heat and Power (CHP), where electrical and heat energy is produced and supplied to the consumers. For the RES to cover both these sectors, a certain flexibility must first be achieved. Research into forecasting methods must be increased so that operators can have better knowledge of how the RES production is going to change in the future. Certain operational practices must be altered like faster dispatch times, which will reduce regulation resources need and larger balance authority areas. To cover the fluctuating electrical energy demand, flexible generation sources can be used, with natural gas combustion turbines and hydropower plants being amongst the most flexible generators. To help with this flexibility and also fulfill the 2035 milestone, that is presented in Table 1, a PtG system which transforms the electrical energy produced by RES into chemical energy can be used for covering the heating needs of consumers and the electrical needs as well. Through the use of such a system surplus electric power can be converted into chemical and then can be used immediately or stored for future use[6, 7].

The last milestone set by the policy is that by the year 2050, all of the energy supplied must come from RES and cover the electrical, heat, industry and transport demand.

Reaching these milestones will not be easy, mainly because it is expected of RES to cover the needs of more than one energy sector, but not impossible. In the past years, much research has been done in developing new and better technologies than before to increase the RES efficiency. Due to this, the number of RES installed in the power system will keep increasing. Unfortunately, these RES work thanks to nature which is often sporadic. As a result of this, a problem is brought to attention connected with the security of supply. That is the issue with surplus power.

Power balance issue

In the electrical system, there are stability criteria regarding the power system frequency at all voltage levels, which state that the frequency must be at $50 \text{ Hz} \pm 0.5 \text{ Hz}$. This criterion requires that the production and consumption of electrical power must always be equal.

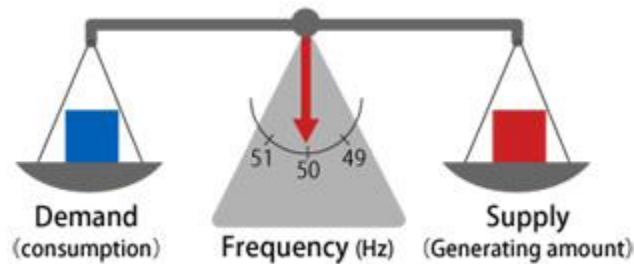


Figure 2 Demand and Supply balance [8]

Higher generation than the load (positive surplus power) will lead to an increase in frequency and having a lower generation than the load (negative surplus power) will result in a decrease in the frequency of the grid, as can be seen from Figure 2. This can lead to un-synchronism of generators and over voltages [9].

However, this obstacle can be overcome by introducing Energy Storage Systems (ESS). An ESS can be used to supply the power system in times of decreased RES production and can also be used to absorb surplus power in terms of increased RES production. Also pairing such a system with a PtG system can ensure that the gas grid, as well as the electrical system, can benefit from surplus power produced by RES.

1.2 Problem Formulation

Taking into consideration that the creation of large ESS is still very expensive and that the efficiency of PtG is very low, the purpose of this master project is to coordinate these two technologies in a manner that fully utilizes their complementary advantages in a grid dominated by RES. The ESS is sized through varying the RES that is installed in the power system. The PtG will create methane (CH_4) which will be pumped into the gas grid from where it can help gas-burner power plants or the transport sector.

The main objectives of this paper are:

- Investigate different ESS technologies available on the market and what services they can perform.
- Investigate different PtG technologies.
- Make an assessment of whether a coordination between an ESS and a PtG would be beneficial

1.3 Project Limitations

The following assumptions and limitations are set.

- The Electrical Power System, RES, ESS and PtG will all be represented by simplified models in order for the complexity of the simulations to be reduced.
- No power flow models will be created for the LV grid to find the best location for each RES.
- No real models will be conducted to back up the results of this paper.

- The steady-state models for power and gas systems are used. These models are used to size the ESS for past events. They are utilized as a way of showing what would have happened if there was an ESS installed in that period of time and will help in determining whether the system will benefit from such a technology.

1.4 Methodology

The following process will be followed to collect all the necessary information needed for completion of this thesis.

First, different ESS services will be presented and compared. The one that fits the problem will be chosen further on. After that different kind of ESS and PtG systems will be presented and compared.

Afterward, a base scenario will be created. This scenario will contain the electrical load data for a set location, over the course of a month (March 2015), in hourly intervals. The weather data will also be collected at the same intervals for this area so that different RES like wind turbines and solar panels can also be modeled.

After choosing the service provided by the ESS, a LV grid will be created, and the ESS will be placed. After that through varying the number of installed RES and using different charging scenarios, the size of the ESS will be found.

Further on, a PtG system will be modeled for covering the gas needs of consumers in the gas grid. This system will be connected with the ESS to find whether or not the size of the ESS can be reduced.

As a final step, the size for a specific ESS technology will be found.

1.5 The organization of the thesis

This thesis is composed of six themed chapters. The first chapter is where the background and motivation, problem statement and methodology are presented. The second chapter is an introduction to the ESS and P2G technologies. Also, different roles for the ESS are looked through in an attempt to find the one that suits the current needs the best. Chapter three presents how different RES systems are modelled. Chapter four introduces the PtG system and its working process. It also explains how production strategy for the PtG is formed. In Chapter five different sizing scenarios are formed and the resultant ESS capacities are analyzed. Chapter six is dedicated to conclusions that are drawn out from this paper as well as tasks for future work.

Chapter 2 Overview of Energy Storage Systems

The following chapter deals with the connection between a system with a high number of Renewable Energy Sources (RES) and Energy Storage Systems (ESS). Different services provided by ESS that can bring greater stability to the system have been explained. Various types of ESS have been presented and compared. The purpose of this chapter is to find the best service or combination of services with the appropriate ESS technology that best fits Denmark's needs for a future with predominant RES.

2.1 Role of the energy storage system in the grid

Balancing the supply and demand in a RES dominant system can be achieved through the use of ESS. The shape of the request consumption profile can be predicted, and the ESS output can be increased or decreased very fast depending on the needs. Having a system dominated by RES makes it harder to maintain a balance between production and consumption due to differences in generation and consumption profiles. Having higher generation from one RES at a certain time does not usually mean that there are consumers in need of that power. Using energy storage systems in such cases can increase the grid flexibility and the grid stability [10].

The applications for ESS can range from Bulk Energy Services (BES) through Ancillary Services (AS), Transmission / Distribution Infrastructure Services (T/D IS) to Customer Energy Management Services (CEMS). [11]

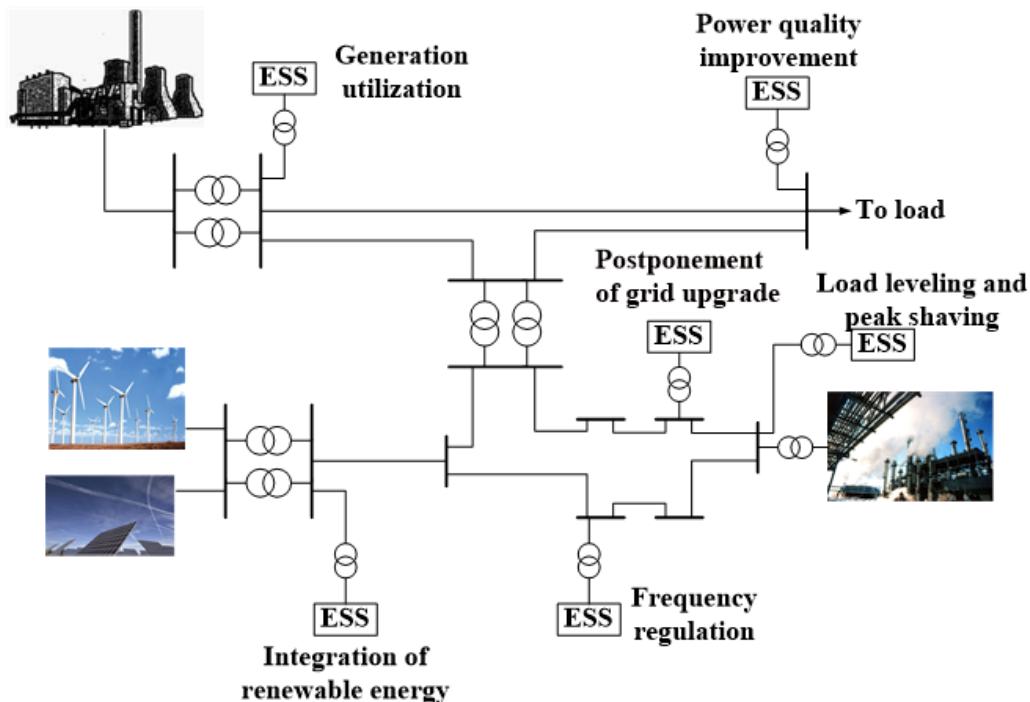


Figure 3 ESS Placement in Grid

Table 2 shows the different services that can be performed by an ESS, while Figure 3 shows a one line diagram of the locations where Energy Storage Systems should be installed to be able to carry out their functions.

BES	AS	TIS	DIS	CEMS
Electric Energy Time-Shift	Regulation	Transmission Upgrade Deferral	Distribution Upgrade Deferral	Power Quality
Electric Supply Capacity	Voltage Support	Transmission Congestion Relief	Voltage Support	Power Reliability
Forecast Hedging	Black Start			

Table 2 ESS Services Source[11]

2.1.1 Bulk Energy Services (BES)

1. **Electric Energy Time-Shift(EET-S)** – The act of purchasing electrical energy in periods with low price and the selling that energy when the price is higher, Time-Shift can also be used to store excess power generation and then release the energy when the RES has decreased production e.g. PV. An Energy Storage System for this size ranges between **1-500 MW** a discharge duration of less than **1 hour** and **250+ cycles** per minimum yearly. Such a service is used for small PV panels and wind farms, but given the size range this service can be further expanded, [11]
2. **Electric Supply Capacity(ESC)** – Such a service can be used to help If there is a need for extra energy in the grid. This type of service is location-dependent and is used as a way to avoid the need to buy extra generation capacity from the electricity market. Such a system can be discharged when there is a lack of RES energy with high load demand and charged when there is excess RES energy with lowered load demand. The ESS size can be between **1 – 500 MW** with a discharge duration of **2-6 hours** and **5 to 100 cycles** per year.[11]
3. **Forecast Hedging (FH)** – A service that is mainly used for renewable systems. With RES it is never certain that the production will match what the owner has promised. This service can then be used to supply the difference between what was forecasted and what is produced.[12]

2.1.2 Ancillary Services

1. **Regulation** – A service used for maintaining the balance between production and demand, Essentially performing frequency regulation. Having greater demand than supply leads to a decrease in frequency and having a greater supply than demand leads to an increase in the grid frequency.[13] Such a system needs to be between **10 and 40 MW** with a discharge duration of **15 to 60 minutes** and must be able to perform between **250 to 10 000 cycles** per year. [11]
2. **Voltage Support(VS)** – Service that maintains the voltage in a certain window of operation. This service is used to offset the reactance in the distribution grid. When there is a voltage drop, the current must increase the power supplied to stay the same. This forces the system to consume more reactive power which drops the voltage further. Further increase of the current brings to shutting down of generators and lines due to self-protection purposes.

Such an ESS need to have a size of **1 – 10 MVAR**. In this mode, the duration is of no interest because no real power is needed from the ESS. A general estimation is made that the operation time should be around 30 minutes.[11]

3. **Black Start(BS)** – A service that energizes the distribution lines, transmission lines and helps to bring back power plants after a grid failure. After energizing the lines and contribute to start the generator, the ESS ramps slowly down as the generator picks up the load. The size should be between **5 and 50 MW**. With work time between **15 and 60 minutes**. The yearly cycles for such a service are usually in the range of **10 – 20 cycles**.[11]

2.1.3 Transmission Infrastructure Services

1. **Transmission Upgrade Deferral(TUD)** – When there is a line that is reaching its maximum carrying capacity, or a substation in the same predicament, ESS are used to take some of the load off and postpone the needed upgrade for a couple of years. Usually, such high loads are reached on specific days for a few hours every year. Such a system is in the **10 – 100 MW** range with a discharge duration between **2-8 hours** and between **10-50 cycles** per year.[11]
2. **Transmission Congestion Relief(TCR)** – Transmission Congestion happens when the customer's energy needs cannot be met. It is said that a system is in such a state while everything is operating at optimum conditions, but the demand can still not be fulfilled.[14] An ESS can be used to store energy while the system is operating normally and then discharge the same energy on peak times. Such a system requires a size between **1-100 MW** with discharge duration of up to **4 hours** and between **50 and 100 cycles** per year.[11]

2.1.4 Distribution Infrastructure Services

1. **Distribution Upgrade Deferral (DUD)** with **VS** – Serves the same purpose as Transmission Upgrade Deferral, of postponing system upgrade by a couple of years. Such a system could be used as voltage support at the same time, by tap changing regulators and switching of capacitors that follow the variations of the load. Tiny amounts of real power are drawn from the ESS in this case. A size for an ESS performing such a service is between **500 kW – 10 MW** with a discharge duration of up to **4 hours** and between **50 to 100 cycles** per year.[11]

2.1.5 Customer Energy Management Services

1. **Power Quality(PQ)** – Such a service is used to deal with voltage magnitude changes, significant variations in the nominal frequency [50 Hz], low power factor, power outage up to a few seconds. All of these factors affect the customer negatively. An ESS thus can be used to deal with all of these disturbances. Size for such an ESS varies from **100 kW to 10MW**. The duration of discharge for such a system ranges from a **few seconds to a quarter of an hour**. Yearly cycles that an ESS has to perform is between **10 and 200 cycles**.[11]
2. **Power Reliability (PR)**– Essentially an Uninterruptable Power System (UPS). If there is a major problem with the grid, e.g. blackout, such a system deals with the needs of consumers it has access to. The size of such a system is dependent on how much power and for how long it must operate. Increasing this so-called “islanded mode” can be done through the use of diesel generators.[11]

Specs Action	Size [MW]	Discharge Duration [h]	Cycles per year
EET-S	1-500	1	250+
ESC	1-500	2-6	5-100
Regulation	10-40	0.25-1	250-10000
VS	1-10 MVAR	0.5	-
BS	5-50	0.25-1	10-20
TUD	10-100	2-8	10-50
TCR	1-100	4	50-100
DUD	0.5-10	4	50-100
PQ	0.1-10	0.002-0.25	10-200
PR	-	-	-

Table 3 Summary of ESS specifications

The following figure, Figure 4, presents a general classification of Electrical Energy Storage Systems. These systems are divided into mechanical, thermodynamic, electrochemical and electromagnetic. In the next sub-chapters, only technologies from the thermodynamic and electrochemical trees will be revised. Main reason for that is because the other branches do not meet the intended need (help in dealing with surplus energy) or Denmark does not have the needed geography for accommodating these technologies.

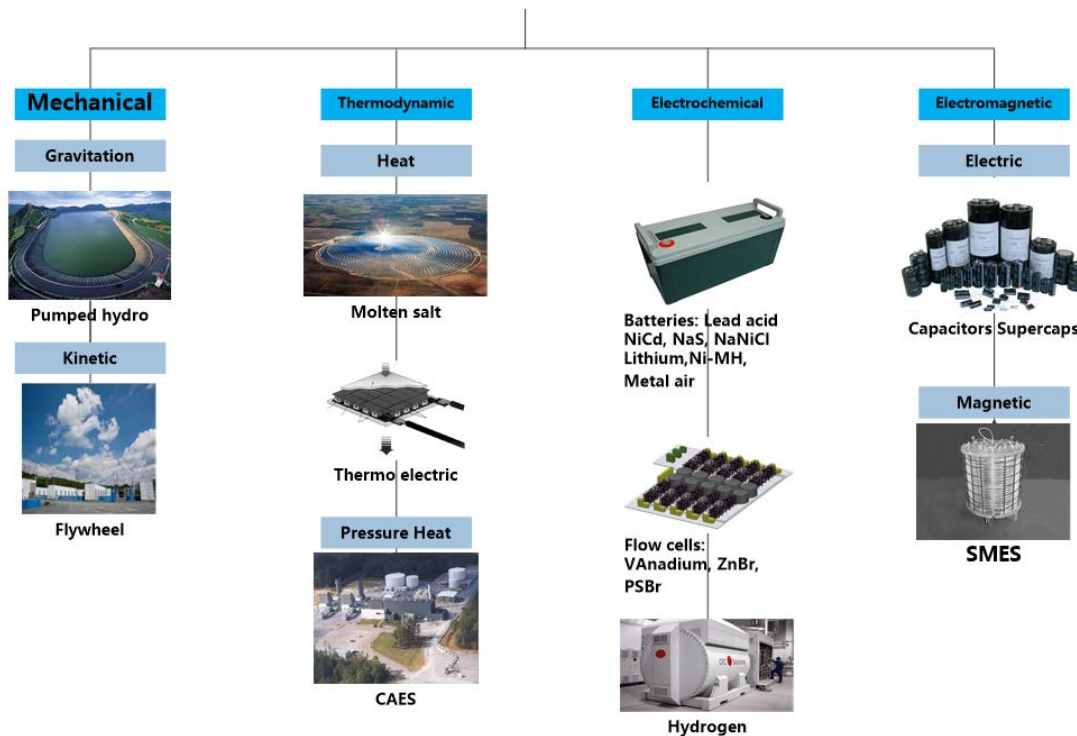


Figure 4 Classification of Electrical Energy Storage

2.2 Electrochemical Energy Storage

With batteries, electrical energy can be converted to chemical energy and held until that energy needs to be discharged. Most of the battery ESS rely on cells to hold the energy. The size depends on the way the cells are connected to each other, voltage level is increased by connecting more cells in a series and capacity is increased by connecting cells in parallel.

There are many different battery technologies on the market. Different kinds of literature and Internet articles separate these four technologies from the rest – Lead – Acid Batteries as the most mature technology out there. Lithium-Ion (Li-Ion) as a widely used technology for electronic devices and with potential for performing utility functions. Vanadium Redox Battery (VRB) as a flow battery is one of them.

2.2.1 Lead-Acid Batteries (LA)

This technology has been around for a very long time. Since the 1870s when lead-acid batteries were first used for ancillary services.[1]



Figure 5 Lead-Acid Battery Discharge/Charge Cycles Source[15]

Figure 5 shows how charging and discharging affects the Lead-Acid Battery. As the name suggest, there is a lead alloy electrodes submerged in an acid electrolyte. From the figure, it can be seen that during discharge Lead Sulfate forms on the electrodes and as more sulfate forms the lower the voltage of the battery. Charging is done at a voltage higher than the nominal battery voltage. While discharging the lead sulfate is reconverted to sulfuric acid and lead. It is also important to mention that some sulfation remains on the plates, which leads to lowered capacity.[15]

Positive aspects of this technology are its maturity and price. Negative aspects include toxicity, self-discharge, temperature sensitive and sulfation. Efficiency is at 75-85 % with a lifetime of 3-10 years depending on the electrode type (different electrodes are used for various applications). Optimal temperature of the surrounding environment is 25°C. [1]

	Voltage Support	Frequency Support	Short Duration PQ	Long Duration PQ	Short Duration PQ + Load Shift+Regulation
Capacity (MWh)	0.003	3	0.006	40	10
Initial costs(\$/kW)					
PCS	153	165	153	215	173
BOP	50	100	50	100	100
Storage	60	315	60	1.258	315
O&M cost(\$/kW-year)					
Fixed	7.3	16.5	7.3	43.5	17.6
Variable	6.7	7	6.7	6.9	6.5

OVERVIEW OF ENERGY STORAGE SYSTEMS

NPV disposal costs(\$/kW)	1.3	0.8	1.3	1.8	1.4
Total Capital Cost (M\$)	2.6	5.8	2.6	15.7	5.9

Table 4 Lead-Acid Cost per Application Source:[1] est.2004\$

Maturity	Capacity(MWh)	Power (MW)	Duration (h)	Efficiency	Lifetime (cycles)	Total cost (\$/kW)	Cost (\$/kWh)
Grid support (ancillary services) and integration of intermittent renewables							
Commercial	200	50	4	85-90	2200	1700-1900	425-475
Commercial	250	20-50	5	85-90	4500	4600-4900	920-980
Demonstration	400	100	4	85-90	4500	2700	675
Grid Support and Power Quality							
Demonstration	0.25-50	1-100	0.25-1	75-90	>100 000	950-1590	2770-3800
Transmission and Distribution Support							
Demonstration	3.2-48	1-12	3.2-4	75-90	4500	2000-4600	625-1150

Table 5 Advanced Lead-Acid Total Costs Source:[1] est.2010\$

Table presents different applications for Lead-Acid technologies and the various expenses associated with these technologies. In the table, PCS stands for Power Conversion System and BOP is Balance of Plant (infrastructure and facility cost). Fixed stands for labor and parts, the variable, is the cost of consumables.

$$InitialCost = (PCS + BOP + Storage) * Power \tag{1}$$

Table presents examples of Advanced Lead-Acid total cost with installed size, capacity, duration efficiency and lifetime cycles.



Figure 6 Lead-Acid Technology around the world[16]

Figure 6 shows the world distribution of the Lead-Acid Battery technology. As it can be expected from such a mature technology, it is spread all around the world. According to [16] this technology nowadays is performing in a wide variety of actions where most of these actions are connected with the integration of RESs to the grid or help regulation. Of course, many sites have been decommissioned or are about to be changed with Lithium-Ion technology.

2.2.2 Lithium - Ion

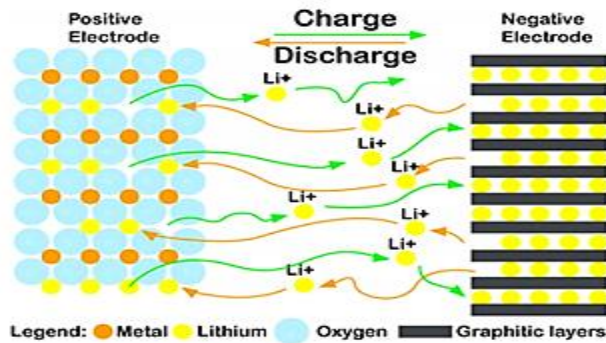


Figure 7 Li-Ion Battery [Utility Scale Energy Storage]

A less mature technology than Lead-Acid. Research into this technology began in the 1970s, but only recently (2000s) this technology has become interesting for utility functions. As it can be seen from Figure , this technology consists of a Metal-Oxide positive electrode and a negative carbon electrode. The electrolyte consists of ether and Li-ions. During charge, the Li-ions move from the positive electrode to the negative. During discharge, the reverse occurs [1].

This technology is characterized by good response time, small size and weight. On the downside, the depth of discharge plays a major role in the overall battery performance, and an external control is needed to manage the battery’s operation[17].

Power (MW)	Efficiency	Lifetime (cycles)	Power cost (\$/kW)	Energy Cost (\$/kWh)	Annual operating cost (\$/kW-yr)	Fixed O&m cost (\$/kW)	Variable O&M cost(\$/kW)
<10	85-95	2000-3000	400 - 1000	500 - 1500	25	0.46	0.7

Table 6 Li-Ion general costs Source:[1]

Maturity	Capacity(MWh)	Power (MW)	Duration (h)	Efficiency	Lifetime (cycles)	Total cost (\$/kW)	Cost (\$/kWh)
Power quality, intermittent renewables integration							
Demo	0.25-25	1-100	0.25-1	87-92	>100 000	1085-1550	4340-6200
Time shift, transmission and distribution support							
Demo	4-24	1-10	2-4	90-94	4500	1800-4100	900-1700

Table 7 Li-Ion Total Costs Source:[1]



Figure 8 Lithium-Ion technology around the world [16]

Figure 8 presents a world view of the distribution of the Lithium-Ion technology. At first glance, it is noticed that this technology is more popular than Lead-Acid technology. This can be due to the low self-discharge rate and the high energy density that this technology presents. The uses of the Lithium-Ion technology around the world are many. Some of the biggest projects perform frequency regulation (South Korea, 48MW, 12MWh), residential energy storage (Germany, 42MW, 21MWh), RES integration (Japan, 40MW, 20MWh)[16]

2.2.3 Vanadium Redox

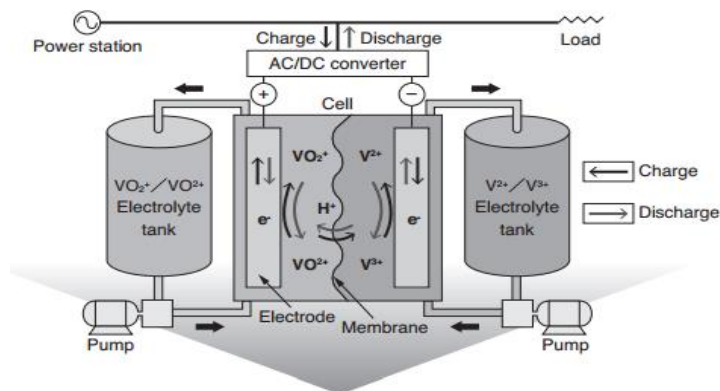


Figure 9 Vanadium Redox Battery Source: [Redox Flow Battery]

This battery is a redox flow battery. The energy and power of such a battery depend on the volume of the electrolyte and the area of electrodes respectively. This technology is as old as the Li-ion battery technology, with NASA starting research on it in the 1970s. The working principle of such a technology is shown in Figure 9. The battery consists of 2 reservoirs that are filled with electrolyte. During a discharge cycle, V^{2+} is oxidized, and an electron is released. During charging an electron is accepted by VO_2^+

and is reduced to VO^{2+} . Also as it can be seen, hydrogen is exchanged in the cell, which is done to keep the neutrality of the charge. The cross diffusion leads to losses for the cycles unless both sides contain vanadium, then there are no losses. VRB is characterized by a long cycle life, but a lowered efficiency, mainly due to the different systems present, like pumps and membranes.[1, 18, 19].

	EET-S [10hr]	TIS/DIS+Regultaion	Renewables EET-S + Regulation	Short Duration PQ + EET-S+Regulation
Capacity (MWh)	100	90	90	67
Initial costs(\$/kW)				
PCS	397	466	466	311

BOP	100	100	100	100
Storage	2125	2125	2125	1417
O&M cost(\$/kW-year)				
Fixed	54.8	56.1	56.1	38.8
Variable	7	-	-	1.9
Total Capital Cost (M\$)	26.2	26.9	26.9	18.3

Table 8 VRB cost per application Source: [1]

Maturity	Capacity(MWh)	Power (MW)	Duration (h)	Efficiency	Lifetime (cycles)	Total cost (\$/kW)	Cost (\$/kWh)
Grid support and integration of intermittent renewables							
Demo	250	50	5	65-75	>10000	3100-3700	620-740
Time shift, transmission and distribution support.							
Demo	4-40	1-10	4	65-70	>10000	3000-3310	750-830

Table 9 VRB cost by Benefit Source :[1]



Figure 10 Global Distribution of Vanadium-Redox Technology[16]

Figure 10 presents a global overview of the distribution of Vanadium-Redox Technology. Compared to the previous two technologies, it can be seen that here the Vanadium-Redox is mostly installed in America, Central Europe, China, and Japan. Some of the biggest Vanadium-Redox projects include a 15MW/60MWh storage system mounted on the island of Hokkaido, Japan and is used for solar integration. A 5MW/10MWh storage system located in Shenyang, Liaoning, China is used for guaranteeing the security and reliability of the GuoDian LongYuan Wind Farm during its operation (power-smoothing, voltage and frequency regulation, active power output). Most of the Vanadium-Redox systems are used to help support the RES systems.[16]

2.2.4 Compressed Air Energy Storage (CAES)

This storage system uses a cavern, usually salt mines. When charging, an electric motor compresses air and pumps it into the cavern. When there is a need for the energy, the air is released through an expansion turbine and combusted to drive a generator. This technology combines many different devices, and that is why the overall efficiency is around 40%. Compressing the air increases the temperature and thus a cooling system must be installed. To generate power, the air must be heated, usually with gas burners, which supply the larger portion of energy that will be converted into electrical energy. This system has a few variations when it comes to the utilization of the process heat needed from the combustion turbine. Diabatic CAES uses only the gas burner and can also recover the heat from the air after the combustion turbine to heat the air that is about to enter the combustion turbine. Adiabatic CAES does not use a gas-burner, but the heat that is produced during the air compression stage. Regarding capacity, such a system is only limited by the size of the cavern, and if there is not one present, an aboveground CAES can be considered (air is stored in human-made vessels) though the capacity of such a system is smaller than when using a natural cavern.[1, 20]

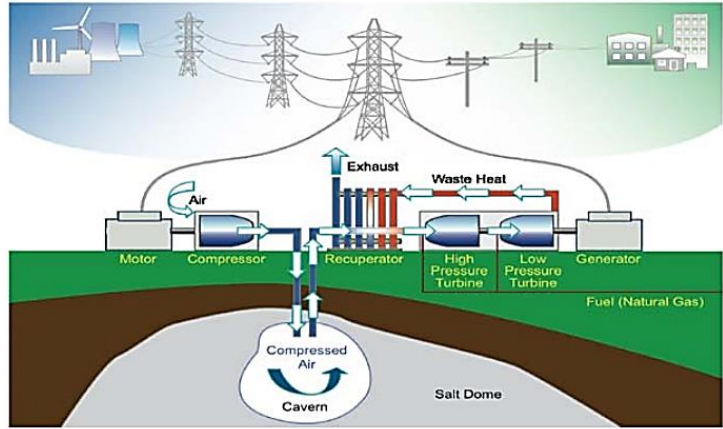


Figure 11 CAES Source [1]

	Small 10MW CAES			Bulk 300 MW CAES		
	EET-S [3/10 hrs]	Renewable EET-S	Renewable Forecast Hedging	EET-S (10 hr)	Renewable EET-S	Renewable Forecast Hedging
Capacity (MWh)	30/100	100	50	3000	3000	1500
Initial costs(\$/kW)						
Combustion Turbine	270/270	300	300	270	300	300
BOP	160/160	200	200	170	210	210
Storage	120/400	400	200	10	18	18
O&M cost(\$/kW-year)						
Fixed	19/24.6	31	27	13	23.6	23.6
Variable	4.7/65	21.9	7.9	58.8	13.1	4.5
Total Capital Cost (M\$)	5.5/8.3	9	7	135	158.3	158.3

Table 10 CAES Cost per application Source:[7]

Type	Size	Maturity	Capacity (MWh)	Power (MW)	Duration (h)	Lifetime (cycles)	Total cost (\$/kW)	Cost (\$/kWh)
Grid support and integration of intermittent renewables								
CT-CAES (underground)	Small	Demonstration	1400-3600	180	8	>13 000	960	120
	Large	Demonstration	1400 - 3600	180	20	>13 000	1150	160
CT-CAES (underground)	Small	Commercial	1080	135	8	>13 000	1000	125
	Large	Commercial	2700	135	20	>10 000	1250	60
Time shift, capacity credit, transmission and distribution support								
CAES (aboveground)	Small	Demonstration	250	50	5	>10 000	1950-2150	390-430

Table 11 CAES Total Costs Source: [7]



Figure 12 CAES world distribution

From Figure 12 it can be seen that this technology is not as popular as the electro-chemical one. All the projects that [16] has information for are located in USA and Europe (2 UK, 2 Germany, and 1 Switzerland). This may be due to the low efficiency and geographical conditions. On the other hand these projects have high Power: Larne, County Antrim, United Kingdom-Generation:330MW/Demand during compression cycle:220MW, Große Hellmer 1E, Elsfleth, Germany – 321 MW, used to absorb night power from the nearby nuclear power plant, one of the caverns is reserved for black-start if the nuclear power plant needs it. Also, two new projects are announced in America with around 300 MW power output each.[16]

2.3 Heat storage

The heat storage technology allows for storing of heat energy for hours, days or even months. This can be done through the use of different materials that change their phase, chemicals or even simple heat storage by the heating material. It is also important to mention that heat storage could also mean

changing electrical energy into cold energy (mostly used for refrigeration purposes). Around half of the total energy demand for the entire world is heat energy. In the future, this value is likely to decrease due to higher energy efficiency. In Denmark's future, where RES will have higher influence, heat storage will play a major role in supply and distribution of thermal energy [21].

2.3.1 Aquifer Thermal Energy Storage (ATES)

This technology uses an underground reservoir to store hot and cold water. As you can see from Figure 13, during the summer, the cold water reservoir is used to cool down the building, and in return, the hot water reservoir is used to heat the building in the winter. There are two modes, a cyclic mode where the wells are switched seasonally and a continuous mode where the wells are not switched. This technology falls under the sensible heat storage category.[22]

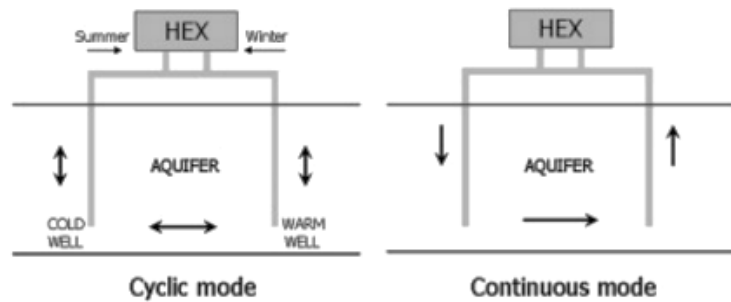


Figure 13 Aquifer Thermal Energy Storage [14]

2.3.2 Pit Thermal Energy Storage (PTES)

Relatively mature energy storage technology is going back to the 1980s and is mainly used for seasonal storage. This technology has been developed by the Danish Technical University (DTU) and since 1995 various demonstration storages have been created with pit sizes from (1 500 m³ to 200 000m³). The largest pit storage in Denmark is located in Vojens and is partnered with a 70 000 m² solar heating plant and is currently used to cover the heating needs of 2000 consumers (45% of consumption is covered). PTES is an excavated area the inside and bottom of which is covered with a special material called High-Density Polyethylene (HDPE). The lid is created from the same material, and it floats on the surface for the pit to be always covered while the water levels are changing. This technology falls under the category of latent heat storage. Figure 14 is an aerial photograph of the Vojens PTES.[21, 23, 24]



Figure 14 PTES Vojens, Denmark Source [The world's largest solar heating plant to be established in Vojens, Denmark]



Figure 15 Heat Storage distribution around the world [16]

No information could be found in particular locations for PTES and ATES (besides Denmark). Figure 15 presents different kinds of Heat Storage technologies all over the world – most are Chilled Water and Ice Thermal Storage which are not very useful in a country like Denmark. Also, not applicable to Denmark, are technologies from the last heat storage category, phase changing materials heat storage. Technologies that fall under this category are the Molten Salt Storage and Storage of Heat with the use of a parabolic trough (curved mirror).

From Figure 15, it can be seen that the Heat Storage is very popular around the world, especially in countries with higher average temperatures and stronger solar radiation throughout the year. Same as with the CAES, the power of such projects is immense, 280 MW Solar Power Plant that uses parabolic trough to store heat located in Gila Bend, Arizona, United States, and a 160 MW power plant that utilizes the Molten Salt Storage technology based in Morocco are amongst the biggest currently operational Heat Storage systems.[16]

2.4 Power-to-Gas (PtG)

This storage technology presents another method of storing electricity in the form of chemical energy. This subchapter focuses on the production and utilization of hydrogen (H₂) and methane (CH₄) Compared to other technologies explained so far, the PtG technology allows for some level of freedom when it comes to utilizing the gas product. The gas can be used for fueling transport vehicles, central heating or it can be transformed back into electricity and help by supporting of the electrical grid. Various PtG systems are either in operation or are still in a Research and Development (R&D) phase but are expected to appear on the market shortly. A few examples are Alkaline Electrolysis (AE), Proton Exchange Membrane (PEM), Chemical and Biological Methanation.[20, 25]

Figure 16 shows the role of PtG in the Danish Power Grid[25].

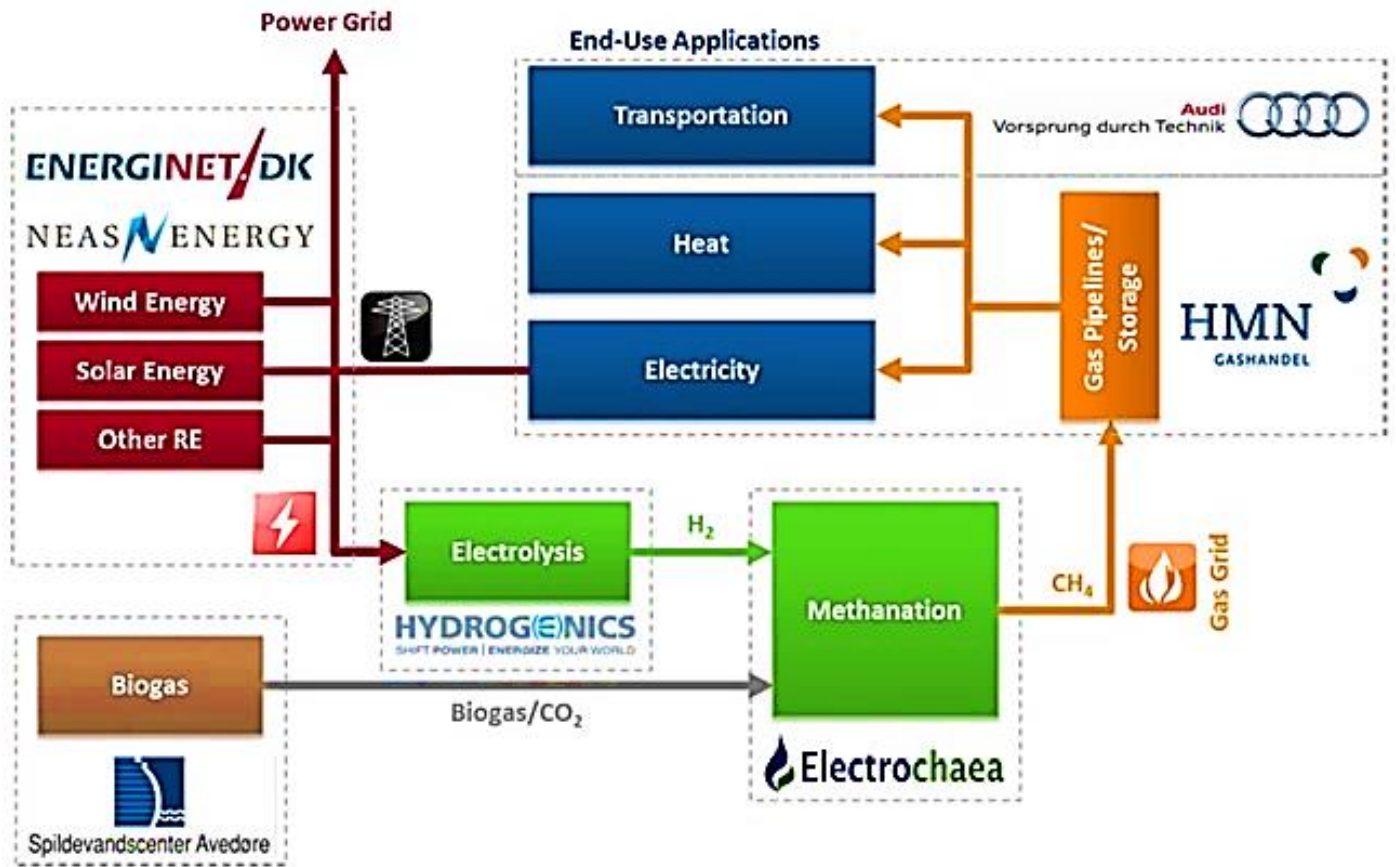


Figure 16 Role of Power - to- Gas in the Danish Grid Source:[17]

2.4.1 Alkaline Electrolysis (AE)

As stated in [20], Electrolysis is a chemical decomposition that is originated from the interaction between electric current and water. This process requires highly pure water with removed minerals and ions. After that, an electric current is applied with the help of which the deionized water is split into hydrogen and oxygen.



Seen from an electrical point of view, the applied DC is the cause of surplus electrons on the cathode and not enough electrons on the anode. The process of a positively charged electron passing from the cathode to the anode, in the water, results in the forming of hydrogen and oxygen. It is also important to mention that the amount of hydrogen that can be added to the natural grid network depends on the content of the natural gas and varies from location to location. [20]

Alkaline electrolysis is a mature technology with a low cost and high durability. The anode and cathode are usually of nickel-plated steel and steel. Hydrogenics do R&D to improve electrolyzers for use in the power-to-gas market.[26]

Table 13 shows the evolution of this technology for years 2011, 2015 and 2020 translated from German to English.[27]

	2011	2015	2020
Delivery Pressure (bar)	<30	60	60
Power Density (kA/m ³)	2-4	<6	<8
Cell Voltage (V)	1.8-2.4	1.8-2.2	1.7-2.2
Load Density (W/cm ²)	1	1	2
Cell Surface max. (m2)	4	4	4
Efficiency (%)	62-82	67-82	67-82
Maturity	Commercial		
Power Consumption per stack (kWh/Nm ³ H ₂)	4.2-5.9	4.2-5.5	4.1-5.2
Power Consumption per system (kWh/Nm ³ H ₂)	4.5-7	4.4-6	4.3-5.7
Production rate H ₂ per stack (Nm ³ /hr)	760	1000	1500
Capacity rate per system (kWe)	3800	5000	7000
Lifetimer (hrs)	90000	90000	90000

Table 13 Alkaline Electrolysis technology evolution Source:[16]

2.4.2 Proton Exchange Membrane (PEM)

Another method for performing electrolysis is through the use of a PEM. Figure 17 shows a general view of this technology. The liquid is transported in the cell, which is gas and water proof. The cell has an anode and a cathode which are in charge of producing oxygen and hydrogen respectively. This technology is still in R&D but already there are plans for significant investments

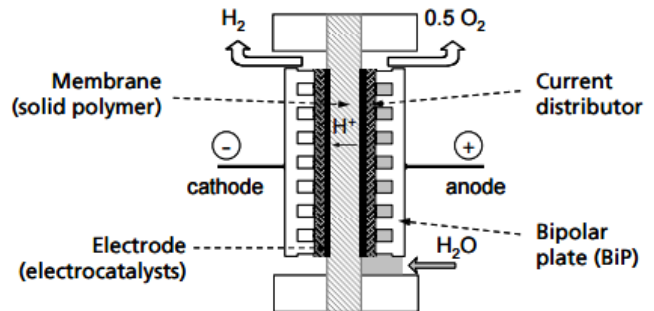


Figure 17 PEM Source:[16]

in the MW scale, which are expected to cost less than alkaline electrolysis.[20]

Table 14 shows the evolution of this technology for years 2011, 2015 and 2020 translated from German to English.[27]

	2011	2015	2020
Delivery Pressure (bar)	<30	60	60
Power Density (kA/m ³)	6-20	10-25	15-30
Cell Voltage (V)	1.8-2.2	1.7-2	1.6-1.8
Load Density (W/cm ²)	4.4	5	5.4
Cell Surface max. (cm ²)	300	1300	5000
Efficiency (%)	67-82	74-87	87-93
Maturity	R&D - Pre - commercial		
Power Consumption per system (kWh/Nm ³ H ₂)	4.5-7.5	4.3-5.5	4.1-4.8
Production rate H ₂ per system (Nm ³ /hr)	30	120	500
Capacity rate per system (kWe)	150	500	2000
Lifetimer (hrs)	20000	50000	60000

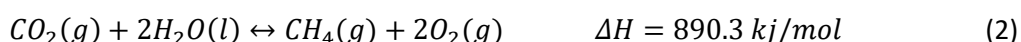
Table 14 PEM technology evolution Source:[16]

2.4.3 Chemical Methanation

Another way of creating Synthetic Natural Gas (SNG) is through the process of methanation. Worldwide around 80 % of the energy produced comes from fossil fuel plants. This process increases the amount of CO₂ emissions in the air, making it dangerous for the climate of the planet and life of humans. One way to reduce the carbon dioxide emissions is by combining the H₂ gas obtained from electrolysis and the CO₂ gas, as shown in equation (3):



Equation (3) is called the Sabatier reaction. Using (2) and (3) gives us:



Using atmospheric CO₂ allows for the methanation plant to be independent of sources of CO₂, which allows building such a plant at a better location. Unfortunately, this process has low efficiency, due to the low number of particles in the air (around 390 parts per million). Thus according to [28], it is more efficient to use CO₂ from concentrated sources like biomass for example.[20, 29, 30]

Chemical methanation occurs through the utilization of a catalyst, which in most cases is Nickel (Ni) due to cost reasons. The process works in two temperature ranges:200-550 and 550 -750 °C.[20] Table 15 shows the characteristics of this technology:

Characteristic	Value
Process temperature (°C)	200-750
Delivery pressure (bar)	4-80
Max. Production capacity (MW _{CH₄})	<500
Maturity	Commercial
Catalyst cost (euro/kg in 2013)	250
Lifetime catalyst (h)	24 000
Deployment time (min)	<5
Cold start time	hours
Methanation efficiency %	70-85

Table 15 Chemical Methanation Characteristic Source: [20, 28, 31]

2.5 Technology Comparison

So far, the three types of technologies that are useful in Denmark, given its geographical situation, have been presented. Most different types of storage are contained in the Electrochemical Energy Storage section. After that is the Heat Storage and the Gas Energy Storage. These technologies have different working principles, explained in 2.2, 2.3 and 2.4, and can help the power system in various ways. For example, the Electrochemical Storage is fast-acting and can help with power regulation, energy time shift, etc. The Heat and Gas Storage have bigger sizes and a high Technology Readiness Level (TRL), where high TRL means technology is well-known and mature, and a low TRL implies that technology is new and often in the phase of basic research [32] . The sensible heat storage also possesses a high TRL level but cannot be used to help with the problem of surplus power.

In order to tackle the problem with raised in Chapter 1, regarding the security of supply and the surplus power, a fast acting Storage System is needed. Such a system can be found by examining the population of the Electrochemical Energy Storage family.

Table 16 Electrical Energy Storage Project Sizes

Lead-Acid		Lithium-Ion		Vanadium-Redox		CAES	
Power	Energy	Power	Energy	Power	Energy	Power	Energy
[MW]	[MWh]	[MW]	[MWh]	[MW]	[MWh]	[MW]	[MWh]
50	200	1-100	0.25-25	50	250	180	1400-3600
20-50	250	1-10	4-24	1-10	4-40	135	1800
100	400					135	2700
1-100	0.25-50					50	250

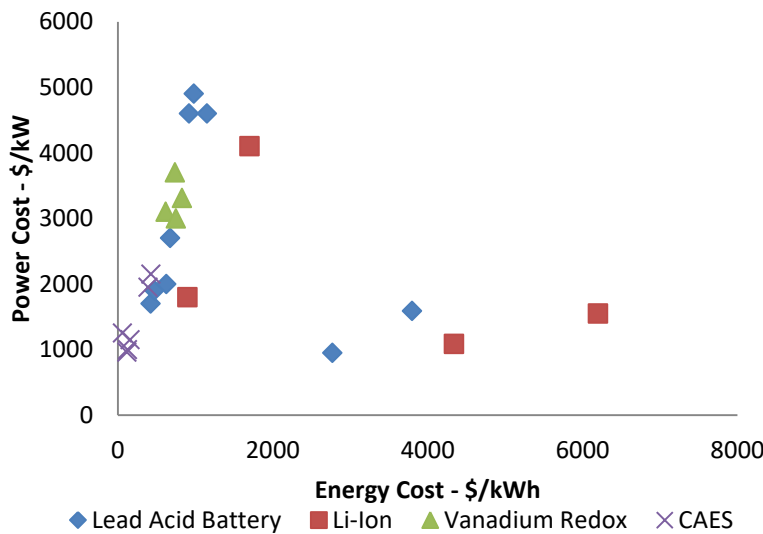


Figure 18 Energy-Power Costs

Application matrix				
	LA	Li-Ion	VRB	CAES
EET-S	-	X	X	X
ESC	-	-	-	-
FH	-	-	-	X
Regulation	X	X	X	-
VS	X	-	X	X
BS	-	-	-	-
TUD	X	X	X	X
TCR	X	X	X	X
DUD	X	X	X	X
PQ	X	X	X	X
PR	-	-	-	-

Table 17 Application Matrix

Table 16 is a comparative table between different storage systems and the energy capacity and power that was achieved. Figure presents the costs of reaching the needed capacity and electricity (\$/kWh and \$/kW respectively). Table is an application matrix presenting the applications. discussed at the beginning of this chapter and have been compared to different ESS technologies. The “X” marks that research have been done into a certain technology and “-” means that the no research has been done into whether that technology can perform certain actions or the technology is just not suitable.

Service that is needed for the future: As it can be seen from Table 17, a lot of R&D has been done by utilizing storage systems for different applications. Storage systems are helping with frequency regulation, time shifting, upgrade deferral, etc. It can also be seen that there is a need for research into the ESC (ESC differs from EET-S with longer discharge duration and fewer cycles per year) and PR. This is the reason why this master thesis will focus on theoretical research into utilizing the market available ESS technologies for ESC and PR applications that will help with the surplus power problem incurred from a large number of RES.

Electrical Energy Storage Systems: From Table 16 and Figure 18 it can be seen that projects with the “battery type” ESS can achieve a power output between 1 and 100 MW (max.50MW for VRB) and store energy between 0.25 and 400,25,250 MWh for LA, Li-Ion and VRB respectively. It is also noticeable that CAES achieves better power (50 – 180 MW) and energy capacity (250-3600 MWh). Using Figure 18, it is also noticed that the CAES achieves better results in the price per kW and kWh. The projects utilizing VRB keep their price per kW and kWh steady around 3100-3700 \$ per kW and 620-830\$ per kWh. The Li-

Ion battery prices for power and energy capacity depend on the service that it is built for – Power Quality and Integration of Renewables has a higher energy cost, while Time Shift, Transmission, and Distribution Support have a higher power cost. The same can be said to be true for the Lead – Acid batteries, prices for power and energy depend on the service provided. Many factors play a role in the price of equipment, location country, etc. It is important to mention that these prices are guidelines and are used to help make the best decision when choosing the ESS that will perform ESC and PR in our hypothetical case.

Heat Storage Systems: Given the geographical location of Denmark and that by the year 2050 the government wants 100% of energy production to come from renewable systems, some thought must be put into how the population will keep their homes warm throughout the year. One way is to store energy in the form of heat in the summer and use it later in the winter. Another solution is to simply use electrical heaters in the winter, though that solution presents an increase in the electrical loads and inevitably large portions of the Distribution network will have to be upgraded. Another solution is to simply use the existing gas network and use the gas created from the PtG system to supply Gas Powered Generators with fuel. From there the gas can be used for heating or, given the fast response time of GPG, for regulation. Even more, the PtG process can be used to supply transportation fuel and can even be stored, and if need be, it can be used to help the Electric Grid.



Figure 5 PtG distribution around the world[16]

Figure 19 presents the location of PtG projects around the world. As it can be seen, the Power2Gas is not that popular around the world. Projects are located in Central Europe, and a 2MW project is in the process of being created in Toronto, Canada. The biggest working project is located in Falkenhagen, Brandenburg, Germany and is used for renewables capacity firming. This project is a demonstration of the entire process chain in creating gas from power (wind power, electrolyzer, gas treatment measurement and injection of hydrogen into the gas grid). The rated power is 1 MW[16].

2.6 Conclusions

In this chapter, different functions for electrical energy storage technologies have been presented and their attributes have been discussed. It was found that electrochemical technologies are used widely around the world to help the power grid with the integration or RES. It was also found that these

techniques, as mature as may they be, still have a quite high price range. It was also found that the electro-mechanical storage systems are not as widely popular worldwide, but on the other hand, have significant power outputs. A conclusion can be made that in a 100% RES future a good way to support the population with reliable electricity and heat is a combination between RES, electrical storage system, and a PtG system. The gas produced from the PtG can be used in a variety of ways from burning it in GPG to help with power system regulation, storing it and when the community needs to be heated it is burned to providing the transport sector with fuel [5, 6].

Chapter 3 Power System with Renewables

The following chapter presents the electrical power system in which the ESS is installed. An explanation on the simulation methods for different facilities in that power system has also been provided.

3.1 Grid Layout

The following sub-chapter gives information about the data used for simulations in this thesis. Figure 20 presents the general idea about the elements in the studied system. From there it is seen that the ESS is put between the electrical substation (or grid) and the consumers. The power grid presented below works at 66 kV. The distances between bus bars are shown below, and information on the cable connecting the bus bars can be found in [33].

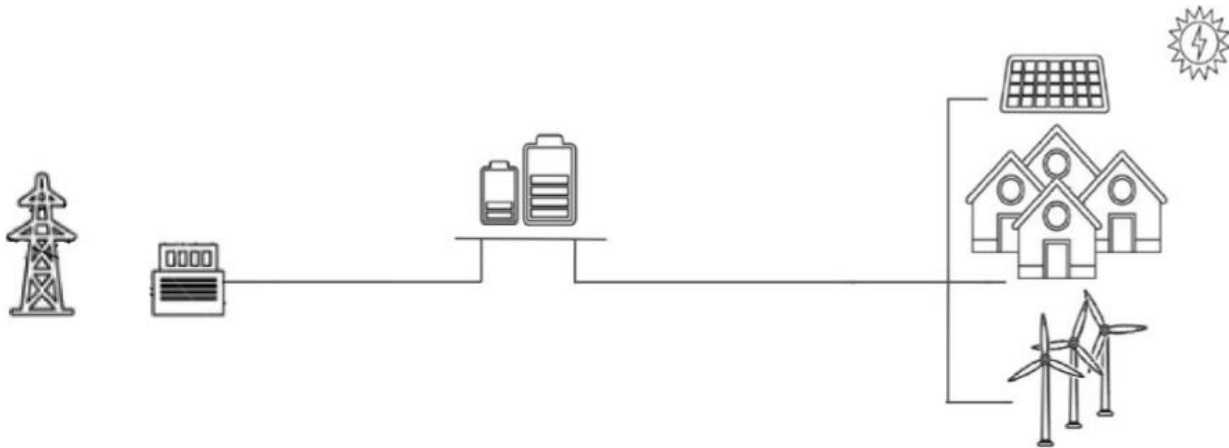


Figure 20 Grid layout Source:[34]

The grid in Figure 20 consists of electrical consumers, ESS and RES (Wind Turbines and Photovoltaics). The consumption data has been obtained from [35] and is given in 15-minute intervals, which due to computing difficulties has been averaged into hourly intervals.

To simulate the working process for the RES, weather data matching the time interval of the consumption data and the geographical location is needed. The wind power generation is determined by the air density and wind speed. Such data is obtained from [36] in the form of hourly intervals. The hourly solar irradiance and the temperature has been obtained from [37] to simulation the PV power output. As a last hourly electricity price data has been obtained from [38].

A program by the name of ESSPC (ESS and PtG Coordinator), has been developed in MATLAB. All the results and figures that are presented further on have been obtained through it. A short manual for this program is in Appendix A including the steps needed to calculate other cases.

3.2 Electrical Demand

Figure 21 represents the electrical demand by the consumers in the grid. This is the demand profile for which the storage system is sized, and the RES have to cover.

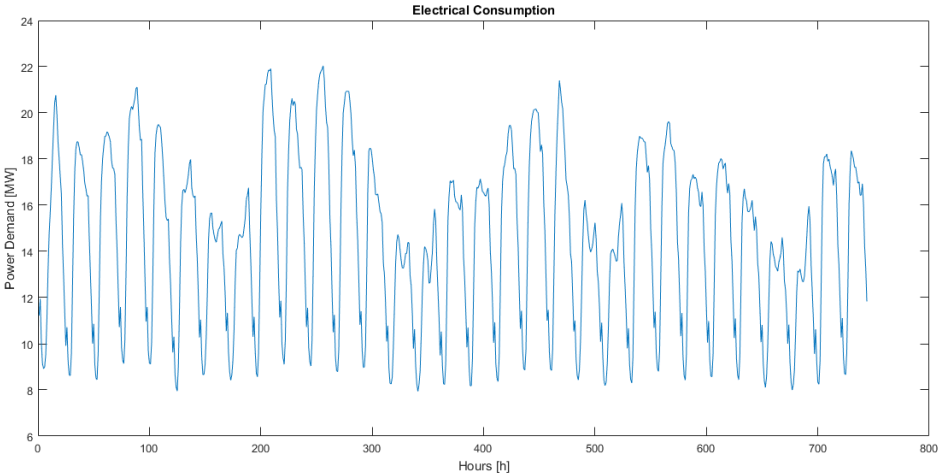


Figure 21 Electrical Demand Consumers

The data presented consists of hourly load demands for the month of March 2015. It is seen that the demand fluctuates from as low as 8 MW to as high as almost 22 MW. The dataset starts from the 1st of March at 00:00, which means that each upward spike represents daytime demand and every valley is nighttime demand, which judging by the graph almost does not change in the course of the month. Each five high spikes are followed by two smaller spikes. Thus it is safe to assume that these seven spikes form the demand for a week. Also, because the power demand is so high in the daytime during the week, we can be confident that the area this profile belongs to is either a city center area, or an area dominated by office buildings and thus support of it is vital to the economy of the city.

3.3 Wind Turbine Modelling

In this sub-chapter, the equations for simulating a Wind Turbine are presented. Using [39] the following formula is used for each datapoint ‘m’:

$$P_{g,wt}^{(m)} = C_{p,wt}^{(m)} * 0.5 * \rho^{(m)} * A^{(m)} * V^{(m)^2} \tag{5}$$

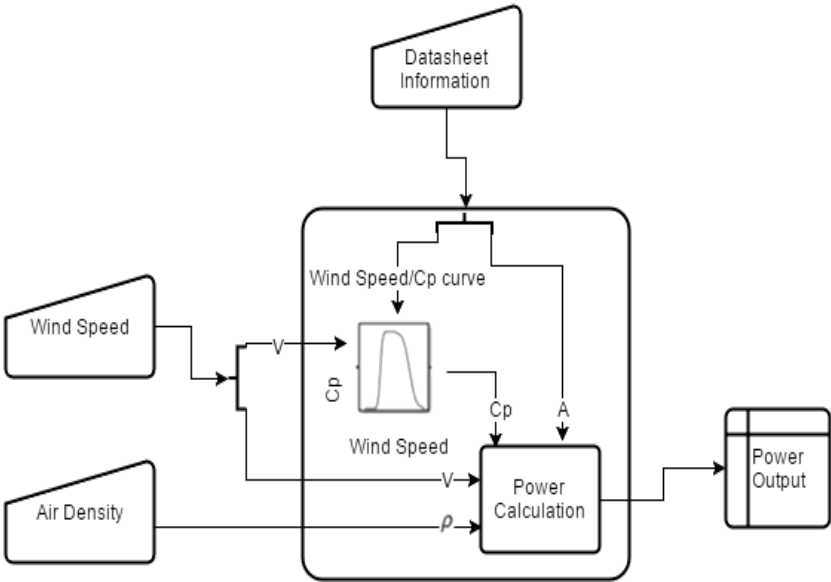


Figure 21 Wind Turbine Simulation

From the datasheet of the wind turbine the wind speed to coefficient of performance of the wind turbine ($C_{p,wt}$) is needed, a curve that shows how the $C_{p,wt}$ changes according to the wind speed. After interpolating the new $C_{p,wt}$ the power output can be calculated. The wind speed to power curve from the datasheet is also used by the program but not in the calculations rather than for visualization of what the manufacturer says the turbine

should produce at different wind speeds. More information on how these curves are represented in ESSPC can be seen in Appendix A.

3.4 Modelling of Photovoltaic Modules

This sub-section presents the mathematical equations used for the PV system [40, 41]:

$$I_p^{(m)} = I_{sc}^{(m)} * [1 - C_1^{(m)} * (e^{(V_p^{(m)}/C_2^{(m)} * V_{oc}^{(m)})} - 1)] \quad (6)$$

Where I_p is the output current and V_p is output voltage and C_1 and C_2 are coefficients obtained through the following equations:

$$C_1^{(m)} = \left(1 - I_{mpp}^{(m)}/I_{sc}^{(m)}\right) * e^{(-V_{mpp}^{(m)}/C_2^{(m)} * V_{oc}^{(m)})} \quad (7)$$

$$C_2^{(m)} = \frac{(V_{mpp}^{(m)}/V_{oc}^{(m)} - 1)}{\ln(1 - I_{mpp}^{(m)}/I_{sc}^{(m)})} \quad (8)$$

In (7) and (8), C_1 and C_2 depend on the following parameters : Short-circuit current [I_{sc}], Open circuit voltage (V_{oc}), Maximum power point voltage [V_{mpp}] and Maximum power point current [I_{mpp}].

$$I_{sc}^{(m)} = I_{scs} * (G^{(m)}/G_s) * [1 + \alpha * (T^{(m)} - T_s)] \quad (9)$$

$$V_{oc}^{(m)} = V_{ocs} + \beta * (T^{(m)} - T_s) \quad (10)$$

$$I_{mpp}^{(m)} = I_{mpps} * (G^{(m)}/G_s) * [1 + \alpha * (T(m) - T_s)] \quad (11)$$

$$V_{mpp}^{(m)} = V_{mpps} + \beta * (T(m) - T_s) \quad (12)$$

I_{scs} , V_{ocs} , I_{mpps} and V_{mpps} are provided from the manufacturer for defined standard test conditions (STC). G_s is the reference solar irradiance and T_s is the reference ambient temperature ($G_s=1000[\text{W}/\text{m}^2]$ and $T_s=25^\circ\text{C}$). α is the current temperature coefficient [$\%/^\circ\text{C}$] and β is the voltage temperature coefficient [$\%/^\circ\text{C}$]. Both are given by the manufacturer. G and T are the solar irradiance and the ambient temperature respectively, and are the input values for the PV model.

According to [40], to increase the accuracy, (9) and (11) must be changed:

$$V_{oc}^{(m)} = V_{ocs} + \beta * (T^{(m)} - T_s) - \Delta V^{(m)} \quad (13)$$

$$V_{mpp}^{(m)} = V_{mpps} + \beta * (T(m) - T_s) - \Delta V^{(m)} \quad (3)$$

Where ΔV is the voltage variation accounted to the solar irradiance

$$\Delta V^{(m)} = V_{ocs} - V_{ocg} \quad (4)$$

V_{ocg} is the open circuit voltage at G

$$V_{ocg} = C_2^{(m)} * V_{ocs}^{(m)} * \ln \left[1 + (1 - I_{scg}^{(m)} / I_{scs}) / C_1 \right] \quad (5)$$

Where I_{scg} is the SC current at G

$$I_{scg}^{(m)} = I_{scs} * (G^{(m)} / G_s) \quad (6)$$

Through the use of (6) → (17), the I-V curve for a given technology can be found for different atmospheric conditions (G and T).

In (2), V_p is the output voltage of the module. The equations up until now are used for simulation of I-V curves for different PV technologies. In MATLAB by simply varying V_p or I_p , I_p or V_p can be calculated respectively. In order to obtain the power P, produced by the module ($P = V_p * I_p$), an assumption must be made regarding V_p .

From [42] the equations for obtaining the voltage of a PV module as a function of the ambient temperature are presented below.

Power produced from a solar module is dependent on its temperature. With an increase in the temperature of the solar module, the current produced increases exponentially, while the voltage is decreased. The higher the temperature of the solar module, the worse the power output is [43].

According to [42], the voltage of a solar module is:

Coldest day of the period

$$V_{max} = (1 + \Delta T * \beta) * V_{ocs} \quad (7)$$

$$\Delta T = T - T_s \quad (8)$$

Hottest day of the period

$$V_{min} = (1 - \Delta T_{emp} * \gamma) * V_{mpps} \quad (20)$$

$$\Delta T_{emp} = (NOCT - NOCT_s) + T \quad (21)$$

where, γ is the power temperature coefficient [%/°C], NOCT is the Nominal Operation Cell Temperature and $NOCT_s$ is the ambient temperature STC value for which NOCT is given. All values are given by the manufacturer.

To obtain V_p , $V_{max}^{(m)}$ and $V_{min}^{(m)}$ need to be obtained as a function of $T^{(m)}$.

$$V_p^{(m)} = \frac{V_{max}^{(m)} - V_{min}^{(m)}}{2} \quad (22)$$

After obtaining V_p , I_p can be found and after that the, power produced by the module is found:

$$P_{g,pv}^{(m)} = I_p^{(m)} * V_p^{(m)} \quad (23)$$

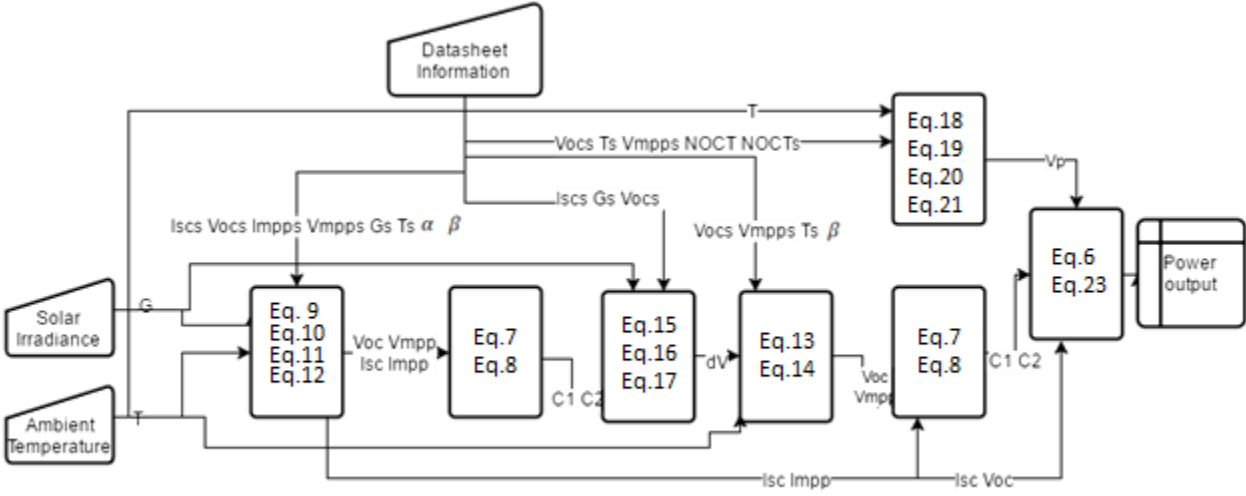


Figure 22 Model framework of PV module

Figure 22 presents the steps and accompanying equations that are performed to simulate the power output of the PV module. First V_{oc} , V_{mpp} , I_{sc} and I_{mpp} are calculate via (9),(10),(11) and (12). After that those values are passed over to be calculated via (7) and (8). As it was mentioned before, the accuracy of (9) and (11) can be increased by changing them. That is done through first finding dV via (15),(16) and (13)and afterwards calculating (13) and (14) which are the transformed (9) and (11). V_{oc} and V_{mpp} are calculated with the use of (7) and (8) again. The next step that is taken is to calculate V_p using (14),(15),(16) and (17). I_p is calculated with the use of (6) and then both I_p and V_p are passed on to (23) which calculates the power outputted by the module for the particular data point “m”. These actions are repeated for every data point of Solar Irradiance and Ambient Temperature that is procured.

3.5 Renewable Power Generation

As explained before, the power system uses two different RES, wind turbines, and photovoltaics. The purpose of this sub-section is to present information on the RES used and simulation results.

3.5.1 Wind Power

Three different wind turbines have been considered for installation in the power system. The Bonus 2300/82.4, NEG Micon 2000/72 and the Nordex N90/2300. Further on in this work, these machines are named Wind Turbines type 1, 2 and 3 respectively.

Error! Reference source not found. presents the power production profile for the first type of turbine in he timeframe of interest, the month of March 2015. Detailed information on how the data is collected and used can be found in Appendix A.

The left y-axis represents the power produced from Wind Turbine type 1 in [kW] and the right axis gives us information on the wind speed, in [m/s]. **Error! Reference source not found.** presents how the power

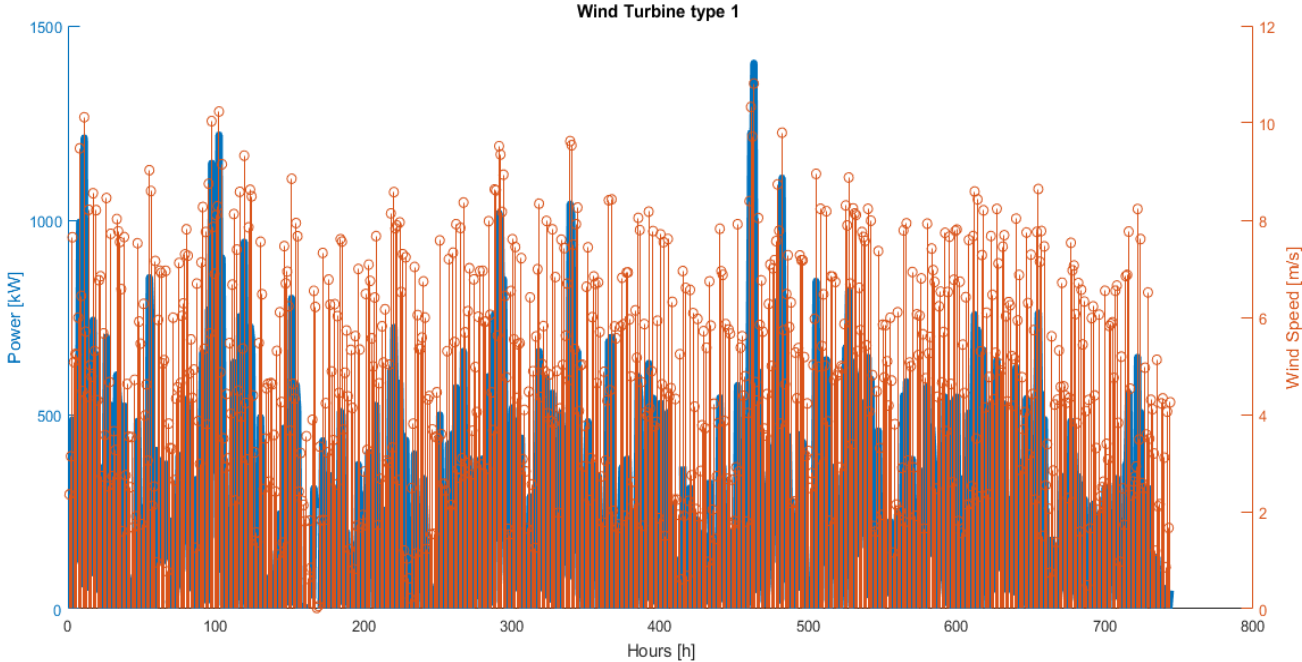


Figure 23 Wind Turbine type 1 power production with wind speed

roduction changes with regards to the wind speed. It can be noticed that the wind speed is mostly in the 4[m/s] to 9 [m/s] window. It can also be seen that the turbine power production fluctuates and produces around 250 [kW] low to as high as 1400 [kW]. To understand the reason for this behavior,

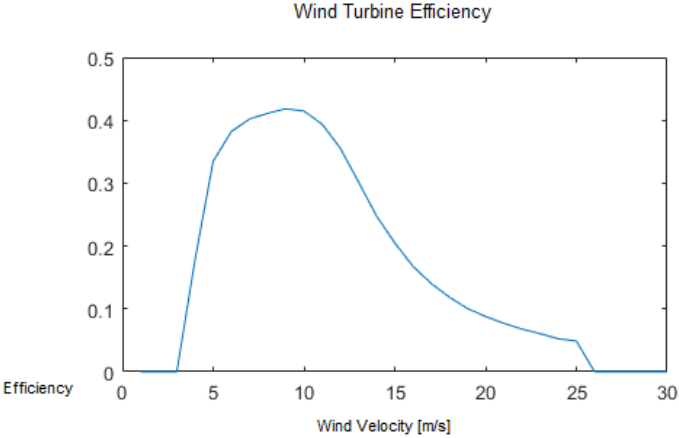


Figure 24 Wind Turbine type 1 Power Curve

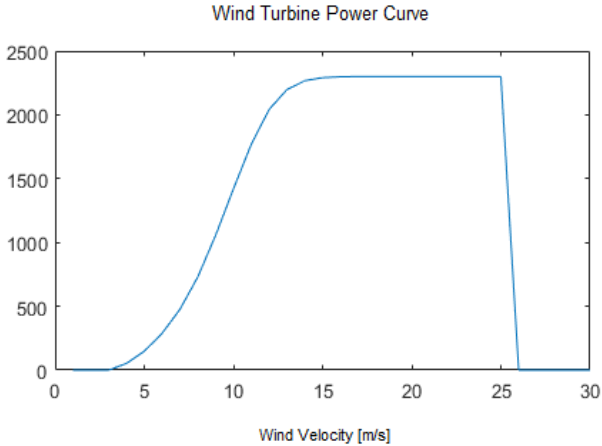


Figure 25 Wind Turbine type 1 Efficiency Curve

Figure 24 and Figure 25 are needed.

Figure 24 is the efficiency curve of the Wind Turbine Type 1. It is noticed that the effectiveness of the turbine reaches its peak when working with the wind around 10 – 11 [m/s]. With the information

obtained from Figure 23, it can be judged that the turbine rarely operates in its most efficient state. Figure , on the other hand, contains information on the power curve, provided from [44]. Here it can be seen that the power production reaches its peak around a wind speed of 15 [m/s] and maintains that production until it reaches its cut-off speed at 25 [m/s]. Unfortunately, due to the poor wind conditions in the zone for the observed timeframe, the turbine can at the very best produce around 60% of its capacity. These factors lead to the poor performance of this technology and will have an effect in sizing the storage system.

Figure 26 shows the production profile of the turbine without the wind speed.

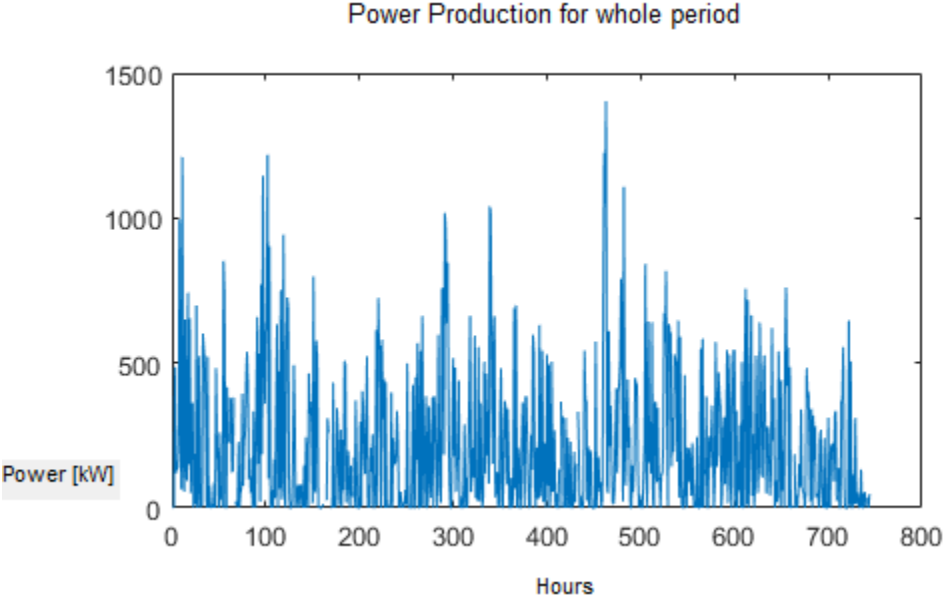


Figure 26 Wind Turbine type 1 power production

After simulation the first turbine technology, the other two technologies are also simulated. With the help of Figure , the performance can be compared. Here the power production is shown in MW and will be used in MATPOWER in that unit while performing the power flows.

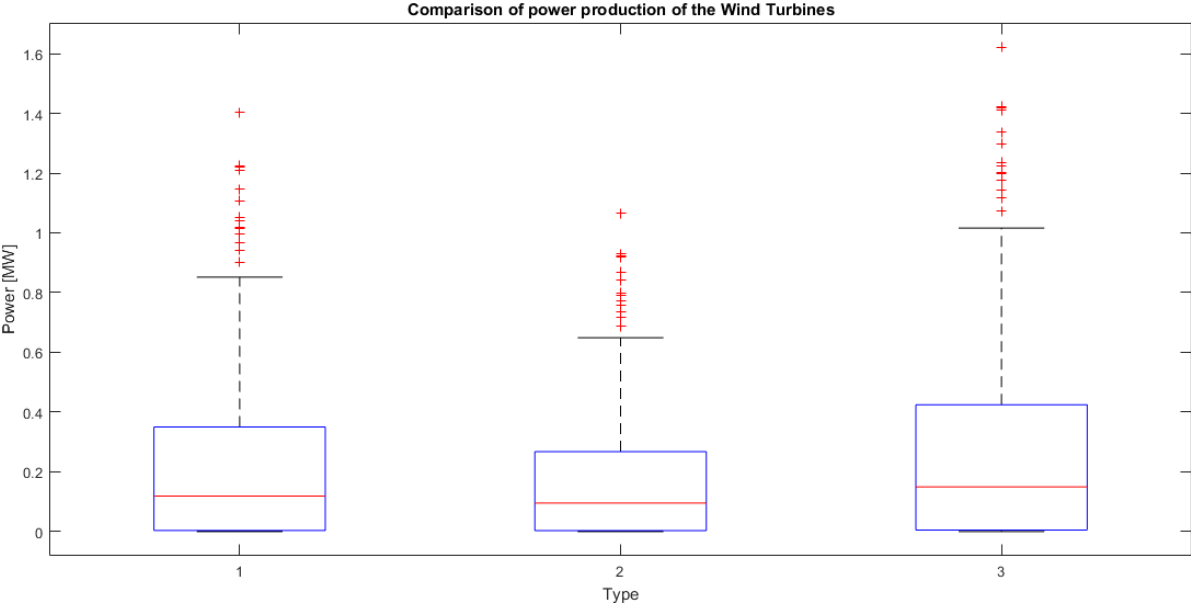


Figure 27 Wind Turbine Comparison

Each box-plot represents the production profile of a wind turbine. The red line inside the box represents the median value of the entire dataset or the middle value of the dataset. Half of the values in the dataset lie beneath the red line and the other half lie above the red line. The box itself represents the inter-quartile range. Seventy-five percent of the values fall beneath the upper quartile (top of the box), and twenty-five percent of the values fall below the lower quartile (bottom of the box).

Judging by the median values, the second turbine production for the period is the weakest. On the other hand, the third turbine type performs considerably better. From the length of the boxplots, it can be judged that the production rates of the three turbines. The second turbine possesses the shortest box-plot among the three. This suggests that the power produced for the whole period does not fluctuate too much. In contrast, the third turbine type, which has a better performance also has the most fluctuating power production. The upper and lower whiskers show us the location of the upper and lower fence of the dataset. Values that lay above these whiskers are considered outliers. Outliers appear very rarely in the dataset and thus lie beyond the whiskers.

From Figure 27 it can be judged that the first turbine can be expected to produce up to 900 kW of power for the given weather conditions, with rare chances for the production to reach as high as 1.4 MW. The second turbine has a lower performance, but the power production also fluctuates less. The maximum power that can usually be produced in that zone is around 700 kW with a chance of reaching 1 MW. The last turbine has the most spread power production with normal production around 1 MW that can reach as high as 1.6 MW. This behavior will affect the size of the storage system negatively, as the power production can vary quite a lot, thus affecting the surplus power in the electrical system more than the other two types. The storage system will have to have a bigger capacity [MWh] to cover these rare power production occurrences.

3.5.2 PV power generation

As with the wind turbines, three different solar module technologies are used in this work. Dymond CS6X-320 P-FG, TSM-245 PC/PA05 and SW 285 Mono. They are again further on referred to as type 1, 2 and 3. The datasheets for this photovoltaics have been obtained from the sites of their respective manufacturers[45-47] and can be seen in Appendix B. The power production of every photovoltaic can be explained using an IV curve such as the one shown in Figure 28. As explained before, to simulate the power production of a solar module, information is needed about the solar irradiance [W/m^2] and temperature[$^{\circ}\text{C}$]. The solar irradiance affects the current of the Photovoltaic, and the temperature

affects the voltage. Figure 28 is an example case using $826 \text{ [W}/\text{m}^2]$ and $28 \text{ [}^{\circ}\text{C]}$ as input information. The blue line corresponds to the current of that module at that solar irradiance, and the red line corresponds to the power that can be produced in [W]. The power production is found through tracing the x-axis voltage, found using Eq.(18-21), to the red power curve. This process is repeated for every hour of the period, and thus we obtain the power production for that hour. Unfortunately, the power produced by a single solar module is not that much, and the search for an optimal number of solar modules will take a very long time to simulate using ESSPC. To decrease the computation time, the modules are connected in solar arrays. The reason for this is that in an array, by connecting modules in series the voltage of the system can be increased, and by connecting modules in parallel the current of the system can increase [40, 41]. Following this rule, Eq. (11) & (12) can be changed, so they obtain the following forms:

$$I_{mpp}^{(m)} = (I_{mpps} * (G^{(m)}/G_s) * [1 + \alpha * (T(m) - T_s)]) * M_p \quad (24)$$

$$V_{mpp}^{(m)} = (V_{mpps} + \beta * (T(m) - T_s)) * M_p \quad (25)$$

where, M_p and M_s is the number of modules connected in parallel and in series respectively.

Using this information, a solar array can be created with far greater power production capabilities than one module. The power production profile of such an array, consisting only of modules of type 1, can be seen in Figure .

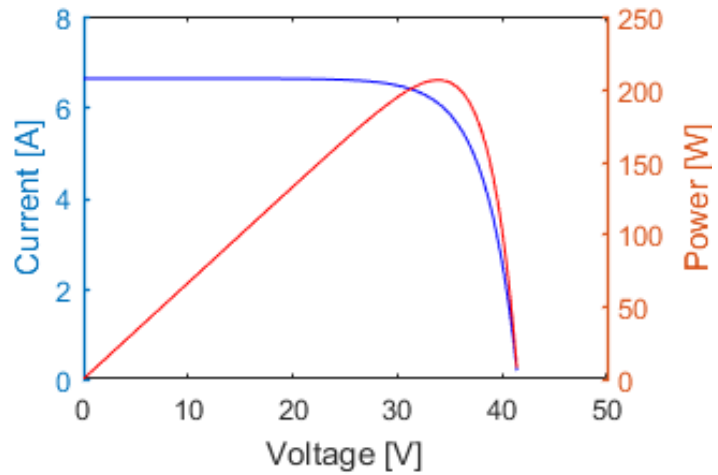


Figure 28 Current-Voltage Curve Solar module type 1 – $826 \text{ [W}/\text{m}^2]$ $28 \text{ [}^{\circ}\text{C]}$.

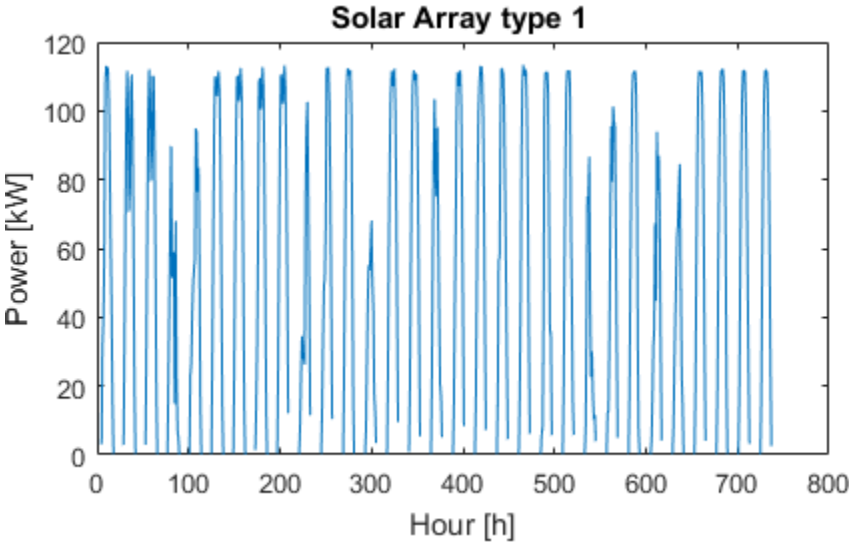


Figure 29 Solar Array power production type 1

To achieve this power production profile, 35 module must be connected in parallel and another 18 in series. The resultant array can at the very best produce around 110 [kW]. Each spike represents daytime, while each valley represents nighttime. It can be judged that except a few days, the arrays will normally produce around 110 [kW] at its peak every day.

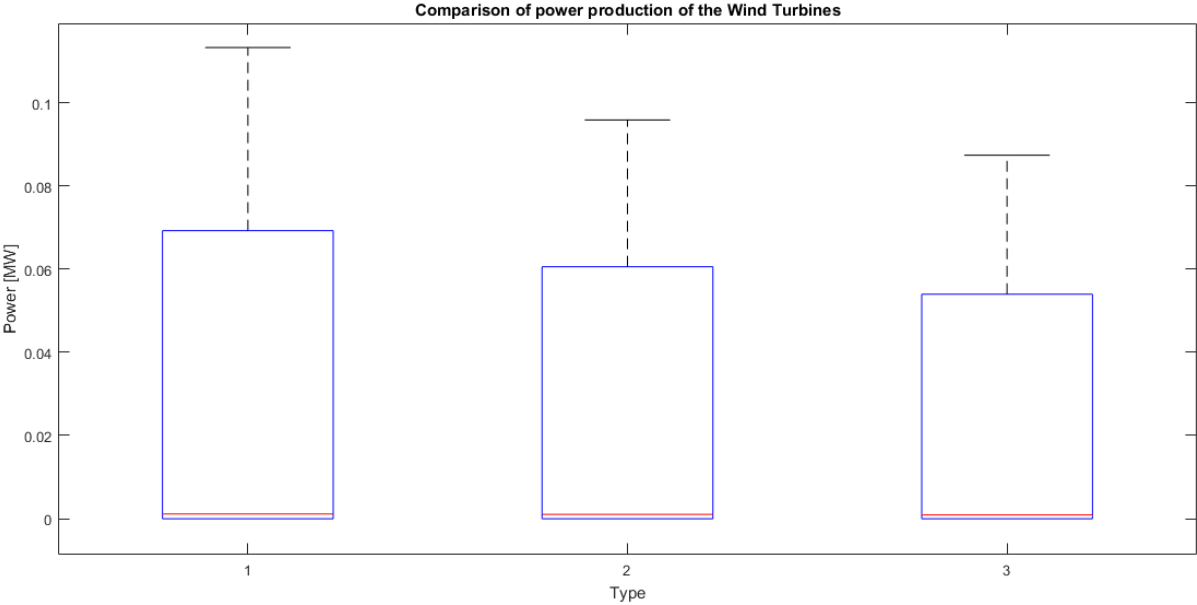


Figure 30 Solar Array comparison

After performing the same actions for the other two solar technologies, a comparison between their production profiles can be made using Figure .

It can be noticed that the median lines lie almost at the very bottom of the boxplot for each technology. This is because the nighttime power production is also included in the datasets. The lack of outlier points are also noticed, which means that any high power production occurrences for this period are not to be expected. The first type possesses the most fluctuating power generation that can reach as high as

0.11 [MW] followed by the second type with around 0.095 [MW] and lastly the third kind with a power production of 0.09 [MW].

3.6 Conclusion

In this chapter, the electrical power grid layout for this master thesis has been examined. After that, the models of the the wind turbine and solar modules have been explained, and the information is given on how to obtain the different variables needed for the models to work. After the simulation of different models, an analysis was performed on their power production and the effect they will have on an ESS.

Chapter 4 Natural Gas System Simulation

The purpose of the next chapter is to give the information on the gas network studied. This includes Information on different elements and simulation methods.

4.1 Supporting Gas Grid

Here, the natural gas grid parameters and a detailed explanation the process used in obtaining $G_{p,PtG}$ are presented.

4.1.1 Natural Gas Grid Parameters

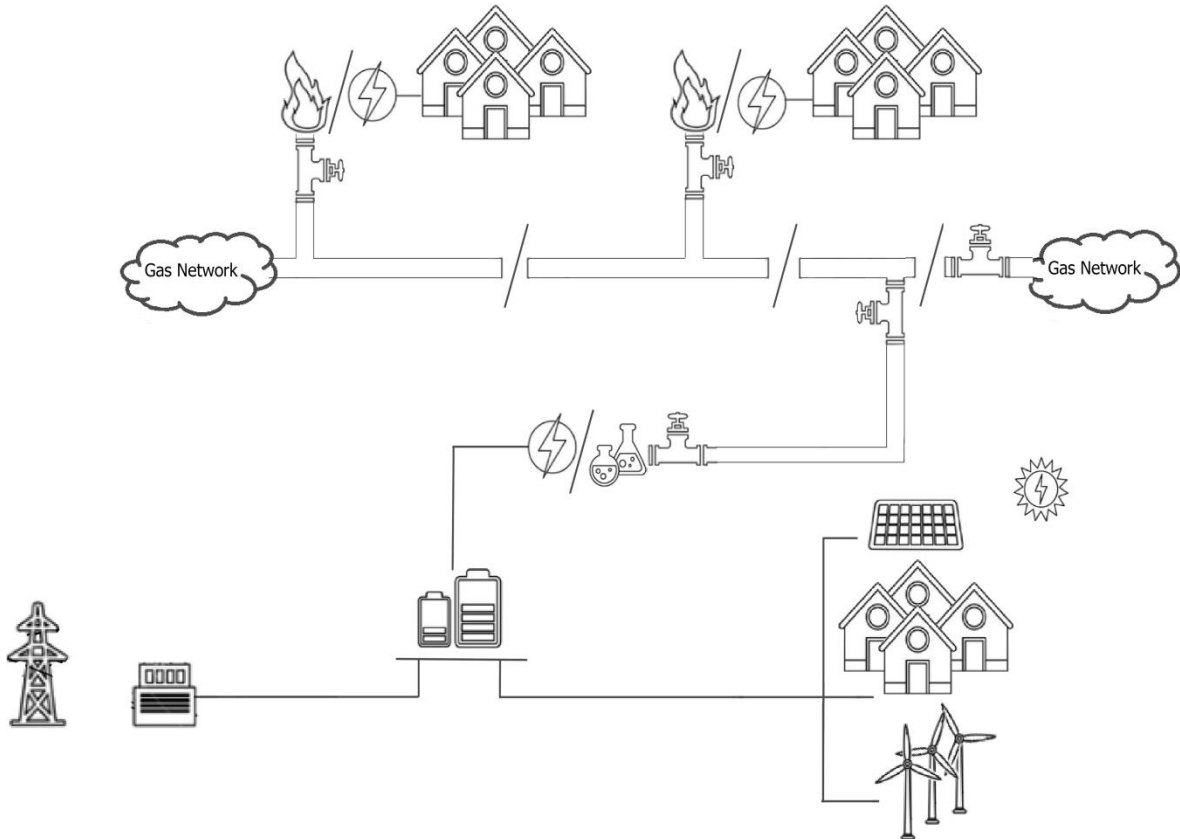


Figure 31 Grid Layout with PtG Source:[34]

Figure 31 shows the combined electrical and gas grid layout that is being used in this thesis. The layout is as simplified as possible. There are two GPGs that perform peak regulation for two different cities. Peak regulation was chosen due to the fact that the PtG system cannot produce significant amounts of synthetic natural gas. A load prediction algorithm is also used for the two cities in an attempt to further decrease the gas demand. An explanation of how the two load prediction algorithms work and how the peak regulation is performed can be found in 4.2. The consumption for the two cities has also been obtained from[35]. To keep track of the gas pressure at different nodes, the amount of synthetic natural gas that has to be produced and with a view to making sure that the normal workflow of the gas grid is not affected, the Newton-Raphson method is used. 4.1.2 gives a detailed explanation of how the Newton-Raphson method works for this layout.

4.1.2 Newton-Raphson method

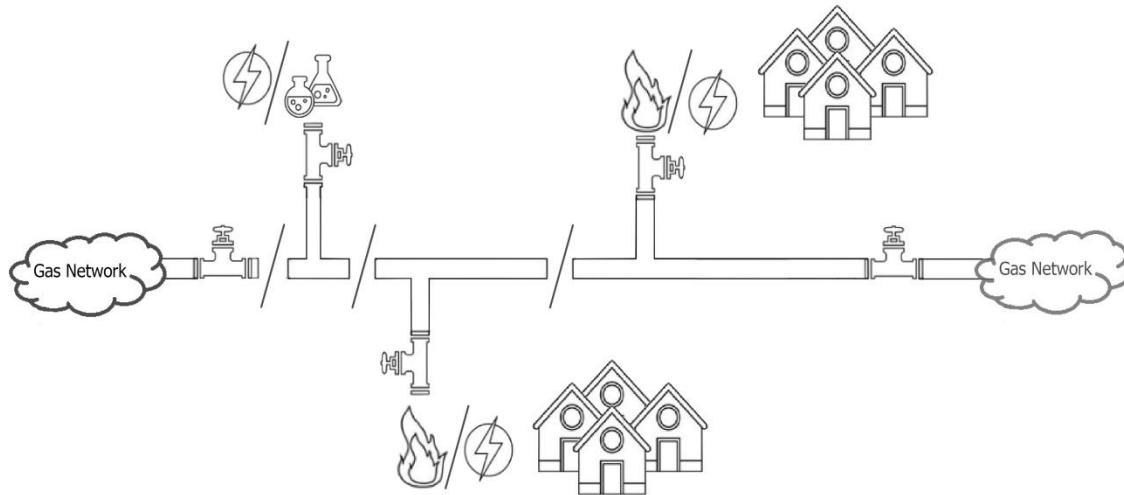


Figure 32 One line diagram Gas Grid Source:[34]

Figure 32 is a one-line diagram representation of the gas grid, shown in Figure 31. To ensure that the PtG system is not affecting the gas grid negatively, the Newton-Raphson method is used. Through that method, we can make sure that the pressure at different nodes and the gas flow in separate pipes is normal. The following publications have been used [20, 30, 48-50] to recreate this method for this work.

Known Parameters

To properly simulate the working process of this grid, some initial information is needed. In our case, that would be the diameter and length of different pipes in the network.

$$D_{0-1} = 280 \text{ mm} \quad D_{1-2} = 250 \text{ mm} \quad D_{2-3} = 250 \text{ mm}$$

$$L_{0-1} = 10 \text{ km} \quad L_{1-2} = 13 \text{ km} \quad L_{2-3} = 12 \text{ km}$$

Aside from that, we also need to know the gas flow rate in the pipeline once it enters our network and at what pressure.

$$Q_{gas,0-1} = 15000 \text{ [m}^3\text{/h]}$$

$$p_0 = 1000 \text{ [kPa]}$$

To create the steady-state model, information about the gas consumption of the two GPGs is needed. That load is marked $G_{d,GPG1}$ and $G_{d,GPG2}$. Information on how these values are obtained, can be found in section 4.2.

Nodal Equations

To analyze the steady-state gas flow distribution in the grid, the following nonlinear equations are obtained. They have been acquired through the nodal gas balance rule, which states that the amount of gas entering a node must be the same as the amount of gas leaving the node.

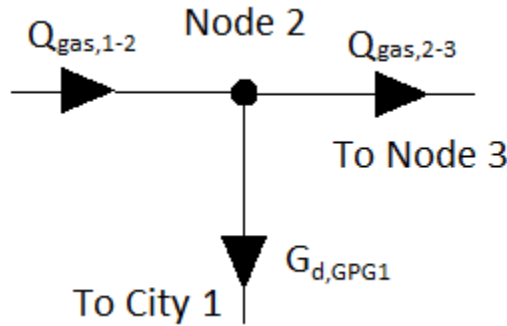


Figure 33 Nodal Gas Balance

For the next step, we need to calculate the resistance coefficient of the different pipelines Z_{k-l} .

$$Z_{k-l} = (6.4575 * 10^{-7}) * L_{k-l} / D_{k-l}^5 \tag{26}$$

After obtaining those values, the following nonlinear equations that represent the gas system can be written:

$$\Delta \Pi_k = p_k^2 - p_l^2 - Z_{k-l} * Q_{gas,k-l} \tag{27}$$

$$\Delta Q_k = Q_{s\ gas,k} - Q_{d\ gas,k} - \sum_{l \in k} Q_{gas,k-l} \tag{28}$$

Newton-Raphson

As mentioned above, the Newton-Raphson method is a popular choice for conducting a steady-state analysis of different gas networks.

$$F(X) = -J * \Delta X \tag{29}$$

To solve the nonlinear equations a point X must be considered, which is close to the actual solution:

$$X = [p_1\ p_2\ p_3\ Q_{s\ gas,1}\ Q_{gas,1-2}\ Q_{gas,2-3}]^T \tag{30}$$

$$F(X) = [\Delta \Pi_k\ \Delta Q_k]^T \tag{31}$$

Moreover, the Jacobian matrix will be given as:

$$J = \begin{bmatrix} \frac{\delta\Delta\Pi_1}{\delta p_1} & 0 & 0 & 0 & 0 & 0 \\ \frac{\delta\Delta\Pi_2}{\delta p_1} & \frac{\delta\Delta\Pi_2}{\delta p_2} & 0 & 0 & \frac{\delta\Delta\Pi_2}{\delta p Q_{gas,1-2}} & 0 \\ 0 & \frac{\delta\Delta\Pi_3}{\delta p_2} & \frac{\delta\Delta\Pi_3}{\delta p_3} & 0 & 0 & \frac{\delta\Delta\Pi_3}{\delta Q_{gas,2-3}} \\ 0 & 0 & 0 & \frac{\delta\Delta Q_1}{\delta p Q_{s, gas,1}} & \frac{\delta\Delta Q_1}{\delta p Q_{gas,1-2}} & 0 \\ 0 & 0 & 0 & 0 & \frac{\delta\Delta Q_2}{\delta p Q_{gas,1-2}} & \frac{\delta\Delta Q_3}{\delta Q_{gas,2-3}} \\ 0 & 0 & 0 & 0 & 0 & 0 \end{bmatrix} \quad (32)$$

To verify the convergence of the Newton-Raphson method, various calculations have been conducted at different initial pressure and gas flow conditions. One set of these values has been chosen as initial conditions for the gas system in this chapter.

4.2 Power-to-Gas Simulation

In this sub-chapter, the equations for simulating the PtG system are presented. These equations were obtained from [30].

$$E_{d,PtG} = G_{d,PtG} * \Delta H * 2.77778e^{-7} \quad (33)$$

Equation (33) gives the energy demand [MWh] needed to transform $G_{d,PtG}$ [mol] into methane. As it is known from eq. (4 Ch.2), the energy needed for turning 1 mol is $\Delta H = 890.3 \text{ kJ}$. In Eq. (33) that value is turned into [MWh] through multiplying ΔH by $2.77778e^{-7}$.

To simplify the equations for the entire process, the constant C_{PtG} is defined. It denotes the conversion of energy from electrical to natural gas form.

$$C_{PtG} = \frac{3600\eta_{PtG}}{LHV} \quad (34)$$

Here, the efficiency (η_{PtG}) is predefined by the user in advance. The energy density of natural gas is presented through its Lower Heating Value (LHV).

Now, $G_{p,PtG}$ [m^3/h] can be obtained, which is the amount of methane that is produced by the PtG.

$$G_{p,PtG} = C_{PtG} * E_{d,PtG} \quad (35)$$

However, if the amount of methane that is needed is known and we only need to know how much energy is withdrawn from the ESS, following equation is used.

$$E_{d,PtG} = \frac{G_{p,PtG}}{C_{PtG}} \quad (36)$$

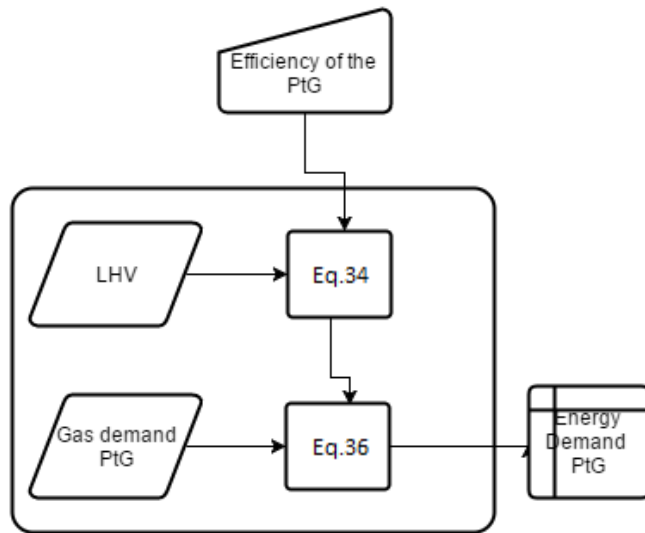


Figure 34 Simulation of PtG

Figure 34 shows the working process of the PtG for this thesis. The model that was created obtains information from the gas – grid and based on that tells the PtG how much methane must be produced. Based on that information our model calculates the needed electrical consumption from the ESS to fulfill this demand. An explanation of how $G_{p,PtG}$ is obtained can be found the next sub-chapter.

4.3 Gas Powered Generator Regulation

In an attempt to help the local consumers of two cities, with synthetic natural gas (SNG) produced from surplus energy from RES, Peak regulation has been chosen to be performed for each city. This service has been selected because GPGs are fast-acting and also the PtG system is not going to be able to produce enough SNG to take care of the base load.

Peak Regulation

Peak regulation is performed through the use of a load prediction sequence in an attempt to minimize the gas demand as much as possible. More information on the working principle of the load prediction algorithms and the way they are used in this work can be found in 4.2.1 and 4.2.2.

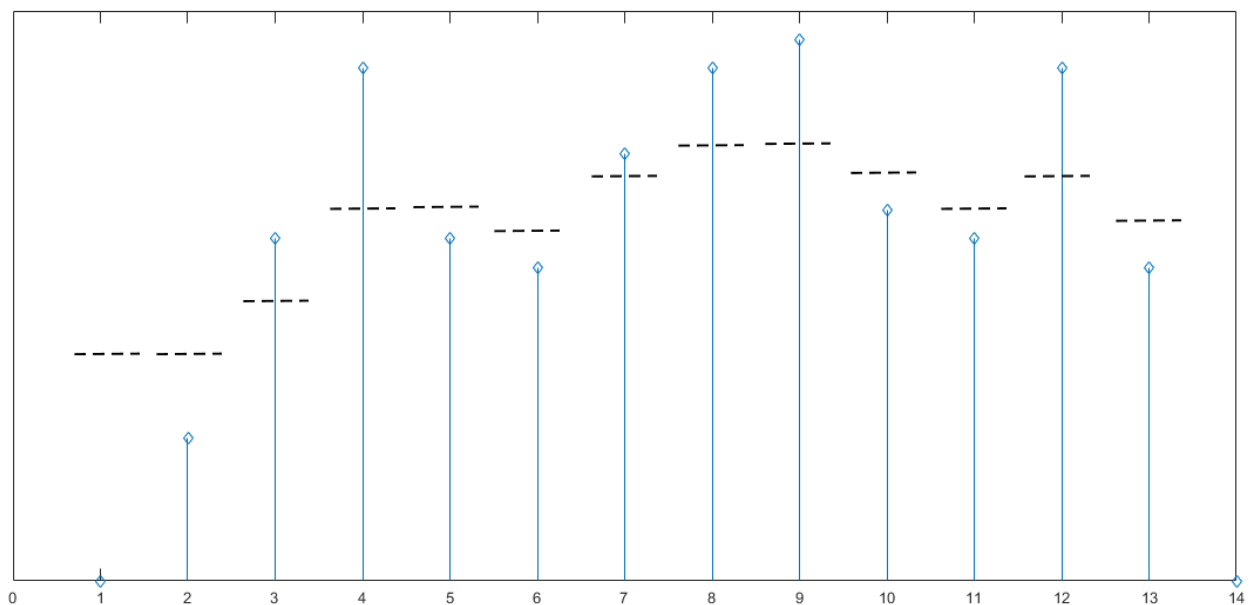


Figure 35 Peak Regulation Example

Figure 35 contains an example of how peak regulation has been utilized in this paper. The blue line represents the consumer demand at different intervals. The dotted line represents the limit the base power sources are prepared to cover. Everything above the dotted line at this moment must be covered by our GPGs.

4.3.1 Kalman Filter⁹

This method works as a recursive estimator. Here, past data is used to predict the next value. A downside of this algorithm is the fact that it is not possible to predict more than one value ahead. The equations through this subchapter have been adapted with the help of these sources [51, 52].

The general equation for the Kalman Filter is:

$$\hat{X}^m = K^m * Z^m + (1 - K^m) * \hat{X}^{m-1} \quad (37)$$

This method is composed of two processes, a prediction process, and an update process. The prediction process output value is used as an input value for the update process. Afterward, the value that is outputted through the update process becomes an input value for the prediction process.

Prediction process:

- Estimation

$$\hat{x}^{m-} = A * \hat{x}^{m-1} + B * u^m + w^{m-1} \quad (38)$$

Here A and B are identity matrices. u_m is a control signal, which identifies that the user has some sort of effect on the outcome. In this work it is assumed that the user has no effect on the outcome, so the control signal is equal to zero. Also, due to the fact that there is only one input signal, Eq.(38) can be minimized to:

$$\hat{x}^{m-} = \hat{x}^{m-1} + w^{m-1} \quad (39)$$

- Prediction error

$$P_{error}^{m-} = A * P_{error}^{m-1} * A^T \quad (40)$$

Update process:

- Kalman Gain

$$K^m = P_{error}^m - H^T (H * P_{error}^m + H^T + R)^{-1} \quad (41)$$

Here, the purpose of H is the same as A and B from Eq.(38), filtering of the signals. Because there is only one signal, H is assumed to be equal to zero.

- Estimate update

$$\hat{x}^m = \hat{x}^{m-} + K^m * (s^m - \hat{x}^{m-}) \quad (42)$$

- Error update

$$P_{error}^m = (1 - K^m * H) * P_{error}^{m-} \quad (43)$$

This algorithm can be summarized by the following figure:

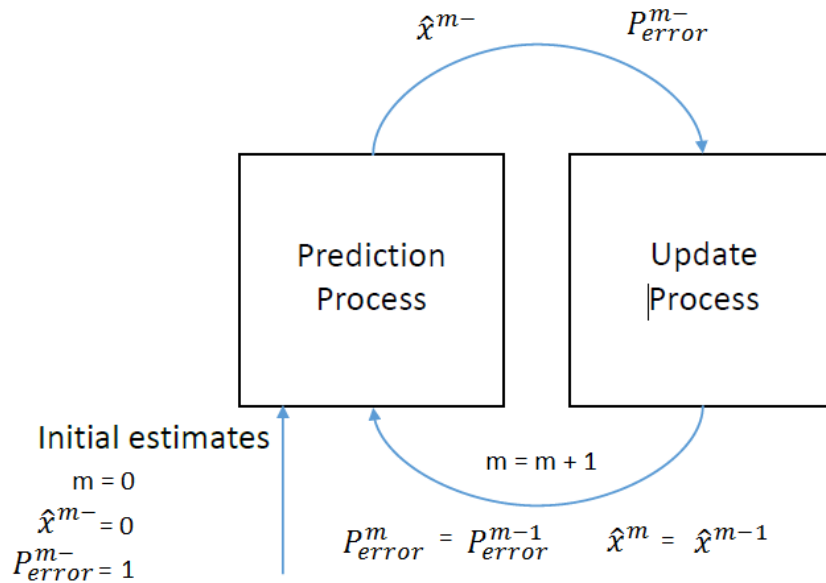


Figure 36 Working principle of the Kalman Filter

The process is first given an estimate of zero and a prediction error of one. After that in the prediction process, through Eq.(39,40) corrects these values and passes the outputs along to the update process which utilizes Eq.(41,42). Then the new \hat{x}^m and P_{error}^m are calculated based on our load data s^m . This whole process is looped until the moment the data runs out for s^m . After that one last iteration is performed and the result is presented through the last \hat{x}^m value.

As mentioned above, s^m is the load data. In an attempt to gain more accurate predictions, the electrical load is divided into hourly values and the load for each hour is predicted based on load data from the previous days at that same hour and the user is presented with an estimation of the load for the next 24 hours. In order to decrease the error, the first week data is used to teach the Kalman Filter. The estimations begin at day 8.

$$n \text{ days } \left\{ \begin{array}{c} \overbrace{\left[\begin{array}{ccc} x_{1,1} & \cdots & x_{1,24} \\ \vdots & \ddots & \vdots \\ x_{n,1} & \cdots & x_{n,24} \end{array} \right]}^{24 \text{ hours}} \end{array} \right.$$

Figure 37 Kalman Filter load data presentation

Then the real value of electrical load demand is compared to the predicted load.

$$P_{d,GPGV} = P_{c,cityv}^m - \hat{x}^m \tag{44}$$

The next step is to find $G_{d,GPGV}$ with the help of $P_{d,GPGV}$. The following equation obtained from [30] is used :

$$G_{d,GPGV} = \left(\frac{3600}{\eta_{GPGV} * LHV} \right) * P_{d,GPGV} \tag{45}$$

4.3.2 Least Error Squares (LES)

This method is a part of the multiple linear regression approaches. Here, the load is estimated based on information about different factors. In this work, the factors used are humidity, wind speed, and temperature[53]. Eq.(21) presents an example of the equation used in the multiple linear regression approaches.

$$\hat{X} = a_0 + a_1 * y_1 + a_2 * y_2 + a_3 * y_3 + \epsilon \quad (46)$$

Where, y_1, y_2 and y_3 stand for humidity, wind speed and temperature respectively and ϵ is an error.

The LES algorithm allows us to predict the load, based on all the available information available have on the electrical consumption and affecting factors.

$$\hat{X} = Y * \theta + \epsilon \quad (47)$$

In matrix form, Eq.(47) will obtain the following form:

$$\begin{bmatrix} S^{m-1} \\ S^{m-2} \\ S^{m-3} \\ \vdots \\ S^{m-n} \end{bmatrix} = \begin{bmatrix} 1 & y_1^{m-1} & y_2^{m-1} & y_3^{m-1} \\ 1 & y_1^{m-2} & y_2^{m-2} & y_3^{m-2} \\ 1 & y_1^{m-3} & y_2^{m-3} & y_3^{m-3} \\ \vdots & \vdots & \vdots & \vdots \\ 1 & y_1^{m-n} & y_2^{m-n} & y_3^{m-n} \end{bmatrix} * \begin{bmatrix} a_0 \\ a_1 \\ a_2 \\ a_3 \end{bmatrix} + \epsilon \quad (48)$$

In Eq.(48), the regression coefficients are the only unknown left. It can be found via the following equation.

$$\theta = (Y^T Y)^{-1} * Y^T S \quad (49)$$

Where S is a matrix containing all the past load data.

An example of how the Kalman Filter and the LES approach data is introduced to the program, created in parallel with this thesis, can be seen in Appendix A.

4.4 Gas Grid Simulation and Demand

As mentioned before, the gas demand from the PtG is formulated from the power regulation needs of two other cities. The working principles of the two algorithms have been presented, and now an algorithm must be chosen that is used to form the gas demand for each city.

4.4.1 Leas Error Squares

A condition of the LES is to have information on the environment, and more importantly, data is needed on the humidity, temperature and wind speed. As shown in section 4.1 the distances between the different GPG are very small, and due to that, the same weather information is used as the one for the Wind Turbines and Solar Arrays

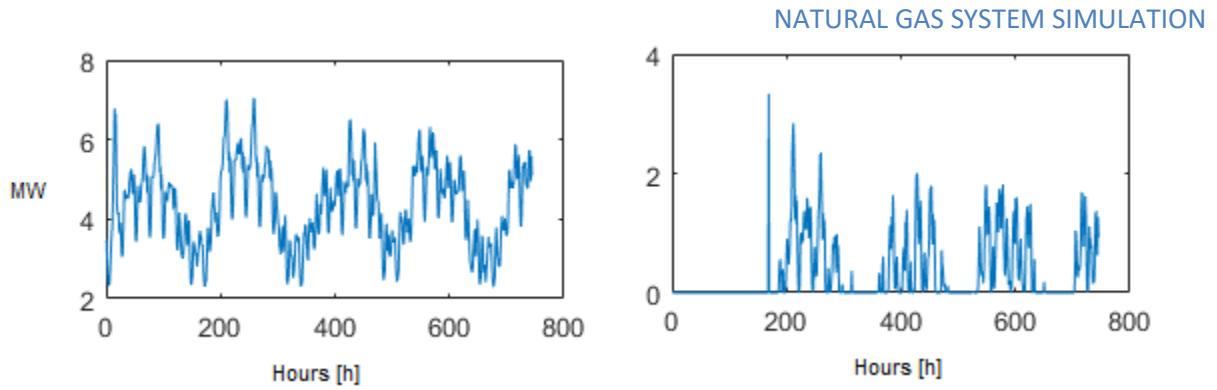


Figure 38 Load profile and regulation profile Area 1 LES

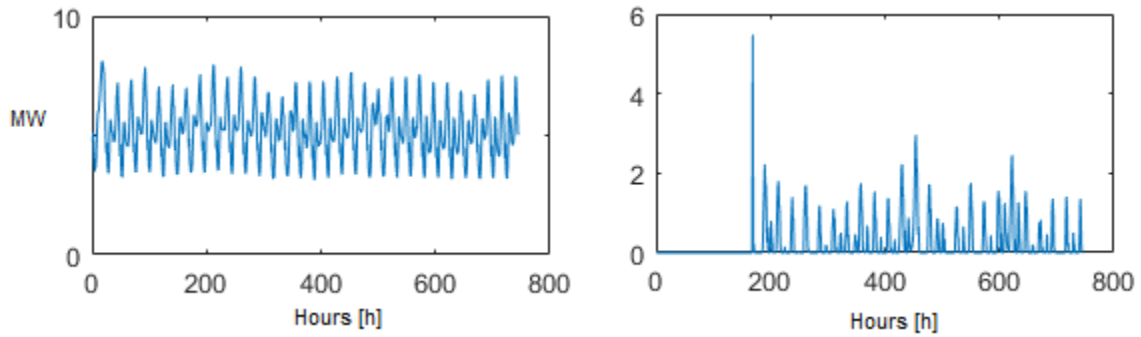


Figure 39 Load profile and regulation profile Area 2 LES

The left part of Figure 38 shows the load of the city for the entire period. The load prediction for the area is obtained and from there the power regulation profile, which is seen on the right. From the load profile, it can be judged that the area is the same as the one for which the ESS is sized, a city center or office complex with loads varying from 2 to 7 [MW]. As it can be seen from the load prediction profile, the LES gathered information on the load and accompanying factors for the first week of operation and started predicting in the second week. The power regulation profile possesses the same outline as the normal load, with peak demand during the week, around 2[MW], and no demand during the weekend. The reason for that is mostly caused by the prediction algorithm overestimating the request, and thus no regulation power is needed.

The profiles on Figure 39 show a different picture than Figure 38. Here the load profile is filled with spikes. Such a profile may belong to either a commercial or residential area. On the right, it can be seen that the regulation profile is full of spikes ranging around 1 - 2 [MW], but the spikes are also in higher number than for the previous area.

4.4.2 Kalman Filter

This time the Kalman filter algorithm is used for predicting the load of the two cities and obtaining the regulation profiles.

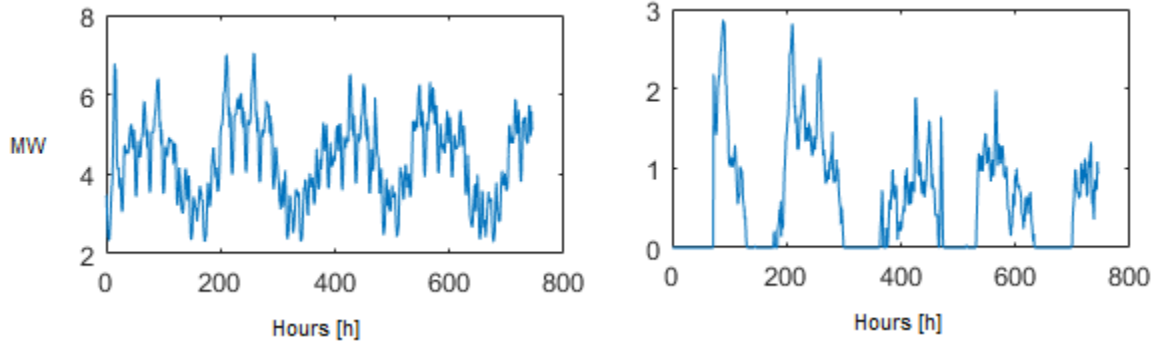


Figure 40 Load profile and regulation profile Area 1 Kalman Filter

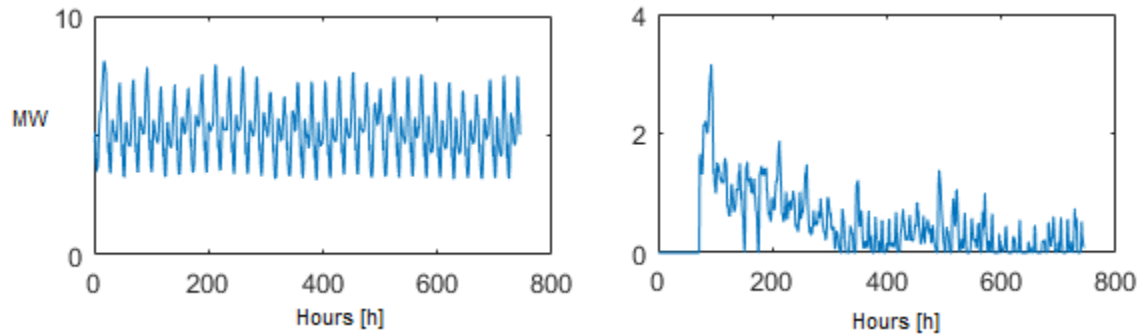


Figure 41 Load profile and regulation profile Area 2 Kalman Filter

First, it is noticed that the Kalman Filter needs less information in order to start working. Figure 40 shows a regulation profile quite similar to the one in Figure 38. The only difference is that now the spikes are more, due to the faster-learning process of the Kalman Filter, and can reach as high as around 2.8 [MW]. The outlook is better when comparing Figure 39 and Figure 41. It can be seen that in the beginning, the regulation profile has relatively high values, but as time goes on, the algorithm is learning, and thus the power demand from the GPG is becoming quite low.

As it became apparent before, different algorithms predict more or less accurately depending on the area. For this case, it is chosen that the gas demand is formed with the help of the LES, for shaping the regulation profile for city 1 and the Kalman Filter for shaping the regulation profile for city 2.

4.4.3 Power-to-Gas Gas Demand

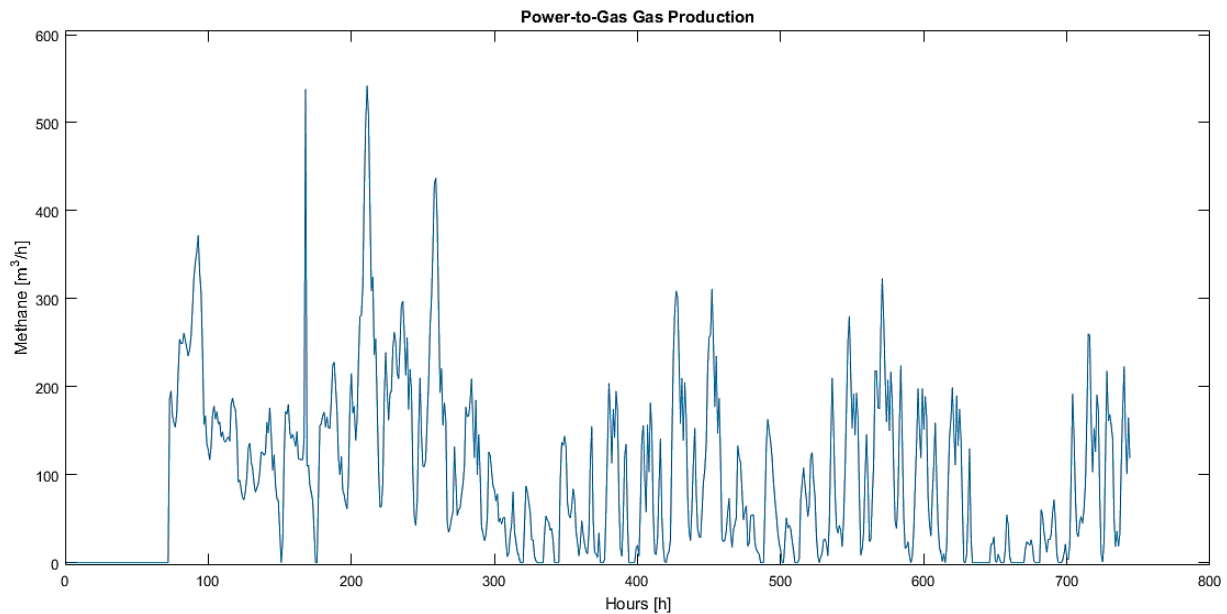


Figure 42 Methane Production PtG

After obtaining the regulation demand for the GPG, it is turned into Gas Demand. Through the Newton-Raphson method, the Gas Demand from the PtG system can be obtained. Figure 42 shows that demand. It can essentially be seen that gas demand profile is a combination of the two regulation profiles for the two zones. This is the reason why it is crucial to choose the right load prediction method for each zone. The profile shows a very high methane demand in the first third of the month of up to 550 [m³/h]. This high rise is essentially due to the effect of the Kalman filter and its inability to be trained for that specific load with less information. After the high rise, the demand lowers and for the rest of the period reach as high as around 300 [m³/h], which is a significant difference compared to the first third.

4.5 Conclusions

In this chapter, some insight has been cast on the combined electrical and gas grid network layout. Afterward information was given on how the PtG simulation is performed and how the demand is obtained through the prediction algorithms. In order to ensure the safe operation of the gas network, the Newton – Raphson method is used.

Chapter 5 Energy Storage and its Optimal Sizing

This chapter contains the results obtained in the course of this master thesis using ESSPC.

5.1. Obtaining the Storage System Size

This section explains how the size of the storage system can be found. First, a case is presented where the storage system is sized only depending on what is imported to the grid or exported. In the second case, the storage system is sized with regards to the price of electricity.

5.1.1 Flowchart for obtaining Storage System Capacity

Figure presents the different methodologies for obtaining the size of the Storage System. First of all, a representation of the Wind Turbines must be created. After inputting all the necessary information, the user can decide to add even more different types of Wind Turbines to the area. After this process has been finished the next step is to simulate the Photovoltaics (PVs). Again a choice can be made regarding the number of types of Solar Modules technologies being simulated. The next step is to present the Load Data (Consumer Data) for the grid where the RESs have been placed. After presenting the Grid Data to ESSPC, the Storage System can now be sized. The only way that this could be done is by varying the different RESs and calculating the Storage System Size for each combination and then getting the combination of RES that gives the smallest Storage System Size. How this is done and what different cases are considered in this thesis can be seen in section 5.3.

5.1.2 Sizing Storage System with regards to the import/export

To find the capacity of the ESS. First, the power input/output of the ESS must be obtained for each data point "m." The Residual Power ($P_{r,g}$) in the grid is the difference between the Generation and Consumption in the grid. If the Residual Power value is positive, the ESS is charged and if it is negative, it is discharged. Of course, unless the ESS is sized for "islanded mode", the ESS cannot charge/dischARGE for the whole value of the Residual Power. The Residual Percentage (R_{per}) is introduced here, which refers to what percentage of the charge/dischARGE power at that time must come from the ESS. The power that is stored/dischARGE from the ESS ($P_{i/o,ss}$) can then be found:

$$P_{i/o,ss}^{(m)} = P_{r,g}^{(m)} * R_{per} \quad (50)$$

Now that the power input/output for each data point is known, the needed energy capacity can be found for the ESS ($E_{cap,ss}$) at every datapoint:

$$E_{cap,ss}^{(m)} = E_{cap,ss}^{(m-1)} + P_{i/o,ss}^{(m-1)} \quad (51)$$

From here, the needed ESS capacity for the entire observed time frame, can be found:

$$E_{cap,ss} = \max(E_{cap,ss}) - \min(E_{cap,ss}) \quad (52)$$

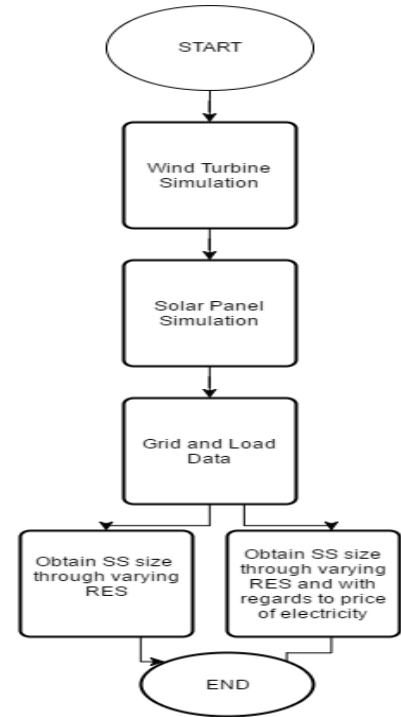


Figure 43 Flowchart Sizing Storage System

5.1.3 Sizing Storage System with regards to the price of electrical power

To find the capacity of the ESS for this case, two more things need to be introduced besides what has been done for the first instance. First the price of power that comes from the higher voltage grid. Second is the use of MATPOWER, package of MATLAB files that can perform PF and OPF calculations. MATPOWER provides information on the power losses in the test grid, also through making the substation bus bar the slack bus, information is provided on the power that enters or leaves the grid through the substation for every hour. Now $P_{i/o,ss}^{(m)}$ is divided in three different parts depending on the Consumption ($P_{c,g}$), Generation ($P_{g,g}$) and Price ($P_{pr,g}$) of electrical power.

If $P_{g,g}$ is greater than $P_{c,g}$

$$P_{c,ss}^{(m)} = (P_{g,g}^{(m)} - P_{c,g}^{(m)}) * R_{per} \tag{53}$$

$$P_{g,ss}^{(m)} = 0 \tag{54}$$

If $P_{c,g}$ is greater than $P_{g,g}$ and $P_{pr,g}^{(m)}$ is greater than the price limit ($P_{prl,g}$)

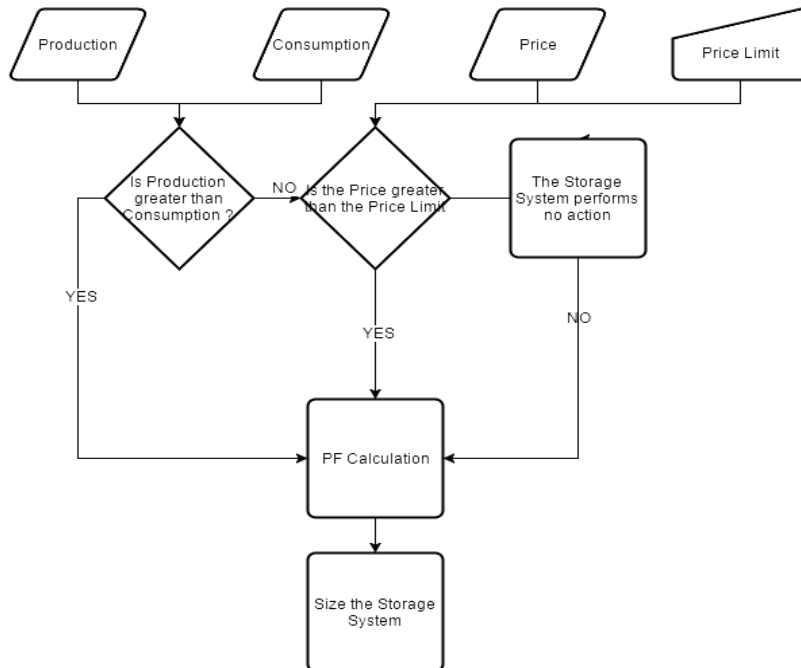
$$P_{g,ss}^{(m)} = (P_{c,g}^{(m)} - P_{g,g}^{(m)}) * R_{per} \tag{55}$$

$$P_{c,ss}^{(m)} = 0 \tag{56}$$

If $P_{c,g}$ is greater than $P_{g,g}$ and $P_{pr,g}^{(m)}$ is smaller than $P_{prl,g}$

$$P_{c,ss}^{(m)} = 0 \tag{57}$$

$$P_{g,ss}^{(m)} = 0 \tag{58}$$



With (53) and (55) the charge and discharge events that were happening in (52) are divided into $P_{c,ss}$ and $P_{g,ss}$. $P_{g,ss}$ is used for what must be produced by the Storage System in order to satisfy the consumers, $P_{c,ss}$ is used for what is unneeded in the LV grid at that data point and needs to be stored. When the system is producing it is taken that it cannot be consuming and vice versa (54) and (56). This is done with MATPOWER, the power flow toolbox can perform Power Flow calculations for only one

Figure 44 Charging Strategy choice tree

data point. Also due to the fact that the storage system is both a Consumer and Generator this division must be made because the consumption and generation data is entered in different fields of the toolbox. From the equations above it can also be noticed that that data is given to MATPOWER through another criterion, the price of power. Here the user sets a PriceLimit where if the Price at that time is higher we choose to support the grid with the help of the Storage System. But if the Price at that time is smaller than the PriceLimit the Storage System performs no action and the grid is supported entirely with cheap power from the higher voltage grid/substation. The choice tree presented in Figure 44 explains this charging strategy.

Figure 45 shows the price of electricity for the month of March 2015. The price is given in \$/MW. It can be seen that at the beginning of the month, the prices vary a lot from as low 10 \$/MW to as high as almost 500 \$/MW. After that, until the end of the month, the prices are considerably lower with the occasional spikes. Here the value of the median and the mean value of the dataset is given. This is done to help the user with their choice in setting a price limit, which as mentioned in Chapter 3, will be used to signal to the ESS that the price from the grid is too high and it should cover the electrical need of the grid.

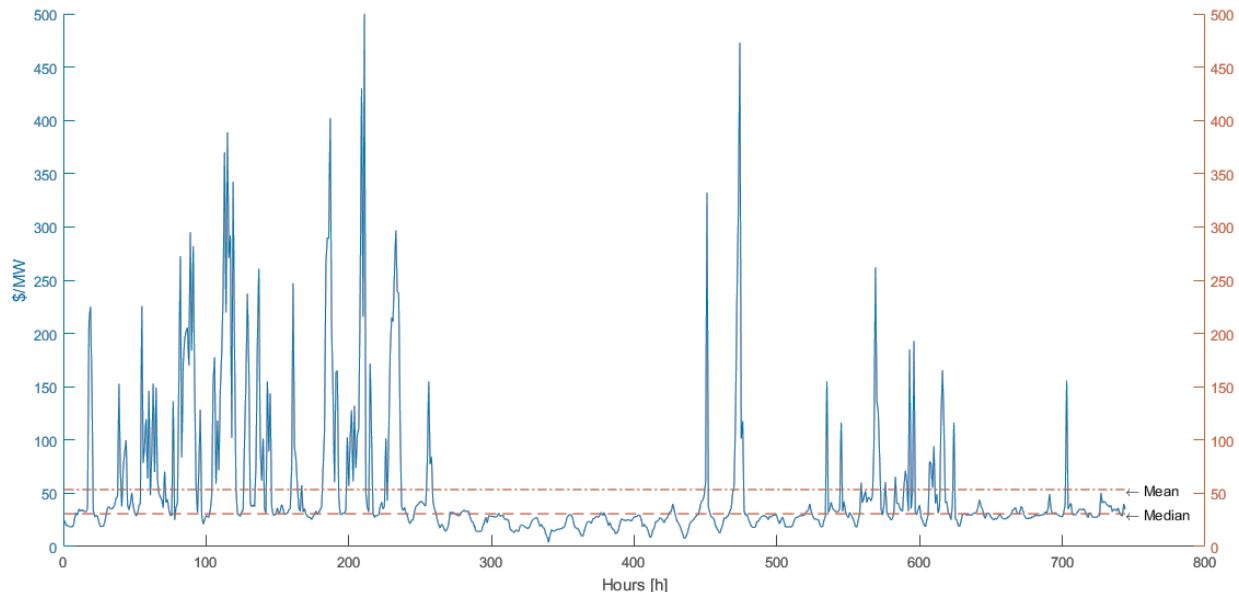


Figure 45 Electrical Power Price

It can be seen that the mean value of the dataset is around 52 \$/MW. The median value, on the other hand, is smaller and is around 30 \$/MW. This is because of a significant portion of the prices, in the given timeframe, are tiny. In ESSPC, the user can observe this information and try different prices and see how that affects the ESS capacity. In this work, 82 \$/MW are set as the price limit. The number of RES is then found to be 13, 9, 12 for Wind Turbines of types 1 2 and 3 and 9 10 9 for Photovoltaics of types 1 2 and three respectively.

5.2 Sizing of the ESS

The size of the ESS depends on the number of installed RES, weather conditions throughout the observed time frame and consumer load. To find the best combination of RES, the following equation is used:

$$P_{g,g}^{(m)} = P_{gn,wt}^{(m)} * x_n + P_{gn,pv}^{(m)} * y_n \quad (59)$$

Where “n” is the number of different models that are available, and WT and PV refer to the power generation from the Wind Turbine and the Photovoltaic respectively.

Obtaining the optimal number of RESs can be found by testing different combinations of RESs and then matching them to the storage system size that they have procured. For example, if the algorithm has access to 2 different WTs and 1 PV model, the equation above will look like this:

$$P_{g,g}^{(m)} = P_{g1,wt}^{(m)} * x_1 + P_{g2,wt}^{(m)} * x_2 + P_{g1,pv}^{(m)} * y_1 \quad (60)$$

From here, different combinations of x_1 , x_2 and y_1 are tested and the *Production* data for each combination is forwarded to help find the size of ESS. The smallest ESS size is then found and traced back to its RES combination.

5.3.1 Sizing Storage System Capacity with Surplus Power Method

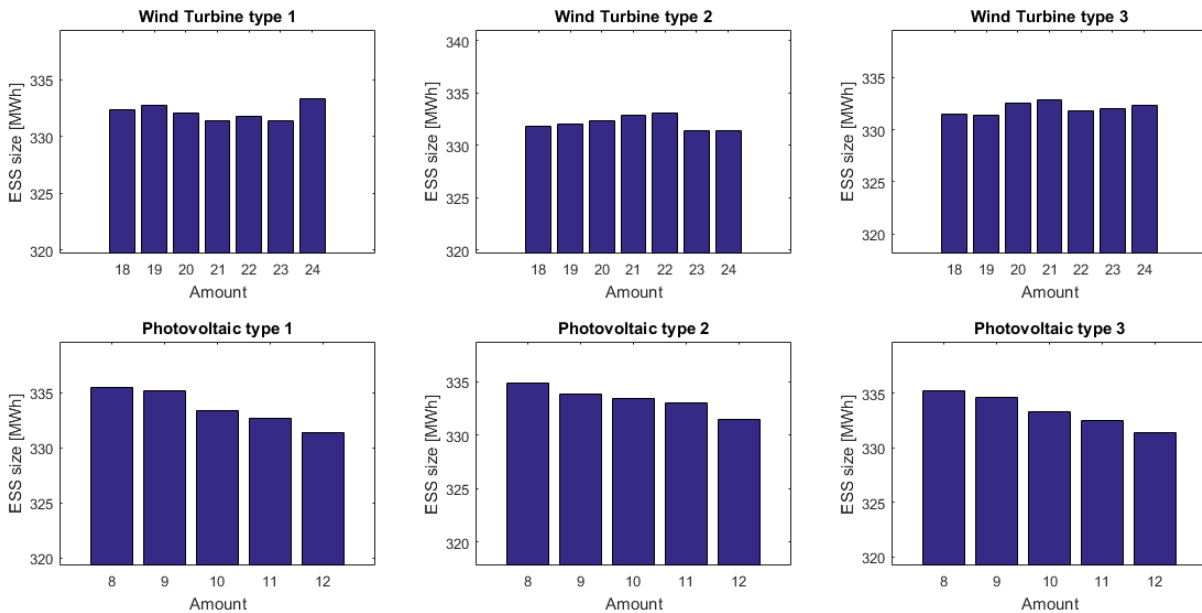


Figure 46 RES combinations Surplus Power

Figure 46 is a representation of all the different ESS capacities that can be achieved with a various number of RES at 50% of the Surplus Power. The graphs have been zoomed-in around the area where the smallest ESS capacity of 331.4 [MWh] is obtained. To achieve this 21 Wind Turbines of type 1 are required, 24 of type 2, 19 of type 3 and 12 of each type of Photovoltaic. It is also noticed that having a smaller number of RES will bring to a slightly larger ESS. Due to this, it is important to mention that this thesis will not make a techno-economic analysis based on the number of RES installed in the grid. In the “Results” section of ESSPC, the user can input different RES combinations and observe how they affect the ESS. Such an observation is performed in 5.3.1 and 5.3.2.

This whole process can be summarized with the following objective function:

$$f(R_{per}, x_{1:n}, y_{1:p}) = \max(E_{cap,ss}^{(1:m)}) - \min(E_{cap,ss}^{(1:m)}) \rightarrow$$

$$\rightarrow E_{cap,ss}^{(m)} + R_{per} \left(P_{g1:n,wt}^{(m)} * x_{1:n} + P_{g1:p,pv}^{(m)} * y_{1:p} \right) - P_{c,g}^{(m)} \quad (61)$$

subject to following constraints:

$$0 \leq f(x_{1:n}) \leq 10$$

$$\text{Constraints: } 0 \leq f(y_{1:p}) \leq 10$$

$$f(R_{per}) = 0.5$$

Here R_{per} is the percentage of power the ESS can cover, be it provide to the system or absorb. This value is 1 only in the time when electricity price is too high for the consumers and the ESS must provide what is demanded.

Error! Reference source not found. 48 and 49, present a comparison between the different ESS apacities with regards to the charging method. Here, only the surplus power charging method is used,

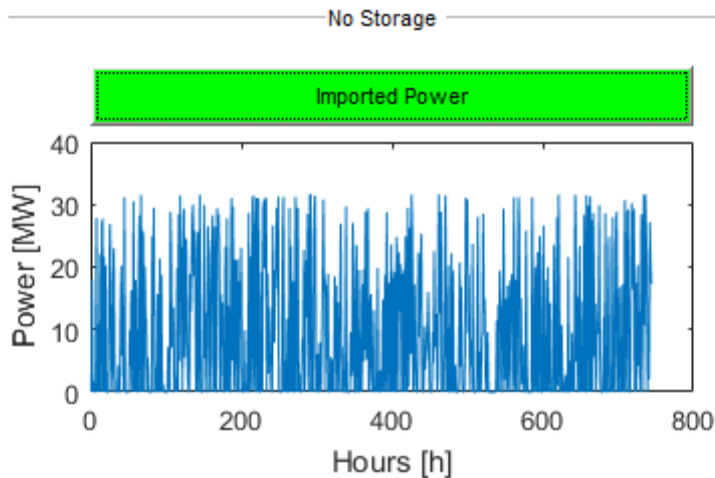


Figure 47 Effect of RES with no ESS

where the ESS is charged based on 50% of the positive surplus energy and discharged based on 50% of the negative surplus power.

Figure 47 presents the hourly power profile that must be covered from the substation. It can be noticed that quite often the external power system must help the power system in keeping the demand covered. The areas where nothing is imported from outside mean that all of the

requests in the grid are covered by the RES and the actual surplus power is transmitted through the substation elsewhere. As it can be seen, these hours are not many. Another noticeable feature is the larger amount of power that has to be supplied from the substation, which reaches as high as 30 [MW]. This is because MATPOWER also calculates the losses from the line. Thus after supplying the power from the substation, a portion of it will be lost in the lines, and only the needed amount will reach the consumers.

Figure 48 presents the behavior of the ESS and the effect it will have on the grid. The first plot shows how the energy inside the ESS changes over the course of the month and the second plot shows the amount of power that is charged or discharged from the ESS every hour. It can be seen that the ESS capacity profile is represented by some different in size hills. Each hilltop represents the end of a cycle of positive RES surplus power, and each valley bottom represents the end of a cycle where the RES could not meet the demand. Also, from the second plot, it can be noticed that due to the high fluctuating power production, mainly from the wind turbines, the charging power at times is more than twice of what is discharged for the whole period. It is also observed that the discharge profile mostly falls in the same window when compared to the charging profile for the entire period. The last plot covers the power that has been imported from beyond the network. On a first glance, when compared to Figure 48 it can be noticed that the ESS has had a positive effect on the system, the power supplied from the substation has decreased, which means fewer losses and that the otherwise lost power can be useful somewhere else.

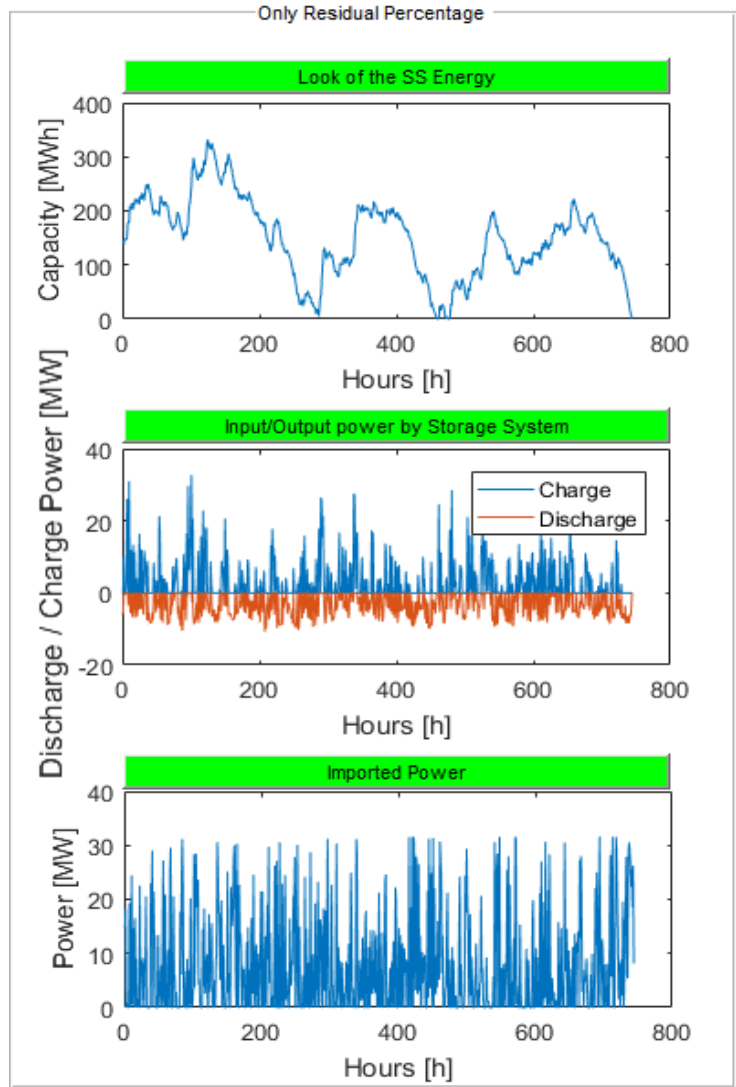


Figure 48 ESS capacity with the Surplus Power method with number of RES for Surplus Power method

5.3.2 Sizing Storage System Capacity with Surplus Power and Price Method

As mentioned before, another method has been devised in sizing the ESS. This method utilizes the electrical power price. Through it, the ESS can supply the power system when the cost of electricity is too high to purchase from outside the system, in the case beyond the substation.

Once again, this process can be presented by the following objective function:

$$\begin{aligned}
 f(R_{per}, x_{1:n}, y_{1:p}, P_{pri,g}) = & ((P_{g1:n,wt}^{(m)} * x_{1:n} + P_{g1:p,pv}^{(m)} * y_{1:p}) > P_{c,g}^{(m)} \rightarrow P_{g,ss}^{(m)} = \\
 & 0, E_{cap,ss}^{(m-1)} + R_{per} \left((P_{g1:n,wt}^{(m)} * x_{1:n} + P_{g1:p,pv}^{(m)} * y_{1:p}) - P_{c,g}^{(m)} \right) + P_{g,ss}^{(m)} \wedge (P_{c,g}^{(m)} > \\
 & (P_{g1:n,wt}^{(m)} * x_{1:n} + P_{g1:p,pv}^{(m)} * y_{1:p})), P_{pr,g}^{(m)} > P_{pri,g} \rightarrow P_{c,ss}^{(m)} = 0, E_{cap,ss}^{(m-1)} + R_{per} (P_{c,g}^{(m)} - \\
 & (P_{g1:n,wt}^{(m)} * x_{1:n} + P_{g1:p,pv}^{(m)} * y_{1:p})) + P_{c,ss}^{(m)} \wedge (P_{c,g}^{(m)} > (P_{g1:n,wt}^{(m)} * x_{1:n} + P_{g1:p,pv}^{(m)} * \\
 & y_{1:p})), P_{pr,g}^{(m)} < P_{pri,g} \rightarrow P_{c,ss}^{(m)} = 0, P_{g,ss}^{(m)} = 0, E_{cap,ss}^{(m-1)} = 0)
 \end{aligned} \tag{62}$$

$$0 \leq f(x_{1:n}) \leq 10$$

Constraints: $0 \leq f(y_{1:p}) \leq 10$

$$f(R_{per}) = 0.5$$

$$f(P_{pri,g}) = \text{user set}$$

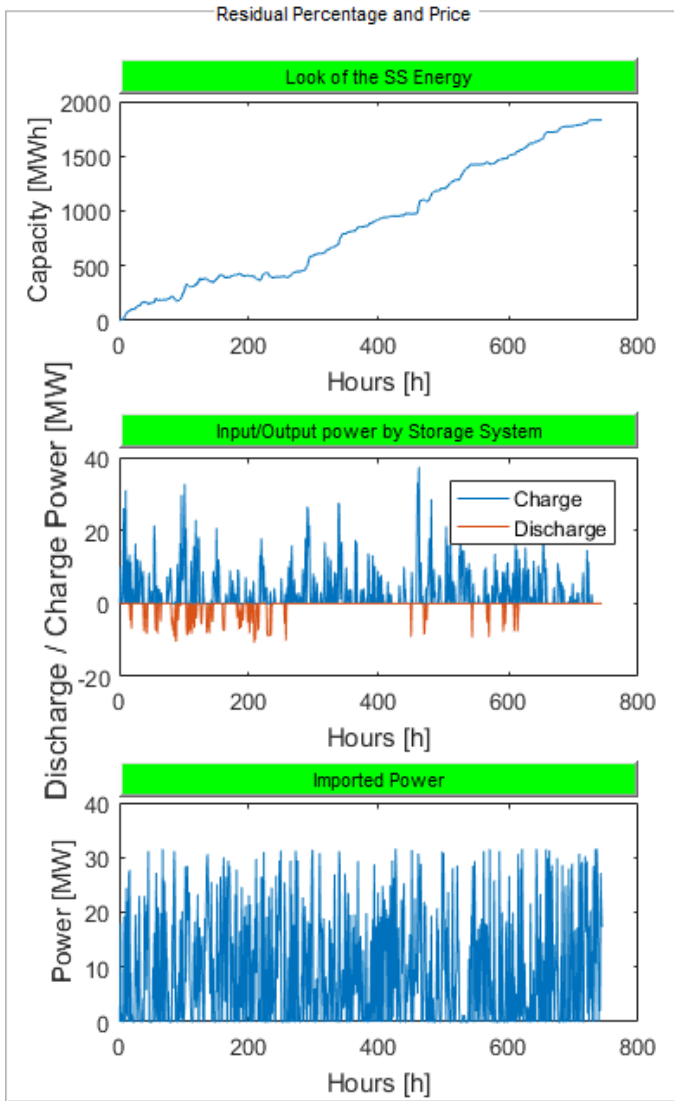


Figure 49 ESS capacity with the Surplus Power and Price method with number of RES for Surplus Power method in Figure 45. The amount of imported power from outside has also worsened, mainly because the ESS is not operational most of the time.

An overview of all the results obtained in sizing the ESS with the surplus power method can observe in Figure 50. The first row presents the total amount of money that have been paid for imported power. It can

Now the next charging method that includes the price of electricity is executed. The number of RES stays the same as the number of RES as before.

Here it can be seen that the ESS is constantly charging throughout the whole month of March. The reason for this behavior is the significant number of RES that is present. Because the number of RES is greater than what this method needs, the ESS almost constantly charges throughout the whole period and at the end reaches a size of around 1800 MWh. It can also be seen that the charging cycles have not increased in number, compared to Figure 48, but some have increased in power. However, the biggest change, which also affects the ESS, is the lack of discharging cycles in the middle of the month. This is due to the change of charging strategy, and those areas where it is noticed a lack of discharging events correspond with the lowest prices of electricity that were observed

Total Price Paid for Imported Power Whole Period

No Storage	Only % of Power	% of Power and Price
4.1446e+05	3.4267e+05	3.7688e+05

Total Size of the Storage System

No Storage	Only % of Power	% of Power and Price
0	331.4224	1.8302e+03

Highest Charge Rate

No Storage	Only % of Power	% of Power and Price
0	30.9950	30.9950

Highest Discharge Rate

No Storage	Only % of Power	% of Power and Price
0	10.7622	10.7622

Figure 50 End results for sizing ESS with optimal number of RES for Surplus Power method

be seen that with no ESS, that value is around 414460 \$, while with a 331 MWh ESS using the Surplus Power method, that value is around 342670 \$. Using the Surplus Power and Price method with this configuration brought worse results in term of the price paid, 376880 \$ and size of the ESS, 1830 MWh. The last two rows showing the highest and lowest discharge rate are the same for both ESS for both methods.

5.4 Sizing ESS with PtG via Surplus Power and Price Method

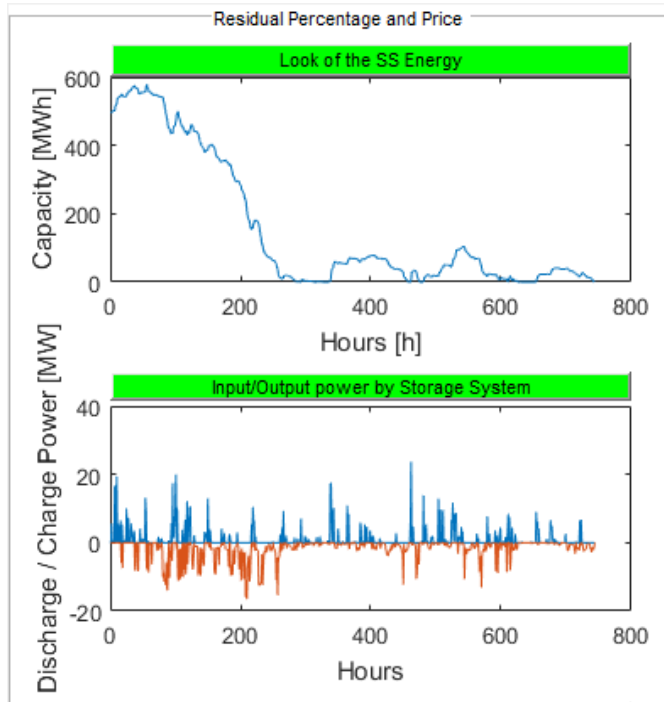


Figure 51 ESS capacity PtG and with the Surplus Power and Price method with combination of RES for Surplus Power and Price method.

In Figure 51 the capacity profile of the ESS working with the PtG, at 85% efficiency(see 2.4.3), can be seen. It is important to mention that 44 Wind Turbines have been utilized (16 from type 1, 13 type 2 and 15 type 3) and 21 Solar Arrays (8, 7, 6 for types 1 2 and 3 respectively). In order to obtain this optimal profile, 10 more Wind Turbines had to be added than for the case in 5.3.2, but on the other hand, the number of Solar Arrays was decreased by 7. What can be noticed from the capacity profile is the shape which is similar to the one obtained in 5.3.2, and it roughly resembles the methane production profile from {methane production Figure}. The charge/discharge profile is quite different from the one before. Now the discharge events have a slightly higher number and are slightly larger, and there are also discharges in places where there were no before. This is due to the charging strategy when the price is in the predetermined limits, in the first case the grid did not need the ESS, but in the case of Figure 51, the ESS is still required. This is the reason why the size is relatively bigger for this ESS than from the one before, because of the effect of the ESS.

Total Price Paid for Imported Power Whole Period

No Storage	Only % of Power	% of Power and Price
4.0295e+05	4.0065e+05	4.3298e+05

Total Size of the Storage System with P2G

No Storage	Only % of Power	% of Power and Price	MWh
0	2.5247e+03	578.4343	

Gas Produced in m³ entire period

No Storage	Only % of Power	% of Power and Price	[m ³]
0	7.0298e+04	7.0298e+04	

Highest Charge Rate

No Storage	Only % of Power	% of Power and Price	MW/interval
0	19.3954	19.3954	

Highest Discharge Rate

No Storage	Only % of Power	% of Power and Price	MW/interval
0	13.2164	13.2164	

Figure 52 End results for sizing ESS with PtG and optimal number of RES for Surplus Power and Price method

The end results can be observed in Figure 52. The results shown before are combined with results from a study that was similar to the one in 5.3.2, sizing the ESS with the RES for Surplus Power and Price Method, but utilizing only the Surplus Power method. Figure 52 is quite different to Figure 50, where the PtG was not used. For starters, due to the increased number of RES, the total price paid for imported power has decreased, but it is

still a bit higher than the total price paid for imported power with no ESS and PtG. The total ESS capacity has also increased from 314 MWh to roughly 579 MWh, which is a change once again brought by the PtG.

This information is proof that for the currently chosen Grids, Consumers, and RES, the combination of ESS and PtG will not bring better results in lowering the ESS capacity. Evidence was also found that the PtG has the potential of lowering the ESS given slightly different starting conditions, like changing the demand profiles, the prediction algorithms and introducing various more RESs.

5.5 Sizing of ESS with Electrochemical Characteristics

Gathering the valuable information from the sections so far, it is known that through the Surplus Power and Price method we obtained the smallest ESS capacity. Afterward coordinating that ESS with PtG did not bring better results.

Lead-Acid		Lithium-Ion		Vanadium-Redox		CAES	
Power	Energy	Power	Energy	Power	Energy	Power	Energy
[MW]	[MWh]	[MW]	[MWh]	[MW]	[MWh]	[MW]	[MWh]
50	200	1-100	0.25-25	50	250	180	1400-3600
20-50	250	1-10	4-24	1-10	4-40	135	1800
100	400					135	2700
1-100	0.25-50					50	250

Table 18 Electrical Energy Storage Project Sizes

Table 18 has already been presented in 2.5, and it is brought it here for easy reference. It can be noticed that the 314[MWh] and the 578[MWh] Storage Systems obtained in the course of this study match the power output of all these projects, but with regards to the size, fit only the Lead-Acid and the CAES technologies. This means that the ESS capacities fit real projects utilizing the Lead-Acid and CAES. So far the ESS is sized without regards to the efficiency. Now, that there is a rough estimation of the parameters are to be needed, one of the following technologies can be fitted, and a real ESS capacity can be obtained.

The Lead-Acid is chosen to be fit, seeing as the 314 [MWh] ESS is the smallest obtained in the course of this study.

In order to perform this task, the Lead-Acid roundtrip efficiency is needed. From 2.2.1 the value of 85% is taken. Also with a view to include the roundtrip effectiveness in the calculations, the following change must be made in accordance with [54].

$P_{i/o,ss}^{(m)}$ is divided into charging and discharging events. Where if $P_{i/o,ss}^{(m)} > 0 \rightarrow P_{i/o,ss}^{(m)} = P_{c,ess}^{(m-1)}$ and if $P_{i/o,ss}^{(m)} < 0 \rightarrow P_{i/o,ss}^{(m)} = P_{g,ess}^{(m-1)}$

For charging events there is

$$E_{cap,ss}^{(m)} = E_{cap,ss}^{(m-1)} + P_{c,ess}^{(m-1)} * \sqrt{\eta_{ESS}} \quad (63)$$

And for discharging events

$$E_{cap,ss}^{(m)} = E_{cap,ss}^{(m-1)} + P_{g,ess}^{(m-1)} * \frac{1}{\sqrt{\eta_{ESS}}} \quad (64)$$

Where η_{ESS} is the efficiency of the chosen ESS.

As explained before, the Lead-Acid battery will be sized with accordance to the Surplus Power and Price method without coordination with the PtG system. For this case the objective function will acquire the following form:

$$\begin{aligned} f(R_{per}, x_{1:n}, y_{1:p}, P_{pri,g}, \eta_{ESS}) = & \left((P_{g1:n,wt}^{(m)} * x_{1:n} + P_{g1:p,pv}^{(m)} * y_{1:p}) > P_{c,g}^{(m)} \rightarrow \right. \\ P_{g,ss}^{(m)} = & 0, E_{cap,ss}^{(m-1)} + (R_{per} \left((P_{g1:n,wt}^{(m)} * x_{1:n} + P_{g1:p,pv}^{(m)} * y_{1:p}) - P_{c,g}^{(m)} \right) + P_{g,ss}^{(m)}) + \\ P_{c,ess}^{(m-1)} * & \sqrt{\eta_{ESS}} \wedge (P_{c,g}^{(m)} > (P_{g1:n,wt}^{(m)} * x_{1:n} + P_{g1:p,pv}^{(m)} * y_{1:p})), P_{pr,g}^{(m)} > P_{pri,g} \rightarrow \\ P_{c,ss}^{(m)} = & 0, E_{cap,ss}^{(m-1)} + R_{per} (P_{c,g}^{(m)} - (P_{g1:n,wt}^{(m)} * x_{1:n} + P_{g1:p,pv}^{(m)} * y_{1:p})) + P_{c,ss}^{(m)} + \\ P_{g,ess}^{(m-1)} * & \frac{1}{\sqrt{\eta_{ESS}}} \wedge (P_{c,g}^{(m)} > (P_{g1:n,wt}^{(m)} * x_{1:n} + P_{g1:p,pv}^{(m)} * y_{1:p})), P_{pr,g}^{(m)} < P_{pri,g} \rightarrow \\ P_{c,ss}^{(m)} = & 0, P_{g,ss}^{(m)} = 0, E_{cap,ss}^{(m-1)} = 0 \end{aligned} \quad (65)$$

subject to following constraints:

$$\begin{aligned} 0 & \leq f(x_{1:n}) \leq 10 \\ \text{Constraints: } 0 & \leq f(y_{1:p}) \leq 10 \\ f(R_{per}) & = 0.5 \\ f(P_{pri,g}) & = \text{user set} \\ 1 & \leq f(\eta_{ESS}) \leq 100 \end{aligned}$$

Figure 53 presents the Lead-Acid capacity found through the aforementioned method. A definite size increase is observed where the ESS now reaches 363 [MWh]. As expected, the profile maintains its previous shape.

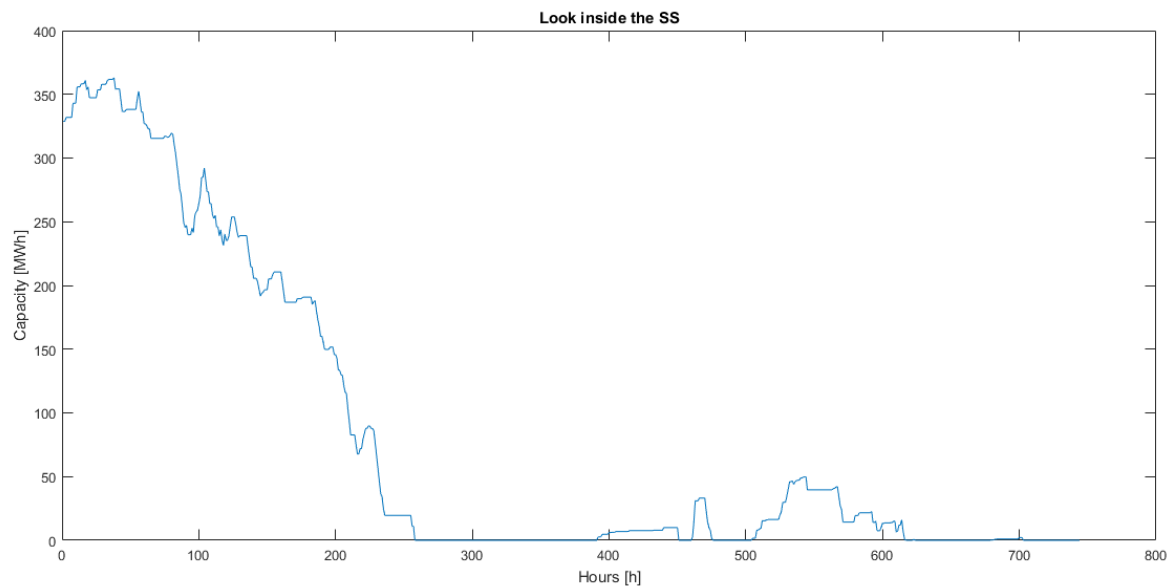


Figure 53 Lead-Acid capacity Surplus Power and Price method without PtG

As for the charge/discharge characteristic, due to the effect of the now added efficiency, it can be noticed that the spikes have slightly larger values than before.

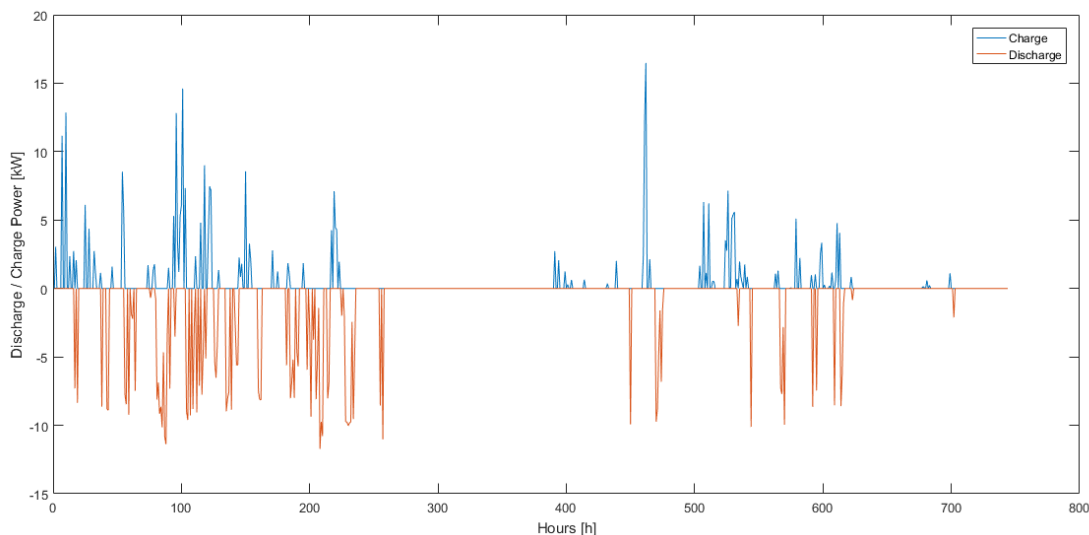


Figure 54 Charge-Discharge characteristic Lead - Acid

5.6 Conclusions

In this chapter results have been obtained on sizing the storage system with different combinations of RES and different methods. It was found that the smallest ESS size is found through the Surplus Power and Size method with number of RES specifically set for that method. Afterwards the effect of the PtG system on the ESS was observed and a conclusion was reached that for this particular case a coordination between the two systems will bring an increase in the ESS size, and thus is not wanted. As a last result, via information obtained from simulations an ESS technology was chosen and the ESS was sized with that particular technology. The results showed that installing a Lead-Acid technology, the ESS will have an increase of size by about 20 [MWh] compared to the perfect case, where the technology has not yet been chosen.

Chapter 6 Conclusion and Future Work

6.1 Conclusions

Coordination between ESS and PtG systems will play an important role in the future power system. Due to the large number of RES that are installed and will continue to be installed, a method for utilizing the excess renewable energy is needed. A number of different technologies have the ability to store this excess energy and then release it when needed. Through the use of different charging methods, an ESS can be optimally sized for taking care of the electrical needs of nearby consumers, as well as the gas demand.

This work introduced a few of the most well-known ESS technologies. The technologies were compared and one that can best perform the task at hand was chosen. In this work, a few charging strategies were developed for charging the ESS with and without connection to the PtG system, as well as a strategy for gas demand from the PtG.

In this master thesis it was found out that it is possible to store surplus energy from RES and store it as electrochemical energy which afterwards can be turned into methane. With the proper charging strategy, tailored to the the given area, the size of the ESS can be optimized to be as small as possible. Furthermore, by setting gas demand strategies with load-prediction algorithms it was found that using the PtG system under these initial conditions will increase the ESS size even though the number of RES is smaller.

6.2 Future work

In the future, the ESSPC can be further enhanced by introducing a number of different features, like for example:

- Easy introduction of a more complicated power grid and the ability to change the position of the ESS.
- Easy introduction of a more complicated gas network with a number of different gas consumers.
- Improving the computation time of the ESSPC, so that more types of RES can be introduced and a more in-depth observation can be performed.
- Introduction of a wider variety of charging strategies.
- Introduction of a wider variety of load prediction algorithms if GPGs are to be used.

Bibliography

- [1] D. G. Rachel Carnegie , David Nderitu, Paul V. Preckel, "Utility Scale Energy Storage Systems," State Utility Forecasting Group 2013.
- [2] ISPRE, "Research and Development on Renewable Energies " ISPRE2011.
- [3] (1/9). Available: <http://www.ens.dk/en/supply/renewable-energy/wind-power/offshore-wind-power/current-offshore-wind-farm-projects>
- [4] M. Bredsdorff. (2015, 01/10). 6/1. Available: <https://ing.dk/artikel/tordnende-succes-39-procent-af-stroemmen-kom-fra-vindmoeller-i-2014-173290>
- [5] B. V. Mathiesen, H. Lund, D. Connolly, H. Wenzel, P. A. Østergaard, B. Möller, *et al.*, "Smart Energy Systems for coherent 100% renewable energy and transport solutions," *Applied Energy*, vol. 145, pp. 139-154, 5/1/ 2015.
- [6] B. V. L. Mathiesen, Henrik; Hansen, Kenneth; Skov, Iva Ridjan; Djørup, Søren Roth;, S. S. Nielsen, Peter; Thellufsen, Jakob Zinck; Grundahl, Lars; Lund, Rasmus, and D. W. C. Sjøgaard; Drysdale, David; Østergaard, Poul Alberg, "IDA's Energy Vision 2050: A Smart Energy System strategy for 100% renewable Denmark," Aalborg University 2015.
- [7] L. Bird, M. Milligan, and D. Lew, "Integrating Variable Renewable Energy: Challenges and Solutions," National Renewable Energy Laboratory, Technical Report September 2013 2013.
- [8] TEPCO, "Tokyo Electric Power Company," N. o. electricity, Ed., ed: TEPCO.
- [9] A. Oudalov, D. Chartouni, and C. Ohler, "Optimizing a Battery Energy Storage System for Primary Frequency Control," *IEEE Transactions on Power Systems*, vol. 22, pp. 1259-1266, 2007.
- [10] "The future role and challenges of Energy Storage," ed: European Commission, 2014.
- [11] G. H. Abbas A. Akhil, Aileen B. Currier, Benjamin C. Kaun, Dan M. Rastler, and A. L. C. Stella Bingqing Chen, Dale T. Bradshaw, and William D. Gauntlett, "DOE/EPRI 2013 Electricity Storage Handbook in Collaboration with NRECA," Sandia National Laboratories 2013.
- [12] G. P. Pierre Pinson, Bernd Klocki, Jody Verboomen, "Dynamic Sizing of Energy Storage for Hedging Wind Power Forecast Uncertainty," presented at the Power & Energy Society General Meeting, 2009.
- [13] D. P. Kothari and I. J. Nagrath, *Modern Power System Analysis*: Tata McGraw-Hill Publishing Company, 2003.
- [14] H. Singh, S. Hao, and A. Papalexopoulos, "Transmission congestion management in competitive electricity markets," *IEEE Transactions on Power Systems*, vol. 13, pp. 672-680, 1998.
- [15] (21/02). *Battery Basics*. Available: http://www.progressivedyn.com/battery_basics.html
- [16] Sandia National Laboratories. (10/06). *DOE GLOBAL ENERGY STORAGE DATABASE*. Available: <http://www.energystorageexchange.org/>
- [17] X. Luo, J. Wang, M. Dooner, and J. Clarke, "Overview of current development in electrical energy storage technologies and the application potential in power system operation," *Applied Energy*, vol. 137, pp. 511-536, 1/1/ 2015.
- [18] T. K. Toshikazu SHIBATA*, Yoshiyuki NAGAOKA, Kazunori KAWASE and a. K. YANO, "Redox Flow Batteries for the Stable Supply of Renewable Energy."
- [19] "Vanadium Redox Flow Batteries: An In-Depth Analysis " EPRI, Palo Alto, CA:2007 1014836.
- [20] P. S. J. H. Lukas Grond, "Systems Analyses Power to Gas," KEMA Nederland B.V., Technology Review 20/06 2013.
- [21] B. E. Allan Schrøder Pedersen, Claus Hviid Christensen, Claus Kjøller, Frank Elefsen, John Bøggild Hansen, Jørgen Hvid, Rambøll, Per Alex Sørensen, Søren Knudsen Kær, Thomas Vangkilde-Pedersen, Thorkild Feldthusen Jensen,, "Status and recommendations for RD&D on energy storage technologies in a Danish context," 31/01 2014.
- [22] J. Kim, Y. Lee, W. S. Yoon, J. S. Jeon, M.-H. Koo, and Y. Keehm, "Numerical modeling of aquifer thermal energy storage system," *Energy*, vol. 35, pp. 4955-4965, 12// 2010.

- [23] (2014, 29/02/2016). The world's largest solar heating plant to be established in Vojens, Denmark. Available: <http://solar-district-heating.eu/NewsEvents/News/tabid/68/ArticleId/367/The-worlds-largest-solar-heating-plant-to-be-established-in-Vojens-Denmark.aspx>
- [24] F. Ulbjerg. (2014). *SOUTH-JUTLAND STORES THE SUN'S HEAT IN THE WORLD'S LARGEST PIT HEAT STORAGE*. Available: <http://www.ramboll.com/projects/re/south-jutland-stores-the-suns-heat-in-the-worlds-largest-pit-heat-storage>
- [25] Hydrogenics. (23/02). *Excess Wind Power Turned into Gas in Denmark Using Hydrogenics Technology*. Available: <http://www.hydrogenics.com/about-the-company/news-updates/2014/02/18/excess-wind-power-turned-into-gas-in-denmark-using-hydrogenics-technology>
- [26] (23/02). *POWER-TO-GAS TECHNOLOGY OFFER NEW MARKET OPPORTUNITIES FOR ELECTROLYSER MANUFACTURERS*. Available: <http://biocat-project.com/news/power-to-gas-technology-provides-new-market-opportunities-for-manufacturers-of-electrolysers/>
- [27] M. G. Tom Smolinka, Jürgen Garche, "Stand und Entwicklungspotenzial der Wasserelektrolyse zur Herstellung von Wasserstoff aus regenerativen Energien", 05/07 2011.
- [28] M. Sterner, "Bioenergy and renewable power methane in integrated 100% renewable energy systems. Limiting global warming by transforming energy systems " 14, Erneuerbare Energien und Energieeffizienz. Renewable Energies and Energy Efficiency Kassel University, 2009.
- [29] S. H. A. K. Sayah, M. Farazar, "CO₂ Abatement by Methanol Production from Flue-Gas in Methanol Plant " *International Journal of Chemical, Molecular, Nuclear, Materials and Metallurgical Engineering*, vol. 4, 2010.
- [30] Q. Zeng, J. Fang, J. Li, and Z. Chen, "Steady-state analysis of the integrated natural gas and electric power system with bi-directional energy conversion," *Applied Energy*.
- [31] M. S. a. A. Bertuccio, "Synthetic Natural Gas (SNG) from Coal and Biomass: a Survey of Existing Process Technologies, Open Issues and Perspectives," in *Natural Gas*, P. Potocnik, Ed., ed, 2010.
- [32] EARTO, "The TRL Scale as a Research & Innovation Policy Tool, EARTO Recommendations," European Association of Research and Technology Organisations 2014.
- [33] "XLPE_Cu_single_core_66_kV_DS_EN," N. Cables, Ed., ed: NKT cables, 2016.
- [34] Dreamstime, "Dreamstime," ed. <https://www.dreamstime.com>: Dreamstime, 2016.
- [35] "Distribution Zone Substation Information," Ausgrid, Ed., ed: Ausgrid, 2016.
- [36] "Modern-Era Retrospective Analysis for Research and Applications (MERRA), version 2," ed. gmao.gsfc.nasa.gov: National Aeronautics and Space Administration (NASA) / Goddard Space Flight Center, 2016.
- [37] "CAMS Radiation Service v2.7 all-sky irradiation (derived from satellite data).", ed: MINES ParisTech (France), 2016.
- [38] "National Electricity Market Price," AEMO, Ed., ed: AEMO, 2016.
- [39] (2016, 18/03). *Windpower Program*. Available: <http://www.wind-power-program.com>
- [40] A. Bellini, S. Bifaretti, V. Iacovone, and C. Cornaro, "Simplified model of a photovoltaic module," in *Applied Electronics, 2009. AE 2009*, 2009, pp. 47-51.
- [41] X. Weidong, W. G. Dunford, and A. Capel, "A novel modeling method for photovoltaic cells," in *Power Electronics Specialists Conference, 2004. PESC 04. 2004 IEEE 35th Annual*, 2004, pp. 1950-1956 Vol.3.
- [42] K. Provence, "Calculating PV Array Voltage," ed, 2013.
- [43] (2013, 20/03). *Solar Panel Temperature Affects Output – Here's what you need to know*. Available: <http://www.solar-facts-and-advice.com/solar-panel-temperature.html>
- [44] (2003). *Wind Turbine Power Calculator*. Available: <http://xn--drmstre-64ad.dk/wp-content/wind/miller/windpower%20web/en/tour/wres/pow/index.htm>
- [45] CanadianSolar. (2016, 16/11). *CanadianSolar*. Available: <http://www.canadiansolar.com/>
- [46] TrinaSolar. (2016, 16/11). *TrinaSolar*. Available: <http://www.trinasolar.com/us/index.html>
- [47] SolarWorld. (2016, 16/11). *SolarWorld*. Available: <https://www.solarworld-usa.com/>

- [48] S. Clegg and P. Mancarella, "Integrated Electrical and Gas Network Flexibility Assessment in Low-Carbon Multi-Energy Systems," *IEEE Transactions on Sustainable Energy*, vol. 7, pp. 718-731, 2016.
- [49] S. Clegg and P. Mancarella, "Integrated Modeling and Assessment of the Operational Impact of Power-to-Gas (P2G) on Electrical and Gas Transmission Networks," *IEEE Transactions on Sustainable Energy*, vol. 6, pp. 1234-1244, 2015.
- [50] M. Abeysekera, J. Wu, N. Jenkins, and M. Rees, "Steady state analysis of gas networks with distributed injection of alternative gas," *Applied Energy*, vol. 164, pp. 991-1002, 2/15/ 2016.
- [51] G. Czerniak. (2013). *Greg Czerniak`s Kalman Guide*. Available: <http://greg.czerniak.info/guides/kalman1/>
- [52] S. A.-h. Soliman and A. M. Al-Kandari, "8 - Dynamic Electric Load Forecasting," in *Electrical Load Forecasting*, ed Boston: Butterworth-Heinemann, 2010, pp. 291-352.
- [53] S. A.-h. Soliman and A. M. Al-Kandari, "1 - Mathematical Background and State of the Art," in *Electrical Load Forecasting*, ed Boston: Butterworth-Heinemann, 2010, pp. 1-44.
- [54] D. Lee, J. Kim, and R. Baldick, "Stochastic Optimal Control of the Storage System to Limit Ramp Rates of Wind Power Output," *IEEE Transactions on Smart Grid*, vol. 4, pp. 2256-2265, 2013.

Appendix A

The following Appendix shows the sequence of actions that must be made in ESSPC so that a custom user case can be created.

Figure 55 shows the starting screen of ESSPC. Here each button brings you to a different window where you can insert data for models or conduct simulations. There is a sequence to creating a proper case. As you can see all the buttons except one are colored in red, and there is only one green button. After pressing the green button and coming back to this window, another green button will appear and so on.

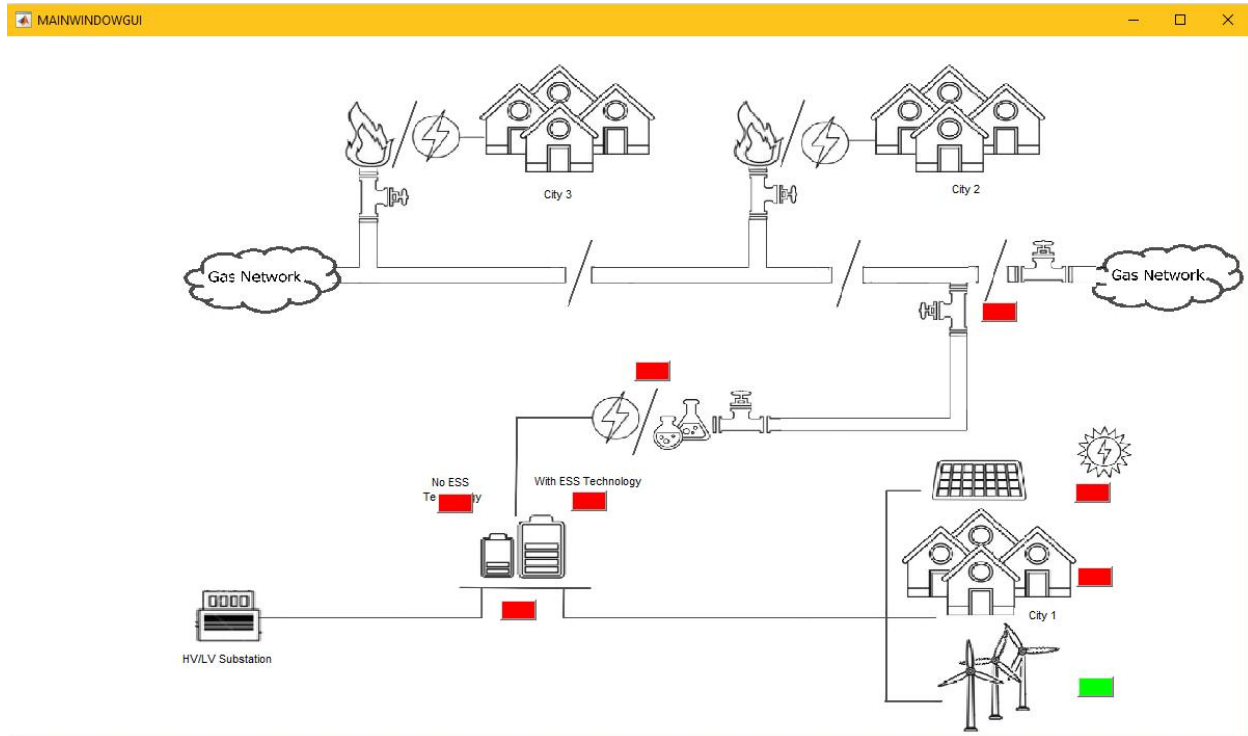


Figure 55 Main Window Screenshot

Figure 55 is a screenshot of the window where the wind turbine information is inserted. As with the main window the areas where data needs to be inserted is marked with green. After filling the green area with the necessary information, merely clicking the left mouse button anywhere in the window will reveal the next green area. The Efficiency Coefficient, Power Curve, and Wind Speed data are necessary for creating a specific wind turbine model. The information is entered with “[]” brackets. Also, it is important to mention that the number of values in all three fields must be equal. Pressing a yellow button will automatically load a wind turbine that has been used in this master thesis.

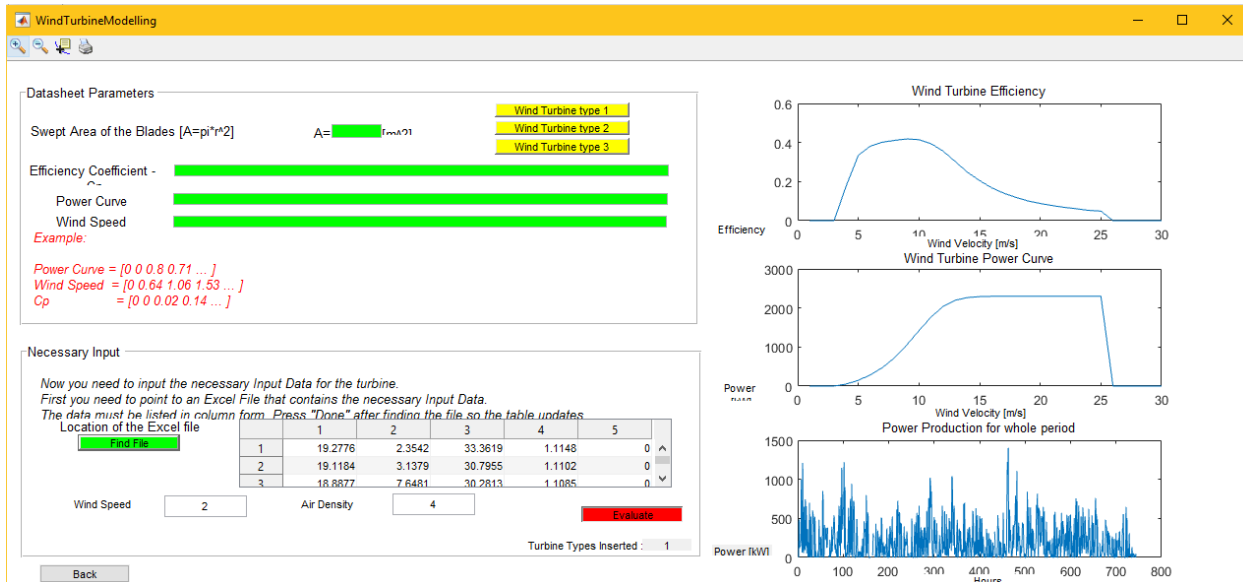


Figure 56 Wind Turbine model creation Type 1

After taking care of the parameters, the next step is to present information on the wind speed and air density. It is preferred that the file is a .xls and contains only values without any text, similar to Figure 57.

$$8760 \text{ hours} \left\{ \begin{array}{l} \overbrace{x_{1,1}}^{\text{Day,Hour}} \\ \vdots \\ x_{1,24} \\ x_{2,1} \\ \vdots \\ x_{365,24} \end{array} \right.$$

Figure 57 Weather Data form

After the data is loaded and is shown in the table ESSPC will need help determining which column contains the needed information. This action is performed by typing the respective number of the column in the fields below the table named Wind Speed and Air Density. The last step is to press the “Evaluate” button, and the graphs will show all the relevant information for that specific wind turbine model. The “Evaluate” button also clears all the fields, so that the user can insert information about the next wind turbine. Pressing the “Back” will bring the user back into the main window and will also show a comparison of the power production of all inserted wind turbines in the form of a box plot.

After returning to the main window, the next button has changed its color from red to green. The solar module window works on the same principle as the previous window. First, the datasheet parameters of the chosen solar module are inserted in the green areas and pressing the yellow button will automatically load information for one of the solar modules used in the thesis. The weather data is inserted the same way as before for the wind turbine models. After that, there is an option to test the solar module by presenting a value for Solar Irradiation and Temperature. The graph below will output an I-V curve for that specific Solar Irradiation and Temperature so that the user can see whether a mistake was made in the data insertion process. In order to make the simulation faster, the user is

presented with the option of combining the solar modules in parallel and/or in series with a view to create a solar array. By pressing the “Evaluate” button, information will be shown on the power production for the whole period with this technology and the fields will clear, awaiting information on the next solar module. Pressing the “Back” button will once again display a box plot of the power production of different technologies for the whole period.



Figure 58 Solar Module model creation Type 1

The next step is to insert the electrical load for the consumers. Again a .xls file containing no words and only numerical values is needed, in a form similar to Figure 59.

$$365 \text{ days} \left\{ \begin{array}{c} \overbrace{\left[\begin{array}{ccc} x_{1,1} & \cdots & x_{1,24} \\ \vdots & \ddots & \vdots \\ x_{365,1} & \cdots & x_{365,24} \end{array} \right]}^{24 \text{ hours}} \end{array} \right.$$

Figure 59 Electrical Consumption Data form

After filling the first table with information, pressing the green “Done ” button will sort the data in the needed form for the study. In the Unit box, the user must define in what units the consumer load is and then the user must press the last green “Done” button which will transform the data into the needed form for the case. Pressing “Done” will also visualize the consumer load information for the whole period in a separate graph.

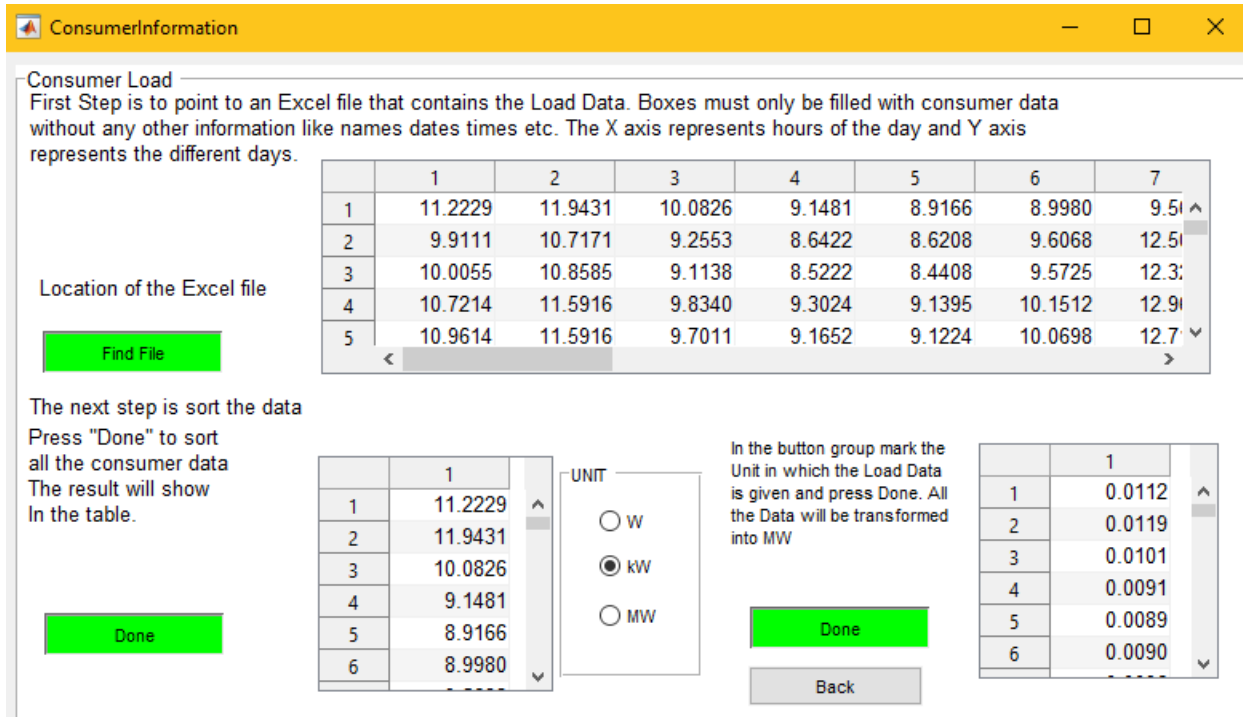


Figure 60 Electrical Load input window

The next step in creating a custom scenario is to supply ESSPC with information on the electrical grid. There are three windows which must be filled containing information on the busbars, branches, and generators. When opening the Grid Information window, you will see that the information is prefilled in all windows. There are two options from there, either you can submit prefilled information in .xls format to fit the different tables, or you can insert the information manually right in the charts. It is important to mention that there are fields which must not be changed and are marked with 999.

GridInformation

Busbar Data

Now you need to present the busbar data. You can either insert the data using the "Find file" button to the side, or you can enter data manually. After you are finished you will have to submit the data to MATLAB

Find File

	BUS	BUS TYPE	REAL POWER DEMAND	REACTIVE POWER DEMAND	SHUNT CONDU
1	1	3	0	0	
2	2	2	999	0	
3	3	2	999	0	

Submit Data

*NOTE: Do not change the 999 value. That is where the Generation and Load Go !!!
Also DO NOT CHANGE BUS and BUS TYPE*

Branch Data

Now you need to present the branch data. You can either insert the data using the "Find file" button to the side, or you can enter data manually. After you are finished you will have to submit the data to MATLAB

Find File

	FromBus	ToBus	R	X	B	rateA	rateB
1	1	2	0.0210	0.0410	0	150	150
2	2	3	0.0180	0.0370	0	150	150

Submit Data

NOTE: DO NOT CHANGE FromBus and ToBus

Generator Data

Now you need to present the generator data. You can either insert the data using the "Find file" button to the side, or you can enter data manually. After you are finished you will have to submit the data to MATLAB

Find File

	Bus	Pg	Qg	Qmax	Qmin	Vg	mBa
1	1	0	0	300	-300	1	
2	2	999	0	300	-300	1	
3	3	999	0	300	-300	1	

Submit Data

Back

Figure 61 Grid parameter information

After providing all the necessary information for creating a custom case, the storage system can now be sized. After opening the window, there are three areas which provide the user with flexibility in sizing the ESS without a PtG system. As before the sequence in which the information is to be filled is marked with green. The first area sizes the ESS with the surplus power method. The user can set limits regarding the number of RES that is to be installed in the grid. The limits are shared by ALL the wind turbine technologies and all the solar module technologies. After pressing "OPTIMUM," ESSPC will calculate the optimum number of RES that is to be installed in order to obtain the smallest ESS size. The optimum number is shown in the tables below, where each value represents the number of RES that must be placed, from each technology. The first row of wind turbine represents the first type of wind turbines and so on.

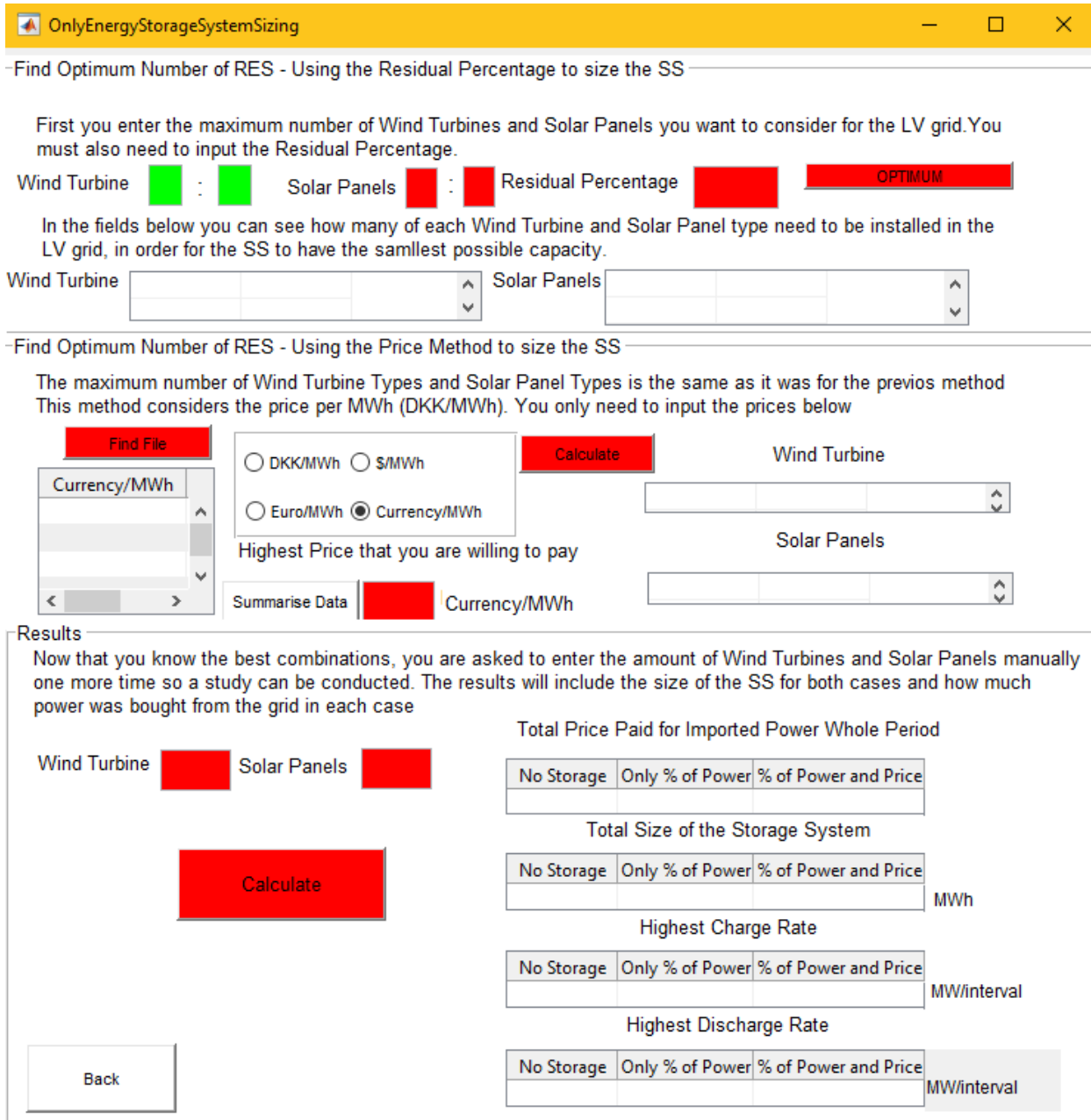


Figure 62 Sizing the ESS without PtG

Next, the ESS can be sized using the surplus power and price method. The data is inserted in a similar way to the one shown in Figure 57. The price can be in different currencies, and the user can choose which type of currency is used and then by pressing the “Summarise Data” button a graph will show the mean and median values of the whole dataset. This can help the user determine the highest price for that period, where the ESS will stay inactive. Similar to before, pressing “Optimum,” ESSPC will calculate the optimum number of RES that is to be installed using this method.

Finally, the user can get more in depth information on the ESS size with different RES combinations. For example, if there are three wind turbines in the scenario and the user wants to see the ESS size for 2 wind turbines of type 1, 3 of type 2 and 5 of type 3, he must enter the numbers in the field in the following form: 2 3 5. The process is similar for the Solar Panels. An example of this can be seen in the figure before. After pressing “Calculate,” a separate window will open with information on the

capacity of the ESS, the power that goes in and out and the amount of power that is supplied from the grid to support the city.

Now, information on the Gas Grid must be inserted. The first step is to fill the information on the gas grid like pressure at the beginning of the pipes, the amount of methane that is entering the area, distances between nodes and pipe diameters. Next step is to set the gas demand from the GPGs and the respective efficiencies. The electrical demand from the GPGs can be calculated through using the Kalman or LES method.

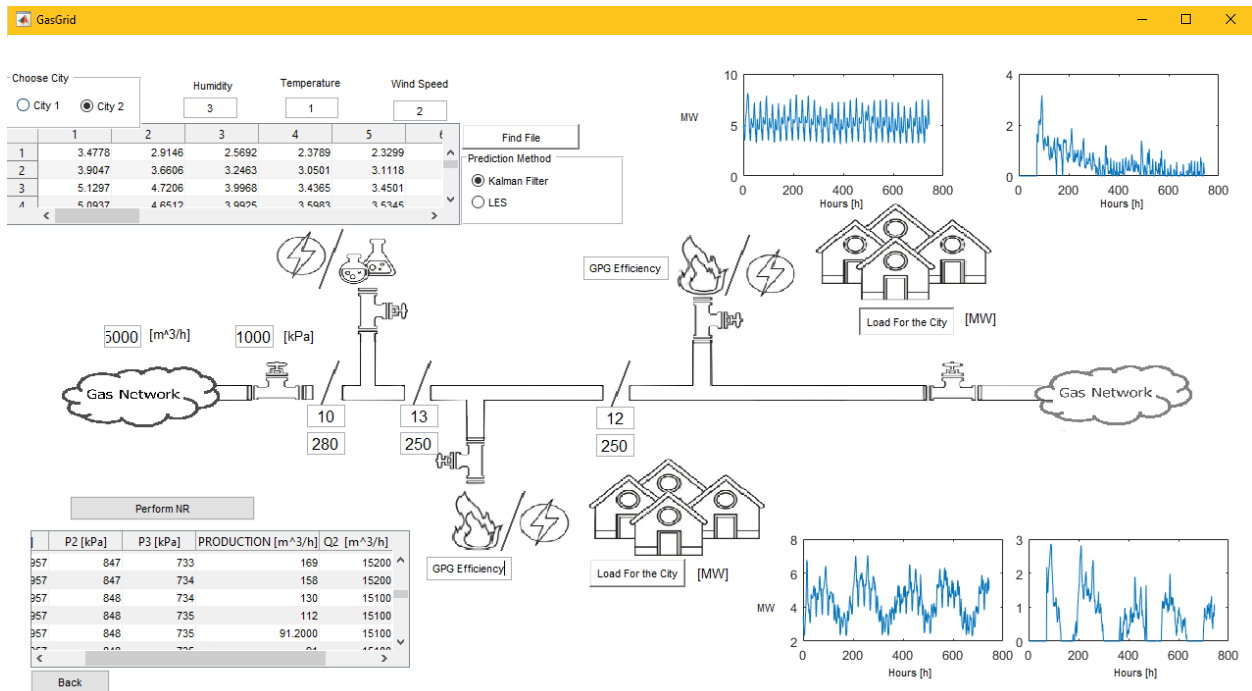


Figure 63 Gas Grid modeling

After choosing the Kalman Filter, the user can then load the electrical load in the different cities and obtain the power demand from the GPGs. If the user wants to use the LES method, information must be supplied on different weather factors (only three for the moment). The factors can be referred to various cities by the markings in the top left corner. As a final step, the demand from the PtG system can be calculated. This is done by pressing the “Perform NR” button, which will give information in the table below about the behavior of the gas grid for each interval.

Sizing the ESS with the PtG is done similar to before.

Using the Residual Percentage size the ESS with P2G

Set the efficiency of the P2G OPTIMUM

Wind Turbine : Solar Panels : Residual Percentage 0.5
 Wind Turbine : Solar Panels

CH4 production in MOI

Find Optimum Number of RES - Using the Price Method to size the SS

The Price Data is the same as in the previous step

Highest Price that you are willing to pay OPTIMUM
 DKK/MWh

Wind Turbine : Solar Panels
 CH4 production in MOI

Results

Now that you know the best combinations, you are asked to enter the amount of Wind Turbines and Solar Panels manually one more time so a study can be conducted. The results will include the size of the SS for both cases and how much power was bought from the grid in each case.

Wind Turbine Solar Panels

Total Price Paid for Imported Power Whole Period

No Storage	Only % of Power	% of Power and Price
<input type="text"/>	<input type="text"/>	<input type="text"/>

Total Size of the Storage System with P2G

No Storage	Only % of Power	% of Power and Price
<input type="text"/>	<input type="text"/>	<input type="text"/>

MWh

Gas Produced in m³ entire period

No Storage	Only % of Power	% of Power and Price
<input type="text"/>	<input type="text"/>	<input type="text"/>

[m³]

Highest Charge Rate

No Storage	Only % of Power	% of Power and Price
<input type="text"/>	<input type="text"/>	<input type="text"/>

MW/interval

Highest Discharge Rate

No Storage	Only % of Power	% of Power and Price
<input type="text"/>	<input type="text"/>	<input type="text"/>

MW/interval

Figure 64 Sizing the ESS without PtG

As a last option, the user can supply ESSPC with roundtrip efficiency for a chosen storage technology. This will give information on how the size changes with regards to the technology chosen and different methods.

ESSRoundTripEfficiency

Set the number of RES

Wind Turbine Solar Panels

Set Round-Trip efficiency for the chosen ESS

Surplus Power method
 Surplus Power and Price method

With Power-to-Gas
 Without Power-to-Gas

Size

Size after round-trip efficiency: [MWh]

Back

Figure 65 Sizing ESS with round-trip efficiency

Appendix B

This Appendix contains datasheet information on the different RES technologies that were used in this thesis.

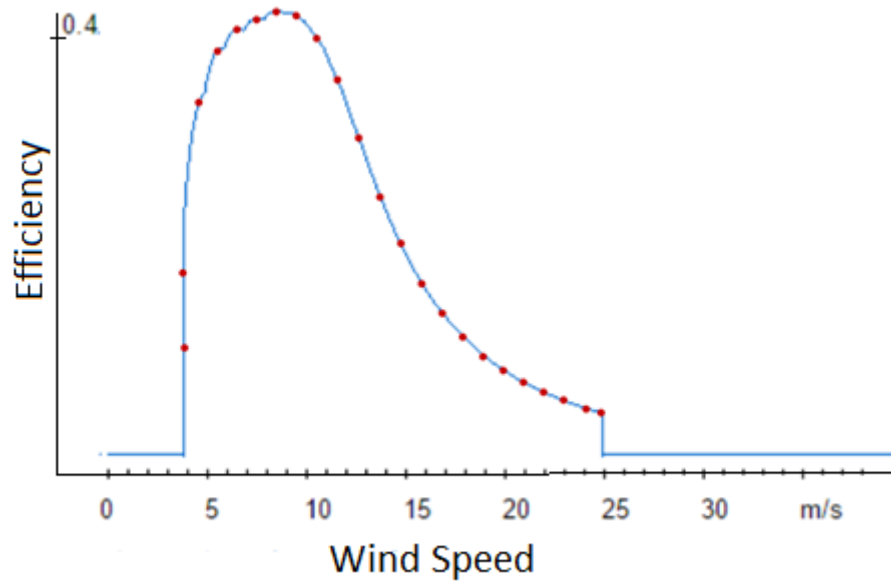
Appendix B.1 Wind Turbines

Name	Bonus 2300/82.4
Rated Power	2300 kW
Swept area blade [m²]	5333

The wind speed and power curve information was obtained in numerical form. The efficiency data was obtained from the figure below. As the figure at the source did not have proper y-axis markings, a program by the name of WebPlotDigitizer was used .

Wind Speed [m/s]	Output Power [kW]	Approx. Efficiency [%]
1	0	0
2	0	0
3	0	0
4	36	0.207189192
5	124	0.353069451
6	226	0.390658229
7	368	0.399607938
8	580	0.417507356
9	811	0.417507356
10	1103	0.412137531
11	1370	0.3915532
12	1633	0.358439276
13	1855	0.321745469
14	1945	0.268942185
15	1988	0.22508861
16	2000	0.183919948
17	2000	0.153490938
18	2000	0.127536781
19	2000	0.109637363
20	2000	0.093527886
21	2000	0.080998294
22	2000	0.070258643
23	2000	0.063098876
24	2000	0.05363715
25	2000	0.050192188
26	0	0
27	0	0
28	0	0
29	0	0

30	0	0
----	---	---

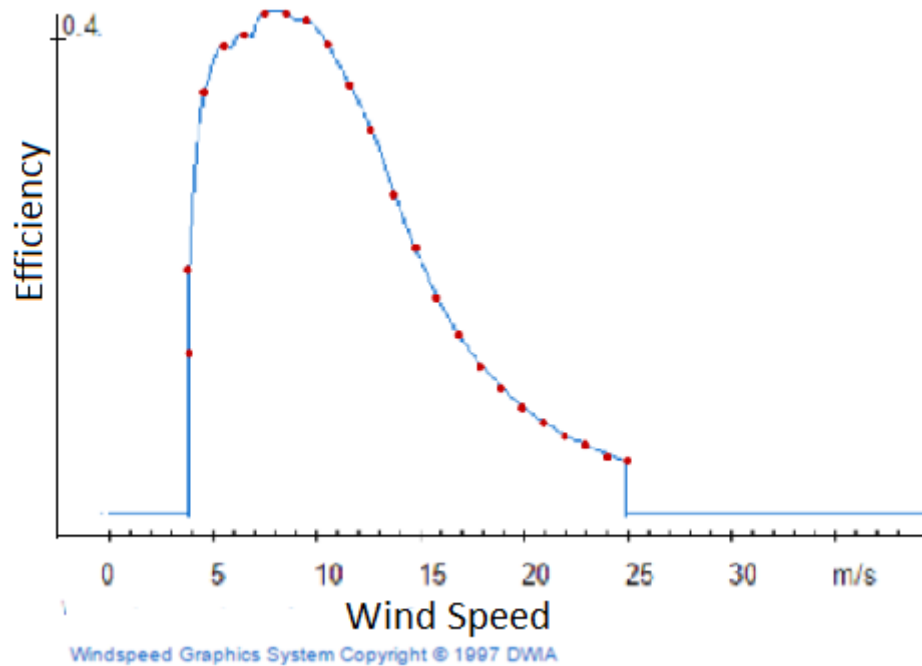


Windspeed Graphics System Copyright © 1997 DWA

Name	NEG Micon
Rated Power	2000/72
Swept area blade [m²]	2000 kW
	4071

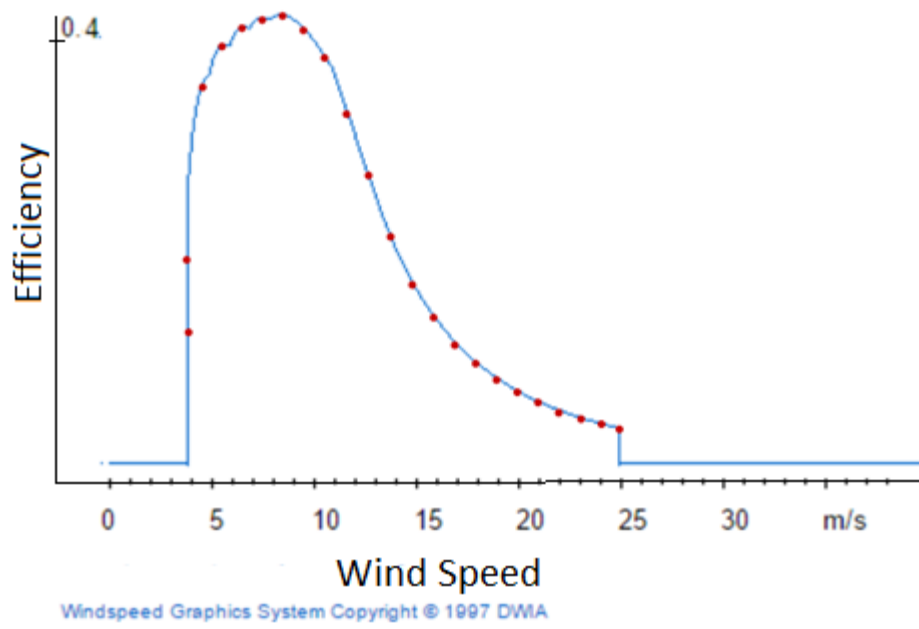
Wind Speed [m/s]	Output Power [kW]	Approx. Efficiency [%]
1	0	0
2	0	0
3	0	0
4	36	0.207189192
5	124	0.353069451
6	226	0.390658229
7	368	0.399607938
8	580	0.417507356
9	811	0.417507356
10	1103	0.412137531
11	1370	0.3915532
12	1633	0.358439276
13	1855	0.321745469
14	1945	0.268942185
15	1988	0.22508861
16	2000	0.183919948
17	2000	0.153490938
18	2000	0.127536781

19	2000	0.109637363
20	2000	0.093527886
21	2000	0.080998294
22	2000	0.070258643
23	2000	0.063098876
24	2000	0.05363715
25	2000	0.050192188
26	0	0
27	0	0
28	0	0
29	0	0
30	0	0



Name	Nordex
Rated Power	N90/2300
Swept area blade [m²]	2300 kW
	6362

Wind Speed [m/s]	Output Power [kW]	Approx. Efficiency [%]
1	0	0
2	0	0
3	0	0
4	70	0.196915556
5	183	0.353660085
6	340	0.390759381
7	563	0.407454065
8	857	0.414873924
9	1225	0.418583854
10	1607	0.4055991
11	1992	0.380557075
12	2208	0.329545542
13	2300	0.273896597
14	2300	0.218247652
15	2300	0.174655978
16	2300	0.144976541
17	2300	0.119934516
18	2300	0.103239832
19	2300	0.088400114
20	2300	0.077270325
21	2300	0.067995501
22	2300	0.058720676
23	2300	0.05306327
24	2300	0.048463987
25	2300	0.043859872
26	0	0
27	0	0
28	0	0
29	0	0
30	0	0



Appendix B.2 Solar Panels

DOUBLE-GLASS MODULE
DYMOND
CS6X-325P-FG

ELECTRICAL DATA / STC*

CS6X	315P-FG	320P-FG	325P-FG
Nominal Max. Power (Pmax)	315 W	320 W	325 W
Opt. Operating Voltage (Vmp)	36.6 V	36.8 V	37.0 V
Opt. Operating Current (Imp)	8.61 A	8.69 A	8.78 A
Open Circuit Voltage (Voc)	45.1 V	45.3 V	45.5 V
Short Circuit Current (Isc)	9.18 A	9.26 A	9.34 A
Module Efficiency	16.14 %	16.39 %	16.65 %
Operating Temperature	-40°C ~ +85°C		
Max. System Voltage	1500 (IEC) or 1000 V (UL)		
Module Fire Performance	Type 3 / Type 13 (UL 1703) or CLASS A (IEC 61730)		
Max. Series Fuse Rating	15 A		
Application Classification	Class A		
Power Tolerance	0 ~ + 5 W		

* Under Standard Test Conditions (STC) of irradiance of 1000 W/m², spectrum AM 1.5 and cell temperature of 25°C.

ELECTRICAL DATA / NOCT*

CS6X	315P-FG	320P-FG	325P-FG
Nominal Max. Power (Pmax)	228 W	232 W	236 W
Opt. Operating Voltage (Vmp)	33.4 V	33.6 V	33.7 V
Opt. Operating Current (Imp)	6.84 A	6.91 A	6.98 A
Open Circuit Voltage (Voc)	41.5 V	41.6 V	41.8 V
Short Circuit Current (Isc)	7.44 A	7.50 A	7.57 A

* Under Nominal Operating Cell Temperature (NOCT), irradiance of 800 W/m², spectrum AM 1.5, ambient temperature 20°C, wind speed 1 m/s.

PERFORMANCE AT LOW IRRADIANCE

Industry leading performance at low irradiance, average relative efficiency of 96.0 % from an irradiance of 1000 W/m² to 200 W/m² (AM 1.5, 25°C).

MECHANICAL DATA

Specification	Data
Cell Type	Poly-crystalline, 6 inch
Cell Arrangement	72 (6×12)
Dimensions	1968×992×5.8mm (77.5×39.1×0.23 in) without J-Box and corner protector
(Incl. corner protector)	1972×996×8.5 mm (77.6×39.2×0.33 in) without J-Box
Weight	27.5 kg (60.6 lbs)
Front Cover	2.5 mm heat strengthened glass
Back Glass	2.5 mm heat strengthened glass
Frame	Frameless
J-Box	Split J-Box, IP67, 3 diodes
Cable	4 mm ² (IEC) or 4 mm ² & 12 AWG 1000 V (UL)
Cable Length	1150 mm (45.3 in), 500 mm (19.7 in) (+) and 350 mm (13.8 in) (-) is optional for portrait installation*
Connectors	Amphenol H4 UTX (IEC), Renhe 05-6 (UL)
Standard	30 pieces, 900 kg (1984.1 lbs)
Packaging	(quantity & weight per pallet)
Module Pieces per Container	660 pieces (40' HQ)

* The application of this short length cable can only be used in portrait installation (clamping mounting method) systems in which the distance between modules should be less than or equal to 50 mm. In the event the distance between the PV modules to be installed is more than 50 mm, please make sure to consult our technical team for evaluation and advice.

TEMPERATURE CHARACTERISTICS

Specification	Data
Temperature Coefficient (Pmax)	-0.41 % / °C
Temperature Coefficient (Voc)	-0.31 % / °C
Temperature Coefficient (Isc)	0.053 % / °C
Nominal Operating Cell Temperature	45±2 °C

TSM-PC05

ELECTRICAL DATA @ STC	TSM-235 PC/PA05	TSM-240 PC/PA05	TSM-245 PC/PA05	TSM-250 PC/PA05
Peak Power Watts- P_{MAX} (Wp)	235	240	245	250
Power Output Tolerance- P_{MAX} (%)	0/+3	0/+3	0/+3	0/+3
Maximum Power Voltage- V_{MP} (V)	29.3	29.7	30.2	30.3
Maximum Power Current- I_{MPP} (A)	8.03	8.10	8.13	8.27
Open Circuit Voltage- V_{OC} (V)	37.2	37.3	37.5	37.6
Short Circuit Current- I_{SC} (A)	8.55	8.62	8.68	8.85
Module Efficiency η_m (%)	14.4	14.7	15.0	15.3

Values at Standard Test Conditions STC (Air Mass AM1.5, Irradiance 1000W/m², Cell Temperature 25°C).
Power measurement tolerance: ±3%

ELECTRICAL DATA @ NOCT	TSM-235 PC/PA05	TSM-240 PC/PA05	TSM-245 PC/PA05	TSM-250 PC/PA05
Maximum Power- P_{MAX} (Wp)	171	174	178	181
Maximum Power Voltage- V_{MP} (V)	26.4	26.6	26.8	27.0
Maximum Power Current- I_{MPP} (A)	6.48	6.55	6.64	6.70
Open Circuit Voltage (V)- V_{OC} (V)	34.0	34.1	34.2	34.3
Short Circuit Current (A)- I_{SC} (A)	6.97	7.04	7.10	7.25

NOCT: Irradiance at 800W/m², Ambient Temperature 20°C, Wind Speed 1m/s.
Power measurement tolerance: ±3%

TEMPERATURE RATINGS

Nominal Operating Cell Temperature (NOCT)	45°C (±2°C)
Temperature Coefficient of P_{MAX}	-0.43%/°C
Temperature Coefficient of V_{OC}	-0.32%/°C
Temperature Coefficient of I_{SC}	0.047%/°C

Sunmodule Plus

SW 285 MONO

PERFORMANCE UNDER STANDARD TEST CONDITIONS (STC)*

<i>Maximum power</i>	P_{max}	285 Wp
<i>Open circuit voltage</i>	V_{oc}	39.7 V
<i>Maximum power point voltage</i>	V_{mpp}	31.3 V
<i>Short circuit current</i>	I_{sc}	9.84 A
<i>Maximum power point current</i>	I_{mpp}	9.20 A
<i>Module efficiency</i>	η_m	17.0 %

*STC: 1000 W/m², 25°C, AM 1.5

†) Measuring tolerance (P_{max}) traceable to TUV Rheinland: +/- 2% (TUV Power Controlled).

THERMAL CHARACTERISTICS

<i>NOCT</i>	46 °C
<i>TC I_{sc}</i>	0.04 %/°C
<i>TC V_{oc}</i>	-0.30 %/°C
<i>TC P_{mpp}</i>	-0.41 %/°C
<i>Operating temperature</i>	-40°C to 85°C